THE MACRO/MICRO MANIPULATOR: AN IMPROVED ARCHITECTURE FOR ROBOT CONTROL

by

ANDRE SHARON

B.S. Mech. Eng., Polytechnic Institute of New York (1981)
S.M. Mech. Eng., Massachusetts Institute of Technology (1984)

SUBMITTED TO THE DEPARTMENT OF MECHANICAL ENGINEERING IN PARTIAL FULFILLMENT OF THE REQUIREMENTS FOR THE DEGREE OF

DOCTOR OF PHILOSOPHY

at the

MASSACHUSETTS INSTITUTE OF TECHNOLOGY

September, 1988

Signature of Author.....
Department of Mechanical Engineering
September, 1988

Certified by.....
Neville Hogan
Thesis Supervisor

Certified by.....
David E. Hardt
Thesis Supervisor

Accepted by.....
Ain A. Sonin
Chairman, Departmental Graduate Committee

THE MACRO/MICRO MANIPULATOR: AN IMPROVED ARCHITECTURE FOR ROBOT CONTROL

by

ANDRE SHARON

Submitted to the Department of Mechanical Engineering in September, 1988 in partial fulfillment of the requirements for the Degree of Doctor of Philosophy

ABSTRACT

Commercially available robotic manipulators are neither accurate, fast, nor well suited to interact with their environment. A macro/micro manipulator system, consisting of a large (macro) robot carrying a small (micro) high performance robot, is proposed as a means of enhancing the functionality of a manipulator. The objective of the research presented in this document is to investigate the inherent features in dynamic performance of such a system, and to evaluate its feasibility.

The effect of a micromanipulator on the stability and performance of a robot system is investigated. It is found that a macro/micro manipulator is an inherently stable physical architecture for endpoint feedback. This configuration is is shown to be well suited for high performance position and force control, enhancing the dynamic range of the robot.

An endpoint position control bandwidth of 28 Hz (15 times higher than the first structural mode of the macromanipulator) was achieved. It is demonstrated through simulation and/or experimentation that the micromanipulator is very useful in compensating for the settling time of the macromanipulator, as well as for dynamic tracking errors encountered in following a prescribed path.

A force control bandwidth of 60 Hz (32 times higher than the first structural mode of the macromanipulator) was achieved against an environment that is five times stiffer than the robot structure. This is beneficial in regulating interface forces and modulating endpoint impedance during constrained motion.

Controller design in the "physical domain" is proposed as a means of retaining physical insight, and narrowing the gap between electro-mechanical design and control systems design. The macro/micro manipulator system is used as a case study in evaluating this approach.

Thesis Supervisor: Dr. Neville Hogan
Title: Associate Professor of Mechanical Engineering

Thesis Co-supervisor: Dr. David E. Hardt
Title: Associate Professor of Mechanical Engineering

MEMBERS OF THE COMMITTEE

Dr. Neville Hogan - Chairman
Associate Professor of Mechanical Engineering
Massachusetts Institute of Technology

Dr. David E. Hardt
Associate Professor of Mechanical Engineering
Massachusetts Institute of Technology

Dr. Woodie C. Flowers
Professor of Mechanical Engineering
Massachusetts Institute of Technology

Dr. Joseph L. Smith, Jr.
Professor of Mechanical Engineering
Massachusetts Institute of Technology

ACKNOWLEDGEMENTS

The Acknowledgements is definitely the most fun section to write. At the very least, it signifies that you are almost done. More importantly (?), it gives you the opportunity to look back on some fond memories.

First I would like to thank my advisors Neville Hogan and Dave Hardt. Neville's ability to absorb technical information (among other things...) is amazing. He always zeros in on the important issues and understands every detail of the problem presented to him. In some respects he lives up the reputation of an MIT professor. In others, he is just "one of the guys," making it especially enjoyable to work with. I have greatly benefitted from his visions.

Dave Hardt and I go back a long way. It seems like after exploring all the alternatives, the path always leads back to his door. I guess that says something about my respect for him. I have learned a great deal from his technical insight and greatly enjoyed working with him again. Directorship of the Laboratory for Manufacturing and Productivity has changed his dress habits but not his personality.

I would also like to thank the other members of my committee, Woodie Flowers and Joe Smith, for their constructive suggestions and for taking the time to be a part of this research.

Professors Kamal Youcef-Toumi and David Gossard were not involved in my research but always had encouraging comments to make. I am grateful.

There are several colleagues and friends here at MIT that I'd like to thank for their friendship and/or help. These include Gary Drlik, Katy Laffey, Zhou-ru Ding, Joe Deck,

Charlie Oppenheimer, Behzad Rasolee, Dov Adelstein, John Bausch, Ahmet Buharali, Tom Fuhlbrigge, and Zvi Shiller.

I would also like to thank my office-mates: Ted Clancy, Tony Koselka, and Gunter Niemeyer. They have always been friendly and supportive.

The members of Neville Hogan's research group have been an enormous source of knowledge and information. My research has greatly benefitted from discussions with them. I have especially benefitted from conversations with Ed Colgate. His departure (he completed his Ph.D.) is a loss to the MIT community, but an asset to Northwestern, where he is presently on the faculty.

Boston is a great place, especially with buddies like Naveed and my Turkish friends whose names I could not even begin to spell. They all helped me explore some of the best "sights" in Boston.

Of course this group would not be complete without my buddy Monsieur Moris Fresko, "mon ami, mon frere". We had some great times in Boston and Montreal.

I would like to thank my sister Jackie and Mers for the use of their house, and more importantly, their laser printer.

I would also like to thank my sister Adina and Jerry for the unlimited use of their Florida residence. Some of my best inspirations came to me on the beach in Ft. Lauderdale.

A thank-you goes to Debbie Faust for all her help and friendship during my stay at MIT. It is greatly appreciated. I am also grateful to Linda D'anna.

I would like to thank the IBM Corporation for its generous support. I am grateful to Phil Summers, Charlie Kelly, Marv Pittler, Dave Grossman, Ed Collins, and especially Jeanine Meyer. I would also like to thank Marilyn Barringer,

Jeanette Ladue, Tony Levas, and Ed Glassman for their help during my stay at MIT.

Then there's Kristen, always understanding and supportive. She also proof-read this document.

To Mom and Dad

TABLE OF CONTENTS

LIST OF FIGURES

LIST OF TABLES

Chapter 1
INTRODUCTION

1.1 Background

As more and more industrial robots find their way to the manufacturing floor, it is becoming evident that there are several technical issues that need to be addressed. These include: coordination between several robots and machines on the manufacturing floor, "intelligence", dynamics of the interaction between a robot and its environment, cycle time, as well as accuracy. The first two issues are addressed by the Operations Research and Artificial Intelligence communities, respectively. It is in response to the latter issues that this research was initiated.

Although robots provide greater versatility and large range of motion, they cannot compete with hard automation when it comes to accuracy and speed. In fact, a robot is slower than a human operator in most applications. Of course the overall productivity of a robot is usually higher than that of a human operator. This, however, is attributed to the fact that humans tend to fatigue quickly in performing repetitive tasks, where as robots thrive on it. Nevertheless, an industrial manipulator generally requires more time to complete one cycle than does a human.

It is clear that robots will never be as fast or accurate as hard automation. After all, hard automation refers to machines that were designed specifically for one task, while robots are designed to be much more versatile in function. In the case of mass-produced disposable consumer products such as

pens, lighters, shavers, etc., machinery can complete upwards of five hundred assemblies per minute. Commercially available industrial robots, equipped with intricate sensing capabilities, can perhaps complete one or two of these assemblies per minute, if at all. Regardless of how technologically advanced future robots may become, the same level of technology can be added to hard automation as well, always resulting in a higher level of performance.

Of course robots have their own virtues. In operations that are not repetitive in nature, and also contain a high degree of uncertainty, hard automation is not appropriate. It is in these types of applications that robots are or should be used. If the length of production runs or life cycle of a product are short, then it obviously does not pay to invest great sums of money developing machinery that will become useless in a short period of time. Hence, choice of automation depends on many factors, both technical and financial.

The fact that human operators can outperform robots in most applications is one of the major reasons why robots are not more widely used. After all, if there was a financial benefit driving the field, there would be many more robots on the manufacturing floor than there are today. It is understandable, and perhaps justifiable, why some managers argue for either hard automation or "human automation".

Almost all industrial robots in use today perform operations requiring minimal, if any, interaction with the environment. Hence, the most common applications are spray painting, arc welding, and simple pick and place tasks. There are, however, many potential robot applications requiring the manipulator to be mechanically coupled to other objects during some phase of the cycle. Examples include: intricate

assembly, handling of fragile objects, grinding, drilling, engraving, etc. During the coupled phase, the dynamics of the robot change, and the position of the end-effector can no longer be controlled independently of the environment. The robot motion is said to be constrained.

During constrained motion, position control no longer suffices. It is the interaction between the robot and its environment that must be controlled. As will be shown in later chapters, however, conventional robot architectures are not well suited for such interactions. Therefore, they are not widely used in such tasks.

Robots are not commonly used in operations requiring high accuracy either. This is due to the inherent design tradeoffs between positioning accuracy and response time that plague conventional robot architectures. The problem of positioning accuracy is caused primarily by unmeasured deflections of the robot structure and transmission system, as well as poor actuator/servo resolution. Poor response time is attributed to low actuator power and control-related problems. Since most commercially available robots derive their endpoint position from transducers located at each joint, the endpoint position is controlled in an open loop fashion. Any measurement error, or deviation of a link from its ideal rigid body behavior, causes the actual endpoint position to differ from the predicted value (see Figures 1.1 and 1.2).

Increasing the stiffness of a structure as a means of improving endpoint accuracy usually results in a more massive structure as well. The increased inertia, however, is detrimental to the response time. Thus, there are inherent tradeoffs between system bandwidth and endpoint accuracy.[1]

It is in response to these problems that the macro/micro

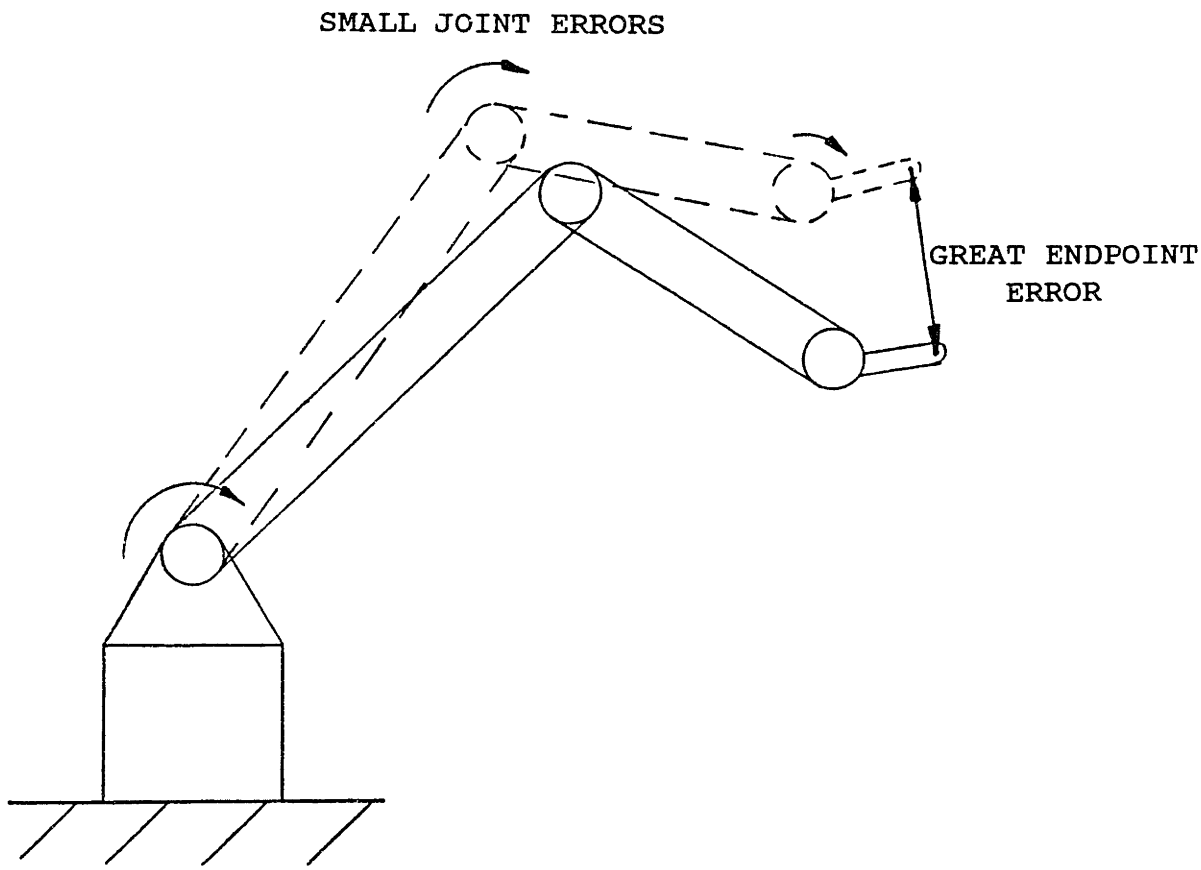

Figure 1.1: Amplification of Measurement Errors.

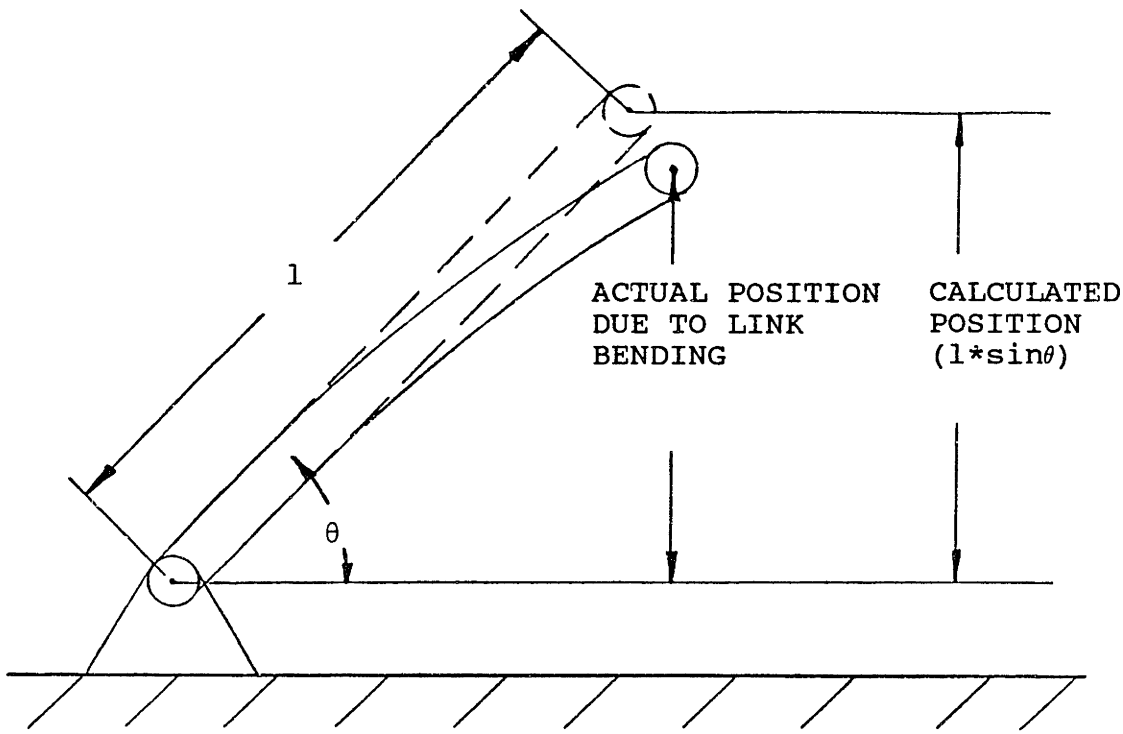

Figure 1.2: Link Bending.

manipulator system is proposed. This architecture consists of a large (macro) robot carrying a small (micro) high performance robot to the vicinity of the task. There, the inherent characteristics of both robots are used, in conjunction with endpoint sensing, to achieve the desired goal. The objective of the research presented in this thesis is to investigate the inherent features in dynamic performance of such a system, and to evaluate its feasibility.

1.2 Thesis Organization

Having introduced some of the problems plaguing robotic manipulators, the rest of this thesis describes how a proposed macro/micro manipulator system solves some of these problems, while inevitably raising a few others.

Chapter 2 describes several approaches to improving robot performance, including the proposed macro/micro manipulator system. Both advantages and disadvantages are discussed in each case.

The stability of the macro/micro manipulator during unconstrained motion, as in welding or spray painting, is analyzed in chapter 3. A robust, high bandwidth endpoint position controller is proposed. It is shown that the micro-manipulator enhances system response time, as well as tracking accuracy.

The force control problem is introduced in chapter 4. A great deal of physical insight is obtained by distinguishing performance issues from stability issues.

In chapter 5, stability of the macro/micro manipulator during constrained motion is analyzed. The system is shown to

be inherently stable in regulating interface forces and modulating endpoint impedance. A robust controller design, based on physical equivalence, maximizing the power flow from the micromanipulator to the macromanipulator through impedance matching is proposed. It is shown that interface force regulation at bandwidths higher than the structural frequencies of the macromanipulator can be achieved.

Chapter 6 describes the experimental verification of the system analysis and performance characterization of the proposed macro/micro manipulator system.

While most of this thesis deals with the design, control, and characterization of a macro/micro manipulator system, chapter 7 is much broader in scope. It attempts to extract concepts observed or developed in working with the macro/micro manipulator system that are generic enough to stand on their own. It is shown how these concepts might be applied to other systems or processes.

Finally, concluding remarks are made in Chapter 8.

Chapter 2

IMPROVING PERFORMANCE

2.1 Desired Characteristics

In order to achieve high productivity and quality, a robot must be accurate, fast, dynamically capable of interacting with variable environments, reliable, and intelligent. If a robot is intelligent but does not possess the dynamic performance necessary to put the intelligence to physical use, then it is nothing more than an intelligent computer system. In fact, some people view the robot as just another peripheral to the computer.

On the other hand, if a robot is dynamically superior, but is not very intelligent in the way that it makes use of its dynamic capabilities, then it obviously is not very effective. Hence, there must be a balance between intelligence and dynamic performance. For example: if a robot is commanded to drill a hole in some medium, it should have the intelligence to evaluate the important properties of the medium, determine a favorable endpoint impedance, and choose a proper drill speed and feed rate. However, it must also have the physical capabilities to execute the given task. This includes accurate positioning of the drill, and the capability to actually modulate its endpoint impedance or dynamics to the required value.

The research presented in this thesis concerns itself only with dynamic performance, and leaves the remaining issues to others.

There have been several approaches suggested by research-

ers for improving the dynamic performance of robots. These approaches are reviewed in the next section.

2.2 Reduction of Bending in Robot Structures

As mentioned earlier, lack of accuracy is caused in part by non-rigid behavior of the robot's links. One way of reducing bending in a link is by increasing the cross-sectional moment of inertia. The easiest way of accomplishing this is to simply increase the cross-sectional area; in other words, to use a "thicker" link. Unfortunately, this implies a larger inertia and response time is greatly sacrificed. The robot becomes little more than a fancy machine tool.

Nevertheless, there are several ways of producing a stiffer link without significantly increasing the mass.

2.2.1 Composite Materials

Through the development of new synthetic materials, it is now possible to build rigid, yet relatively light structures. By electing various combinations of materials, the designer can more precisely control the characteristic behavior of a structure. These composites possess high strength-to-weight and stiffness-to-weight ratios, improved corrosion and wear resistance, and increased fatigue life.[2] Furthermore, fiber orientation can lead to preferred directions of bending, allowing for more design flexibility.

This is a good passive way of increasing link stiffness. It does not add to the number of actuators, nor to the control

problem. Due to the fact that the structural resonant frequencies are generally higher in composites, achievable controlled performance is improved.

While composite materials can reduce bending, they cannot completely eliminate it. Thus, some positioning error due to beam bending as well as amplification of transducer measurement errors will still exist. Hence, it is argued that composites are not a means to a complete solution, but rather an improvement that would complement all the other approaches.

2.2.2 Active Link Stiffness Control

If the amount of bending occurring in a link is known, then it can conceivably be compensated for, in an active manner, in order to eliminate displacement of the endpoint.

One possible solution involves construction of a link composed of an outer and inner beam.[3] A pair of perpendicular actuators is placed at one end between the two beams. As soon as bending of the load bearing outer beam is somehow detected, the appropriate actuator generates a force necessary to eliminate the displacement of the outer beam endpoint. Hence, the stiffness of the beam is actively controlled in real time (see Figure 2.1). This system will theoretically eliminate the static effect of bending in links.

While this approach eliminates static bending and improves static accuracy, there are several remaining problems besides that of measuring the amount of bending. First, whatever errors exist at each link sum up to produce a larger endpoint error. Second, the encoders' measurement errors are still amplified through the length of each link. Finally, longitudinal displacement of a link cannot be corrected unless

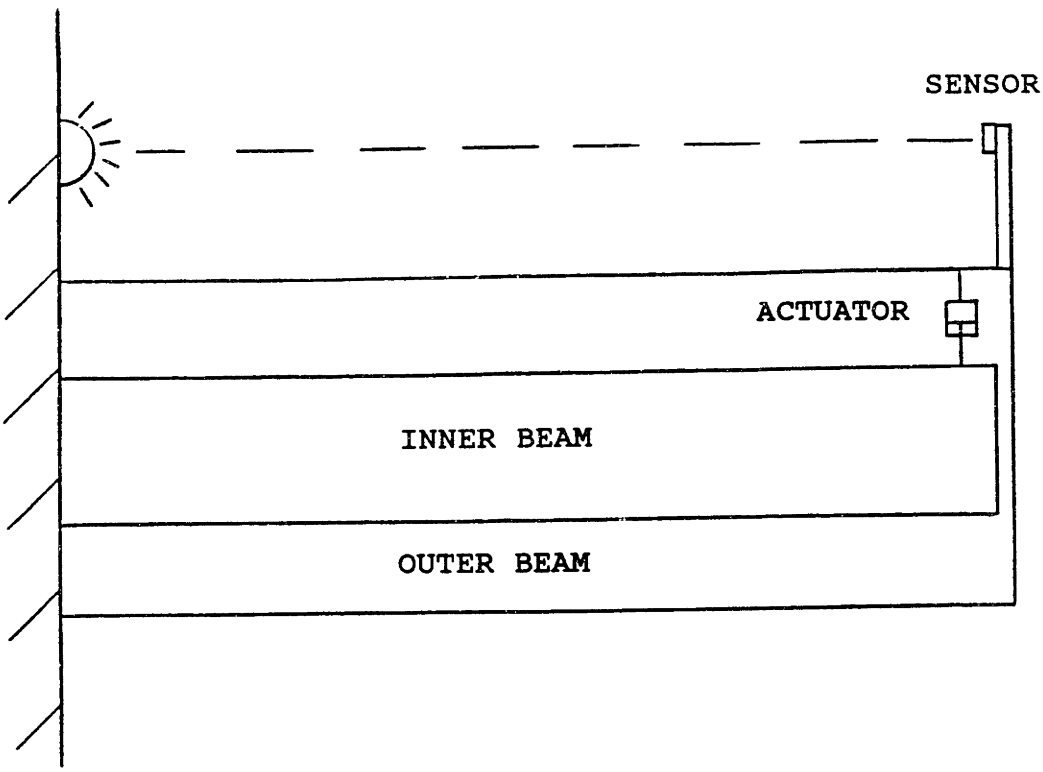

Figure 2.1: Active Stiffness Control of a Robot's Link.

a telescoping link with three actuators is used. Thus, many actuators are needed for a multi-degree-of-freedom robot.

2.2.3 Local Support

Since robots are designed for large range of motion in a sizable workspace, great bending moments are created, especially when the manipulator is fully extended. In order to reduce this large moment arm, the robot can attach itself to a local support in the vicinity of the task location.[4,5] After completing the operation, the robot would detach itself and move on to the next operation where it would again attach itself to another local support. Thus, there would be several local supports in the workspace, located near every critical operation (see Figure 2.2).

There are at least three major benefits from this system. First, the moment arm (distance between the tool and the support of the robot structure) is greatly reduced and bending is therefore virtually eliminated. Second, since the local support may be well defined in the robot coordinate system, the position of the endpoint relative to the support may be very accurately determined, and thus the absolute position of the endpoint will be known. Finally, the dynamics of the robot can be altered depending on how and where it attaches itself to the environment. This in turn leads to more control in interacting with the environment.

On the other hand, the local support concept may inhibit the versatility of a robot application. A local support area must be provided for each point where a critical operation is performed. If there are many such points, it may become very

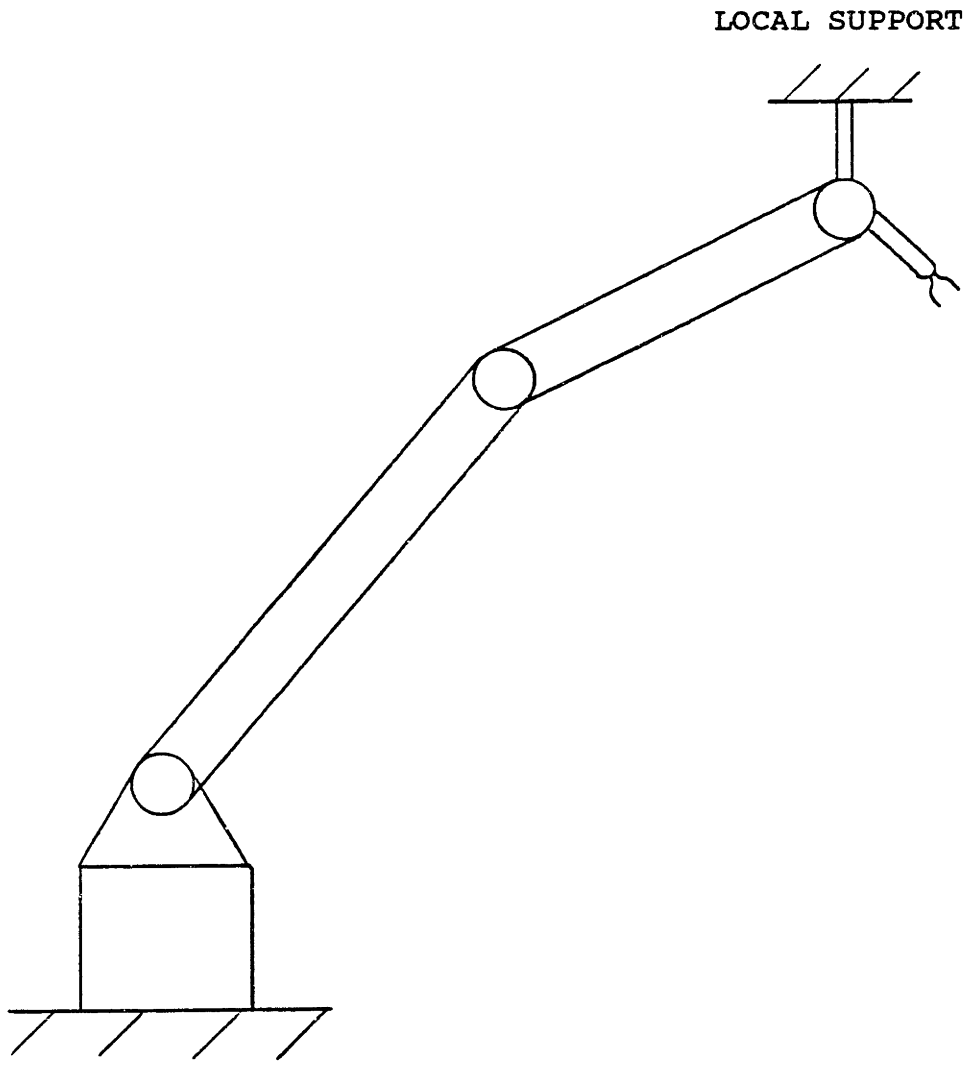

Figure 2.2: Local Support.

difficult to provide the required support areas, especially as the robot work space becomes cluttered with many tools and fixtures. Furthermore, different support areas might be needed for different production runs.

2.3 Endpoint Position Control

If the absolute position of the robot's end-effector is measured, the accuracy of a robot would theoretically be limited only by the measurement device and/or actuator/servo resolution. Thus, if the position of the end-effector is fed back to the controller, the various actuators can react accordingly to keep the endpoint at the desired location (see Figure 2.3). This approach has been rigorously pursued by Cannon.[6]

There is one major problem that immediately stands out: endpoint measurement. A measurement system must be devised that can detect not only the position of the endpoint, but the crientation as well. The measurement must be fast since the data is processed in real time, and it must be accurate over a large workspace.

There are several approaches to this endpoint measurement problem including laser optics and sonics. However, due to fixtures in the workspace, the end-effector is sometimes shielded from view of the base receiver, creating more problems. Nevertheless, feasibility is becoming more promising with time and progress is being made.

There are other problems as well. While the static position of the endpoint can be accurately controlled, dynamic performance is very difficult to achieve. The actuators

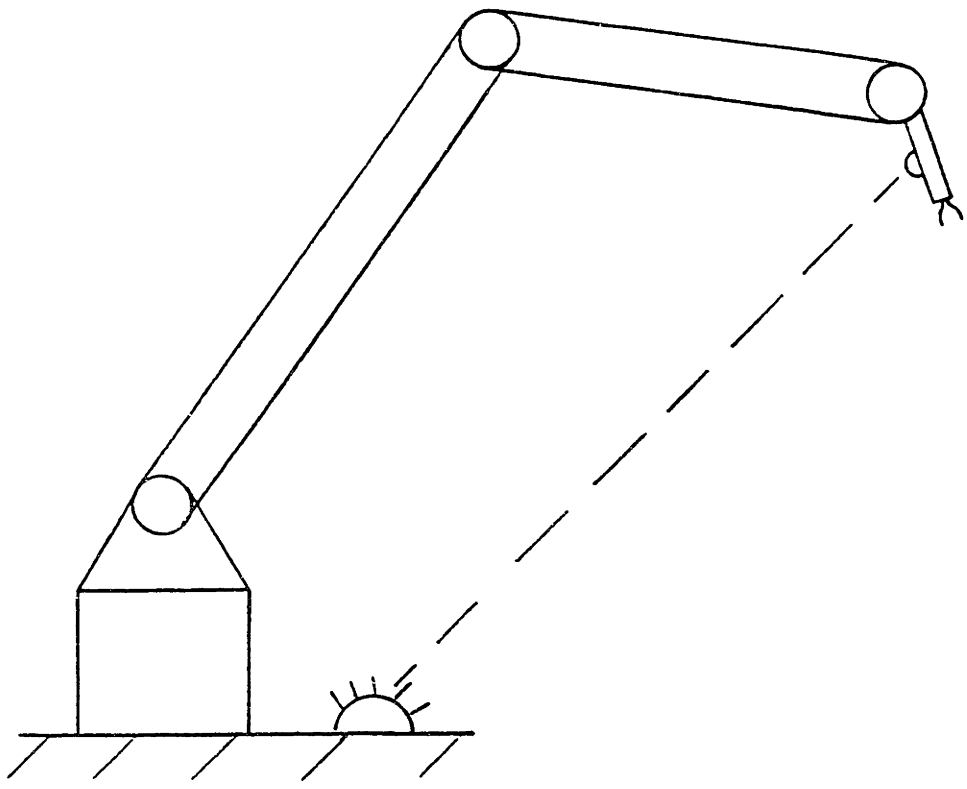

Figure 2.3: Control About Manipulator's Endpoint.

transmit forces to the point of measurement via a dynamic system, resulting in non-collocated control and associated instabilities.[7] Furthermore, there is a physical limitation on the achievable bandwidth due to the time required for a wave to travel the length of the flexible structure.[6]

Finally, there is yet another problem. Since in most robots the actuators are positioned in series, correction of a small endpoint error requires movement of several if not all the manipulator actuators. Thus, each actuator must provide high speed and good response for large motion, while at the same time provide very accurate and quick response for fine motion.

2.4 Proposed Solution: Macro/Micro Manipulator

It is clear that the absolute endpoint position can best be obtained by measurement of the endpoint rather than any other point on the robot. This is the only position that would result in true closed loop control of the robot endpoint. However, sensor location is only one variable in a control system. Actuator location is another.

Thus, to improve dynamic performance without sacrificing accuracy, a macro/micro manipulator system is proposed. This is comprised of a large (macro) robot carrying a small (micro) high performance robot to the vicinity of a task. There, the distinct inherent characteristics of the macro and micro robots are used in conjunction with endpoint sensing to achieve the desired goal(see Figure 2.4).

The objective of the research presented in this thesis is to investigate the inherent features in dynamic performance of

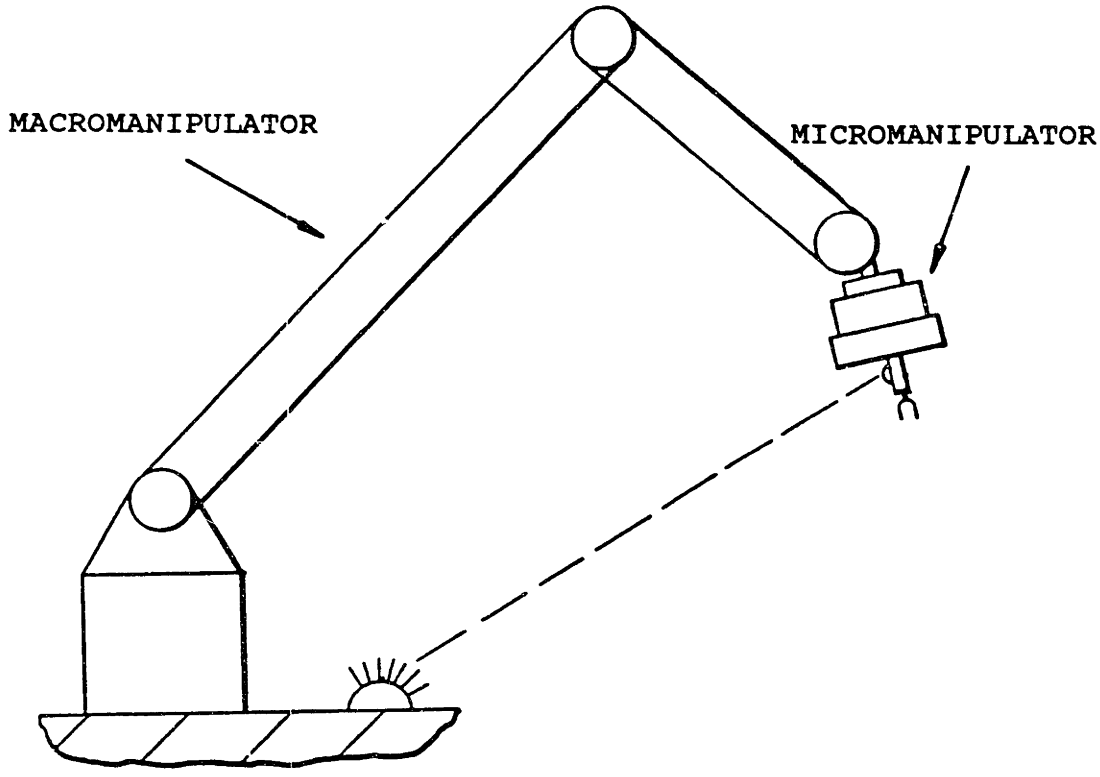

Figure 2.4: Macro/Micro Manipulator System.

such a system, and to evaluate its feasibility.

2.4.1 Advantages

In theory, a macro/micro manipulator offers all the features of a small high precision robot for local operations, while at the same time retaining the versatility, speed, and large range of motion of a bigger robot.

Intuitively, there are several concrete advantages. First, the endpoint dynamics of the robot can be modulated locally using the micromanipulator. This would enhance the system's capability to successfully interact with its environment.

Second, the endpoint inertia of the robot is physically reduced, requiring less control effort in responding to varying conditions. Furthermore, when a robot makes the transition from unconstrained motion to constrained motion, an impact occurs. Force transients during such impacts are directly related to the inertia of the colliding members. Yet, regardless of how much force an actuator can produce, by the time the controller reacts to these force spikes, they are over and the damage is done. When the macro/micro manipulator experiences an impact, it is the low inertia of the micromanipulator that is first seen at the interaction port, hence reducing the magnitude of the associated force transients. Thus, a macro/micro manipulator can achieve a smoother transition between unconstrained and constrained motion, allowing it to have a higher approach speed in contacting the environment.

Finally, the actuators of the macromanipulator could be

specially designed for high speed and large range of motion, while those of the micromanipulator for high acceleration and precise motion.

The advantages cited in this section are based on intuition, and may or may not prove to be true. In the remaining chapters, these advantages will be analyzed and characterized.

2.4.2 Disadvantages

Again, an endpoint position and orientation measurement system is necessary. As mentioned earlier, this is difficult to achieve, but not impossible. However, there are many applications where the absolute position of the robot's endpoint is not required. Instead, its position relative to a work-piece, while interacting with it, is of primary importance. Since during this phase the robot is confined to a small area of the work-space, accurate position measurement is more easily achieved.

Since there are twice as many actuators in a macro/micro manipulator than in a conventional robot, cost is increased. Some of this additional cost, however, can be absorbed by reducing the cost of the large robot because it no longer requires as accurate actuators and encoders.

Finally, it would seem that doubling the number of actuators would increase the complexity of controlling the system. However, as will be seen in later chapters, the additional actuators actually improve stability and greatly reduce the control problem.

2.4.3 History

The idea of placing a high resolution actuator near the endpoint of a tool is quite old. It has been commonly used in hard automation. These are generally open loop devices, however. The purpose of the additional actuator was to improve static accuracy, or cycle time. Since hard automation usually consists of heavy machinery, redundant actuators are often employed to reduce the inertial burden. This results in a lower cycle time since a higher acceleration can be achieved.

The concept of a macro/micro manipulator as a general means of improving a robot's controlled dynamic performance, however, was first demonstrated at MIT in 1983 (see Author's S.M. Thesis[8]). A five degree-of-freedom hydraulic micro-manipulator that could accelerate a 50 lb. mass at 45G's was designed and fabricated. A preliminary system analysis was performed, and the results were verified experimentally.

At this point, a distinction should be made between the proposed macro/micro manipulator system and work done by others involving the placement of a small end-effector on the tip of a robot. In the last few years, several researchers concluded that a fast end-effector at the end of a robot could be advantageous in some applications. However, in most of the work presented in the literature, the end-effector is added on to the robot for a specific purpose.

Hollis[9] developed a fine positioning device that could move a 100 gram load at resolution of 0.5 microns. This is very useful in electronic component fabrication.

Van Brussel and Simmons,[10] Cutkosky and Wright,[11] Asakawa et al,[12] Kazerooni and Guo,[13] developed active versions of the passive remote center compliance device (RCC) introduced by

Whitney.[14]

Salisbury,[15] and Jacobsen et al[16] developed dextrous hands to be attached to manipulators. These hands are multi-fingered, and provide several additional degrees of freedom for intricate manipulation.

Recently, the term micromanipulator has taken on a new dimension. Mechanical structures, measured in microns, are now fabricated out of Silicon, using chip fabrication techniques.[17]

Most of the work done by others, mentioned above, concerns itself only with the design and control of the end-effector. The work does not address the fact that the end-effector is attached to a robot that has dynamics of its own. Thus, the dynamic coupling between the robot and the end-effector is not considered. Although high performance specifications are cited, they generally refer to the capabilities of the end-effector when attached to ground. These specifications are not indicative of the true system performance unless the mass of the end-effector plus load is much lower than the endpoint inertia of the robot, or the end-effector is operated at a bandwidth lower than the structural resonant frequencies of the robot. Otherwise, the dynamic coupling between the robot and end-effector may lead to instability.[18]

In contrast, the work described in this thesis treats the macro/micro manipulator as a whole system. Dynamic coupling between the macro and micro manipulators is of primary concern, since it is shown to be the most detrimental factor. In fact, the micromanipulator is used as a means of reducing the effect of the the undesirable dynamics of the robot. The system is analyzed as a whole, and robust controllers that reduce the effect of the dynamic coupling are proposed.

Similarly, true system performance is evaluated and not just that of an isolated micromanipulator.

Since the introduction of the macro/micro manipulator concept in the author's S.M. thesis, the only other work, known to the author, that treats the system as a whole, is that of Cannon's group - more specifically Chiang,[19] and Tilley and Cannon.[20] Their approach, however, is quite different as will be pointed out in later chapters.

Finally, the concept of a macro/micro manipulator, as described in this thesis, is proposed as general means of improving a robot's performance, not specific to one application. A robot is a general purpose automation device. A macro/micro manipulator is proposed as the next generation robot.

Chapter 3

UNCONSTRAINED MOTION OF A MACRO/MICRO MANIPULATOR

3.1 Effect of a Micromanipulator on System Stability

Since the micromanipulator is carried by a robot that exhibits a dynamic behavior of its own, the entire system must be analyzed as a whole. In order to determine the effect of the micromanipulator on the stability of the overall system, a simple model is introduced (see Figure 3.1).

The system shown in Figure 3.1a represents a flexible, one degree of freedom robot structure. This structure is actuated at the base, as are most commercially available robots. The actuator force is denoted by f, while the joint dynamics are lumped into B_1 and M_1. The structural dynamics of this system or link are lumped into B_2, K, and M_2. However, since the system is taken to be very flexible, the endpoint position (X_2) must be measured and controlled, rather than having its position derived from the base motion. This system will hence forward be referred to as "System A".

In Figure 3.1b, a similar model is used to represent a one degree of freedom macro/micro manipulator. The structural dynamics of the macromanipulator are lumped into B_1, K, and M_1. The micromanipulator is denoted by f along with some corresponding damping and inertia; B_2 and M_2. Again, the endpoint position (X_2) is measured and is to be controlled. This system will be referred to as "System B".

Strictly speaking, a one-axis macro/micro manipulator contains two actuators, and is more accurately modeled as shown in Figure 3.2. However, if the position of M_1 is

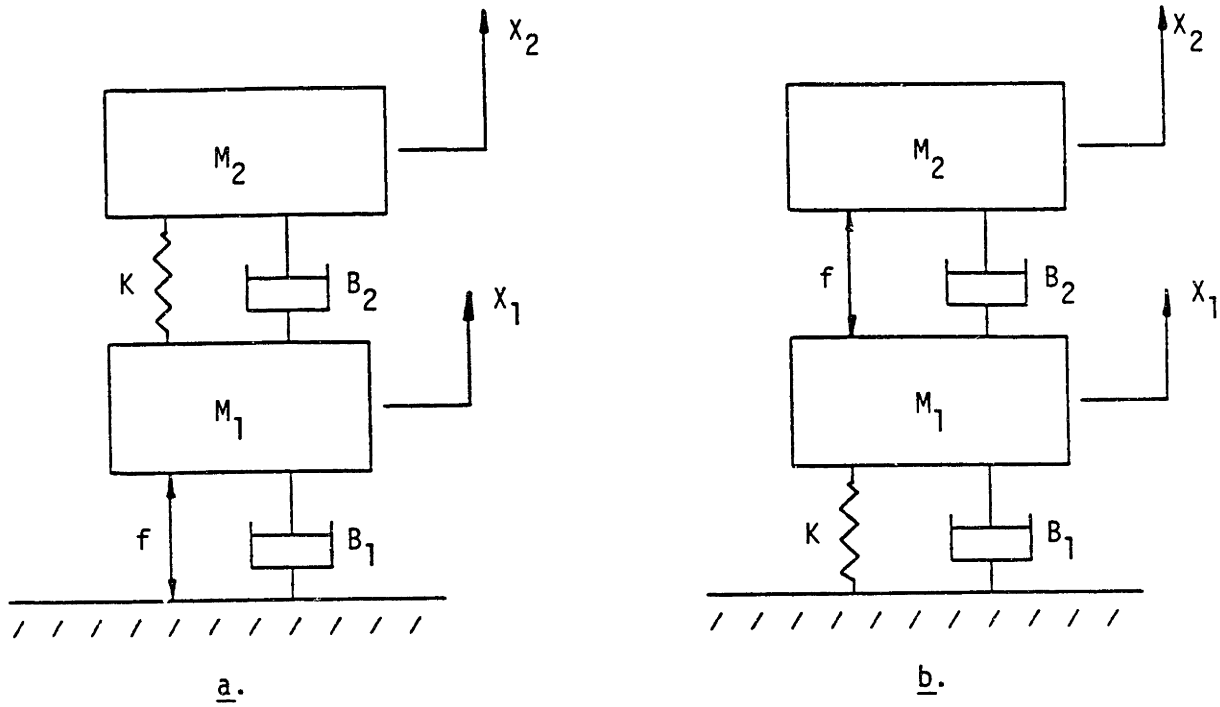

Figure 3.1: a. Model of a One-Axis Flexible Robot Structure.
b. Model of a One-Axis Macro/Micro Manipulator.

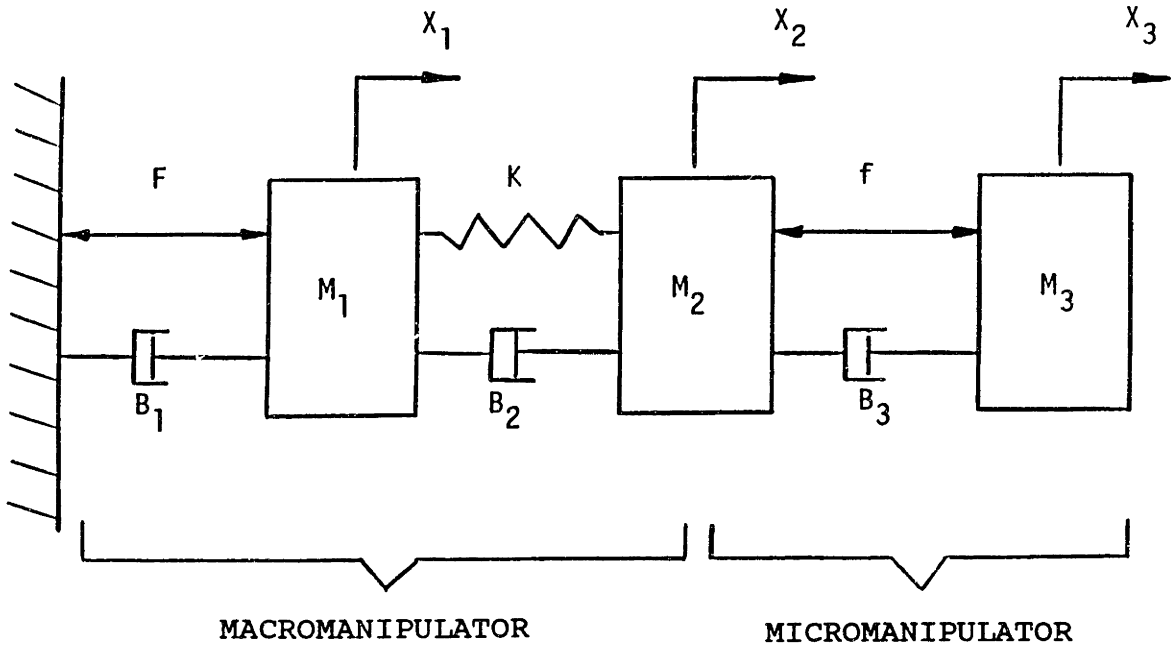

Figure 3.2: Two-Actuator Model of a One-Axis Macro/Micro Manipulator.

regulated about zero with an infinitely stiff feedback loop, the system in Figure 3.2 collapses to that of Figure 3.1b. As will be seen in the next chapter, this is actually the worst case scenario.

Bond graphs are used to analyze the two systems.

System A

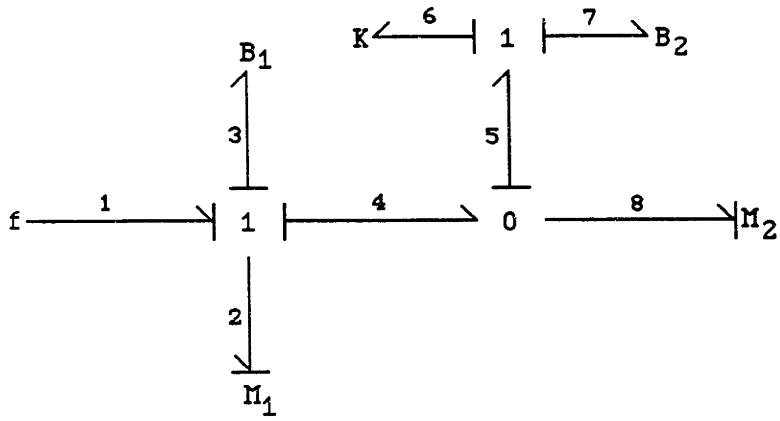

State Variables: V_{M1}, V_{M2}, F_K

$$\dot{V}_{M1} = (1/M_1)F_2 \tag{3.1}$$

$$F_2 = f - F_3 - F_4 \tag{3.2}$$

$$F_3 = B_1 V_{M1} \tag{3.3}$$

$$F_4 = F_K + F_7 \tag{3.4}$$

$$F_7 = B_2 V_7 \tag{3.5}$$

$$V_7 = V_5 = V_{M1} - V_{M2} \tag{3.6}$$

so:

$$\dot{V}_{M1} = (1/M_1)[f - B_1 V_{M1} - F_K - B_2 (V_{M1} - V_{M2})] \tag{3.7}$$

$$\dot{V}_{M2} = (1/M_2)F_8 \tag{3.8}$$

$$F_8 = F_4 \tag{3.9}$$

so:

$$\dot{V}_{M2} = (1/M_2)[F_K + B_2(V_{M1} - V_{M2})] \tag{3.10}$$

$$\dot{F}_K = KV_6 \tag{3.11}$$

so:

$$\dot{F}_K = K[V_{M1} - V_{M2}] \tag{3.12}$$

Putting above equations in the form:

$$\dot{\underline{X}} = A\underline{X} + B\underline{U} \tag{3.13}$$

$$\frac{d}{dt}\begin{bmatrix} V_{M1} \\ F_K \\ V_{M2} \end{bmatrix} = \begin{bmatrix} -\frac{B_1+B_2}{M_1} & -\frac{1}{M_1} & \frac{B_2}{M_1} \\ K & 0 & -K \\ \frac{B_2}{M_2} & \frac{1}{M_2} & -\frac{B_2}{M_2} \end{bmatrix} \begin{bmatrix} V_{M1} \\ F_K \\ V_{M2} \end{bmatrix} + \begin{bmatrix} \frac{1}{M_1} \\ 0 \\ 0 \end{bmatrix} \begin{bmatrix} f \end{bmatrix} \tag{3.14}$$

If the output of the system is taken to be:

$$Y = [0\ 0\ 1] \begin{bmatrix} V_{M1} \\ F_K \\ V_{M2} \end{bmatrix} \tag{3.15}$$

then $G(S) = C[SI-A]^{-1}B$ (3.16)

where

$$C = [0\ 0\ 1] \tag{3.17}$$

If X_{M2} is an augmented state such that

$V_{M2} = d/dt(X_{M2})$ (3.18)

then:

$$\frac{X_{M2}}{f} = G(S) = \frac{K}{S[M_1 M_2 S^3 + (B_1 M_2 + B_2 M_2 + B_2 M_1) S^2 + (B_1 B_2 + KM_1 + KM_2) S + B_1 K]} \tag{3.19}$$

System B

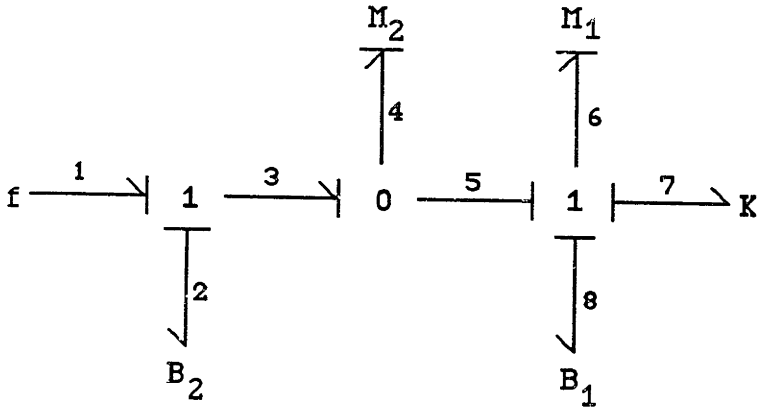

State Variables: F_K, V_{M1}, V_{M2}

$$\dot{F}_K = KV_{M1} \tag{3.20}$$

$$\dot{V}_{M2} = (1/M_2) F_4 \tag{3.21}$$

$$F_4 = f - F_2 \tag{3.22}$$

$$F_2 = B_2 [V_{M2} - V_{M1}] \tag{3.23}$$

so:

$$\dot{V}_{M2} = (1/M_2) [f - B_2 V_{M2} + B_2 V_{M1}] \tag{3.24}$$

$$\dot{V}_{M1} = (1/M_1) F_6 \tag{3.25}$$

$$F_6 = -F_4 - F_K - B_1 V_{M1} \tag{3.26}$$

so:

$$\dot{V}_{M1} = (1/M_1) [B_2 V_{M2} - B_2 V_{M1} - F_K - B_1 V_{M1} - f] \tag{3.28}$$

In matrix form:

$$\frac{d}{dt}\begin{bmatrix} V_{M1} \\ F_K \\ V_{M2} \end{bmatrix} = \begin{bmatrix} -\frac{B_1+B_2}{M_1} & -\frac{1}{M_1} & \frac{B_2}{M_1} \\ K & 0 & 0 \\ \frac{B_2}{M_2} & 0 & -\frac{B_2}{M_2} \end{bmatrix} \begin{bmatrix} V_{M1} \\ F_K \\ V_{M2} \end{bmatrix} + \begin{bmatrix} -\frac{1}{M_1} \\ 0 \\ \frac{1}{M_2} \end{bmatrix} \begin{bmatrix} f \end{bmatrix} \tag{3.29}$$

The output of the system is:

$$Y = [0\ 0\ 1] \begin{bmatrix} V_{M1} \\ F_K \\ V_{M2} \end{bmatrix} \tag{3.30}$$

If X_{M2} is an augmented state as in equation 3.18, then using equation 3.16 yields:

$$\frac{X_{M2}}{f} = \frac{M_1 S^2 + B_1 S + K}{S[M_1 M_2 S^3 + (B_2 M_1 + B_1 M_2 + B_2 M_2) S^2 + (B_2 B_1 + K M_2) S + B_2 K]} \tag{3.31}$$

It is seen in the transfer function above that the macro/micro manipulator introduces two zeros in the numerator.

Using the following parameter values:

System A	System B
$M_1 = 0.0169$ lb·sec^2/in	$M_1 = 0.0169$ lb·sec^2/in
$M_2 = 0.005$ lb·sec^2/in	$M_2 = 0.005$ lb·sec^2/in
$B_1 = 0.13$ lb·sec/in	$B_1 = 0.013$ lb·sec/in
$B_2 = 0.013$ lb·sec/in	$B_2 = 0.13$ lb·sec/in
$K = 24.0$ lb/in	$K = 24.0$ lb/in

results in the root locus plots shown in Figure 3.3. The parameter values used here are representative of the macro/

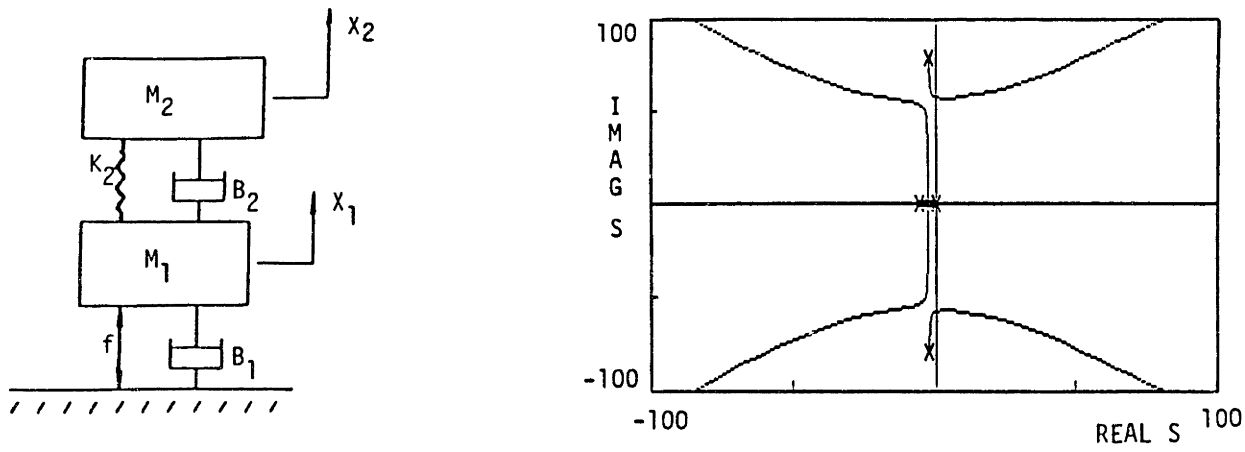

a.

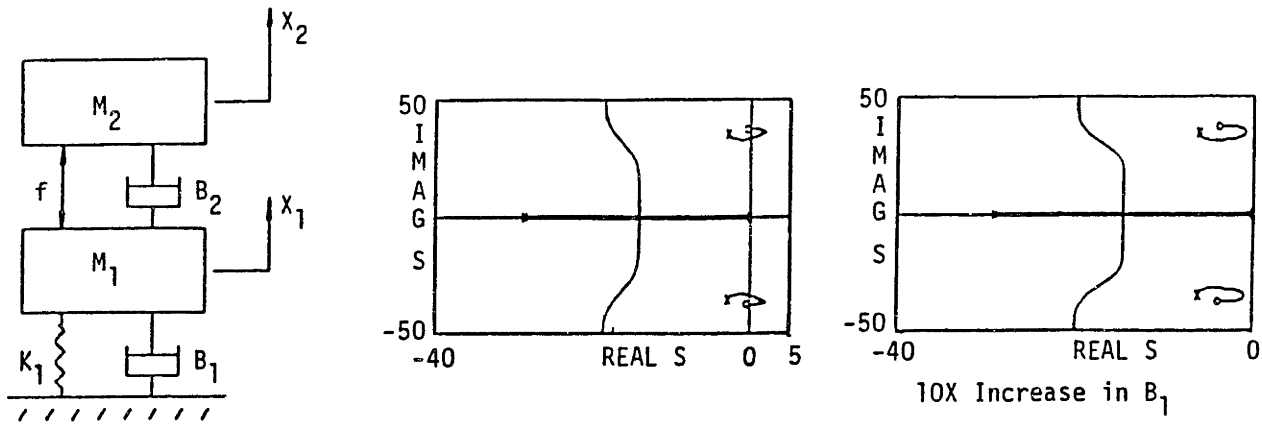

b.

Figure 3.3: a. Root Locus ($f=-KX_2$) of Flexible Robot Structure.
b. Root Locus ($f=-KX_2$) of Macro/Micro Manipulator.

micro manipulator system described in the author's Master of Science thesis.[8]

It is seen in the root locus of system A that instability results very quickly as the gain increases to the point corresponding to the structural resonance of the system. Since there are four poles and no zeros in the system, the poles will head towards forty-five degree asymptotes, resulting in two unstable poles. This is a reasonable result since the actuator force is transmitted through a dynamic system to the point of measurement. Achieving stability in such a system is very difficult and there is a physical limitation on the achievable bandwidth due to the time required for a wave to travel the length of the flexible structure.[6]

The root locus of system B, on the other hand, shows that while the complex poles associated with the macromanipulator become unstable en route to the zeros, the system is inherently stable at high frequencies. Since there are two additional zeros in this system, yet still the same number of poles, the resulting asymptotes are at +90 and -90 degrees.

The Bode plot of Figure 3.4 confirms that the system is stable at frequencies below as well as above the resonance frequency caused by the structural dynamics of the macromanipulator. It is only at frequencies close to the structural resonance of the macromanipulator that the system goes unstable. Furthermore, if the structural damping of the macromanipulator (B_1) is increased by a factor of 10, the imaginary pole-zero combination moves to the left, such that the poles no longer cross into the right-half plane as they approach the zeros. Hence, the system remains stable at all frequencies (see Figure 3.3b). If the structural damping (B_2)

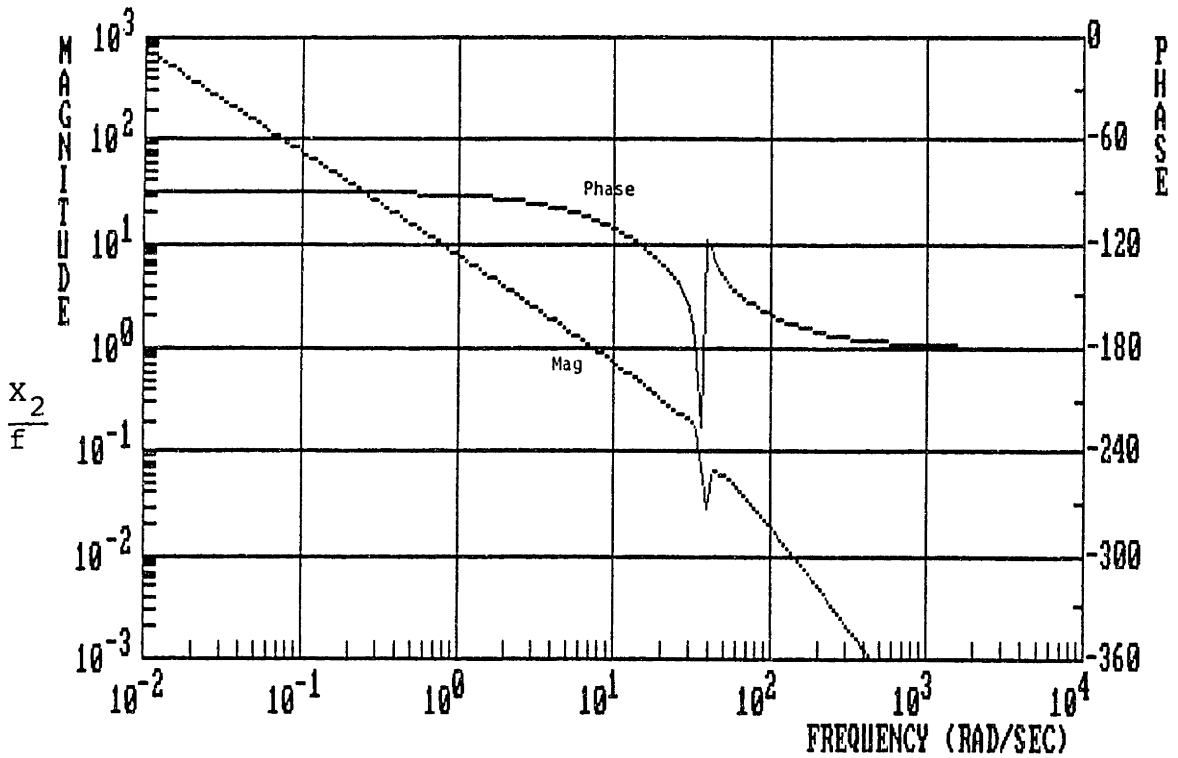

Figure 3.4: Open Loop Bode Plot of Macro/Micro Manipulator.

in System A is increased by a factor of 10, the system continues to be unstable at high frequencies, as is seen in Figure 3.5.

While System B may seem to be a case of collocated control and measurement, it in fact is not. The position of M_2 is measured with respect to ground, while the actuator force does not originate from ground. It is applied between M_1 and M_2. Thus, to achieve collocated control and measurement, $(X_2 - X_1)$ must be measured and fed back, rather than only X_2.

The state equations derived for system B are valid for this case as well. The output, however, must represent the difference in position between the two masses. The resulting transfer function between $(X_2 - X_1)$ and f becomes:

$$\frac{(X_2 - X_1)}{f} = \frac{(M_1 + M_2)S^2 + B_1 S + K}{S[M_1 M_2 S^3 + (B_2 M_2 + B_1 M_2 + B_2 M_2)S^2 + (B_2 B_1 + KM_2)S + B_2 K]} \quad (3.32)$$

While the denominator remains the same as before, the numerator is slightly different. Namely, M_2 appears in the numerator. This reduces the natural frequency of the zeros such that they are just below the imaginary poles. This induces the poles to approach the zeros in a counter clockwise fashion, without crossing into the right half plane. Hence, stability is preserved at all frequencies (see Figure 3.6), as expected with collocated control and measurement.[7] However, since the position of M_2 with respect to ground is of interest, robustness is increased at the expense of accuracy.

Although System B, representing a simple macro/micro manipulator, is not always stable, it is inherently more stable than a conventional robot (System A) when endpoint position feedback is required. It is seen that a macro/micro

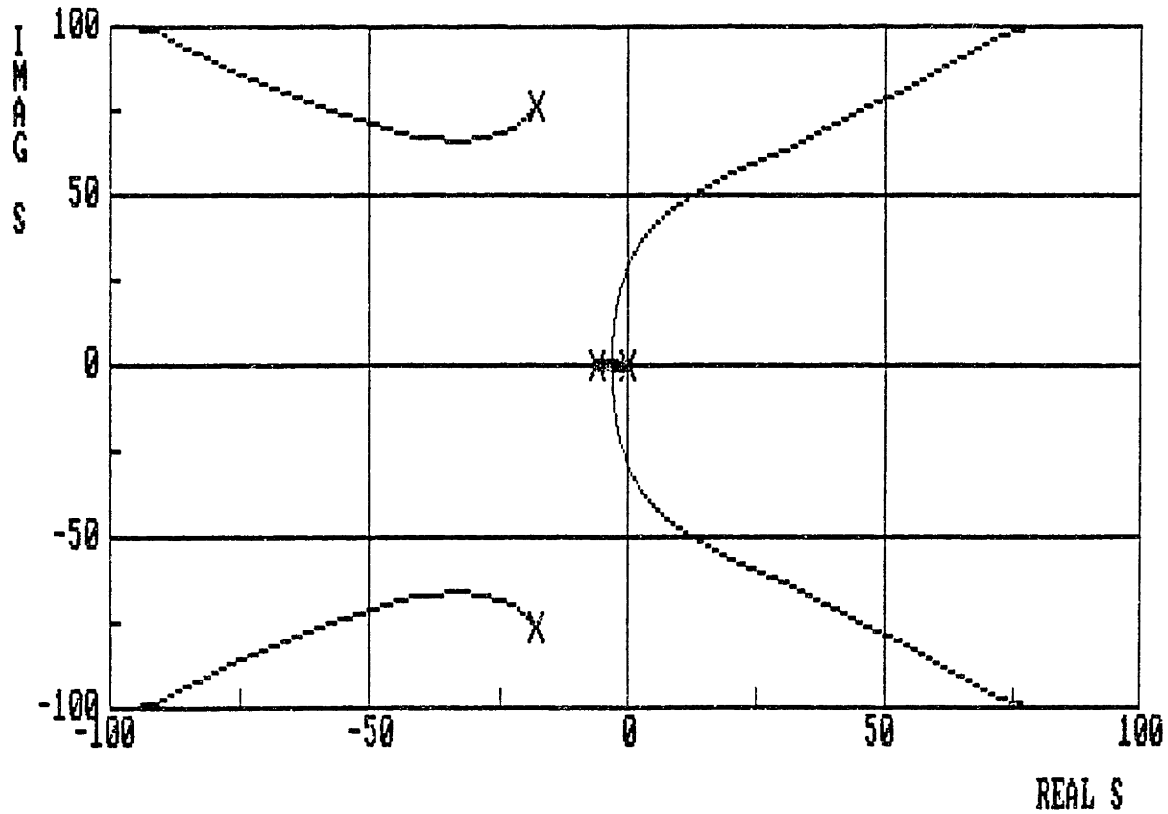

Figure 3.5: Root Locus ($f=-KX_2$) of Flexible Robot Structure With a 10X Increase in Structural Damping.

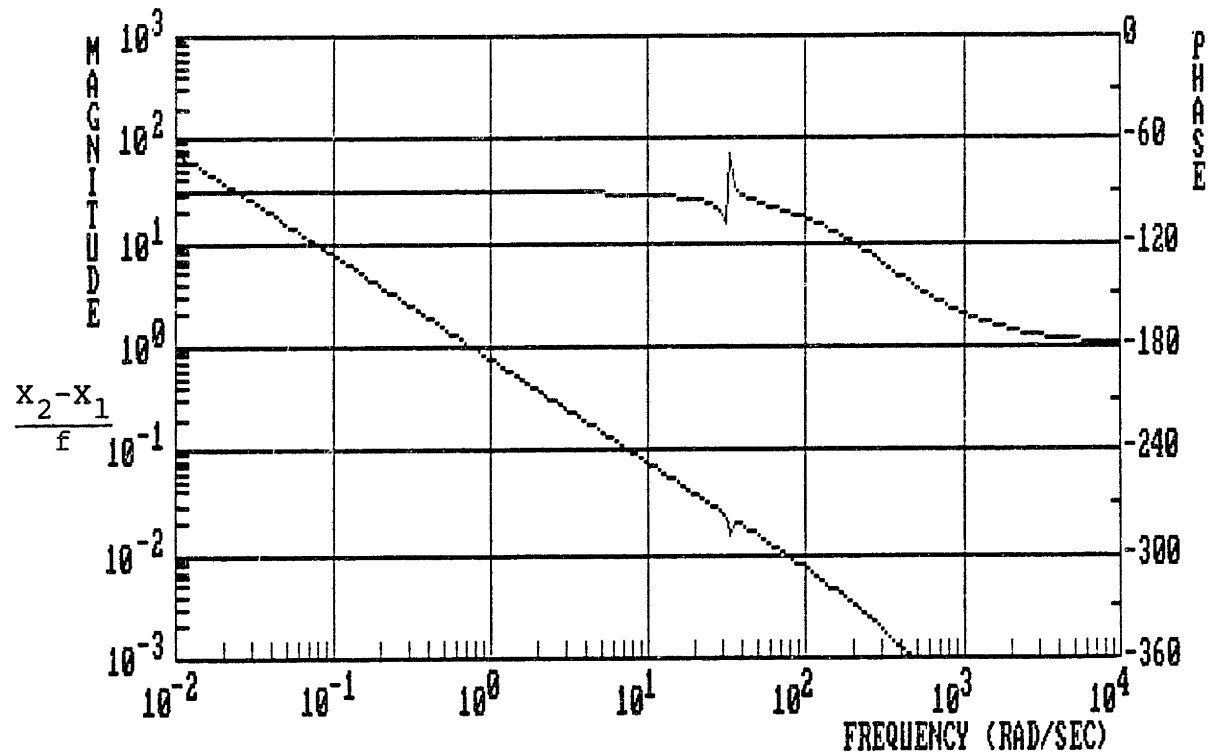

Figure 3.6: Open Loop Bode Plot of Macro/Micro Manipulator With Collocated Control and Measurement.

manipulator is stable at all frequencies, except in the neighborhood of the structural resonant frequencies of the macromanipulator. If the structural damping of the macromanipulator is high, then the macro/micro manipulator maintains stability over all frequencies. Similarly, as was pointed out in the author's Master of Science thesis,[8] if the effective endpoint inertia of the macromanipulator is much greater than the inertia of the micromanipulator and load, then the system remains stable over all frequencies. Of course real systems exhibit unmodeled higher order dynamics and are not stable at arbitrarily high frequencies.

3.2 High Bandwidth Endpoint Position Control

The inherent stability of a macro/micro manipulator at high frequencies does not necessarily guarantee good performance. Examining the Bode plot of Figure 3.4, it is seen that the phase margin at high frequencies is very low. This would result in stable but very oscillatory behavior at high bandwidths. Thus, a controller must be devised that will stabilize the system at frequencies in the neighborhood of the structural resonance of the macromanipulator, as well as provide a higher phase margin for improved performance.

One way of stabilizing the system is by attempting to cancel out the undesirable structural dynamics of the macromanipulator. The performance of such a controller, however, is highly dependent on a precise model of the system. While this may work in theory or even in tightly monitored laboratory situations, it is extremely difficult to achieve in real systems.[6,8] It is thus beneficial to develop a controller

that is not model-sensitive, and requires only minimal knowledge of the system dynamics.

A more robust way of stabilizing the macro/micro manipulator is by increasing the structural damping (B_1) of the macromanipulator, as was pointed out in Figure 3.3b. However, increasing structural damping is physically difficult to achieve, although not impossible.[21]

A realizable and robust approach to stabilizing the system is through endpoint velocity feedback. If the control law prescribed to the micromanipulator is of the form:

$$f = -G_1 X_2 - G_2 \dot{X}_2 ,$$

then as long as G_2 is taken to be large enough, the system becomes stable over the entire frequency range, as is shown in the Bode plot of Figure 3.7 where G_2 was taken to be 4. Feeding back $\dot{X}_2$ biases the root locus to the left, such that the complex poles no longer cross over to the right half plane on the way to the complex zeros. Thus, the phase in the Bode plot of Figure 3.7 does not dip below the -180 line, illustrating that the system remains stable. It is important to note that feeding back $\dot{X}_2$ is not equivalent to increasing B_2 since $\dot{X}_2$ is the absolute velocity of M_2 with respect to ground, while B_2 is the damping between M_2 and M_1. In fact, increasing B_2 does not stabilize the system as does feedback of $\dot{X}_2$.

Besides stabilizing the system, feedback of $\dot{X}_2$ also raises the phase margin at high frequencies since the robot dynamics are enclosed within the loop. This is illustrated in the well-damped step response of Figure 3.8a. An endpoint position control bandwidth well above the structural resonant

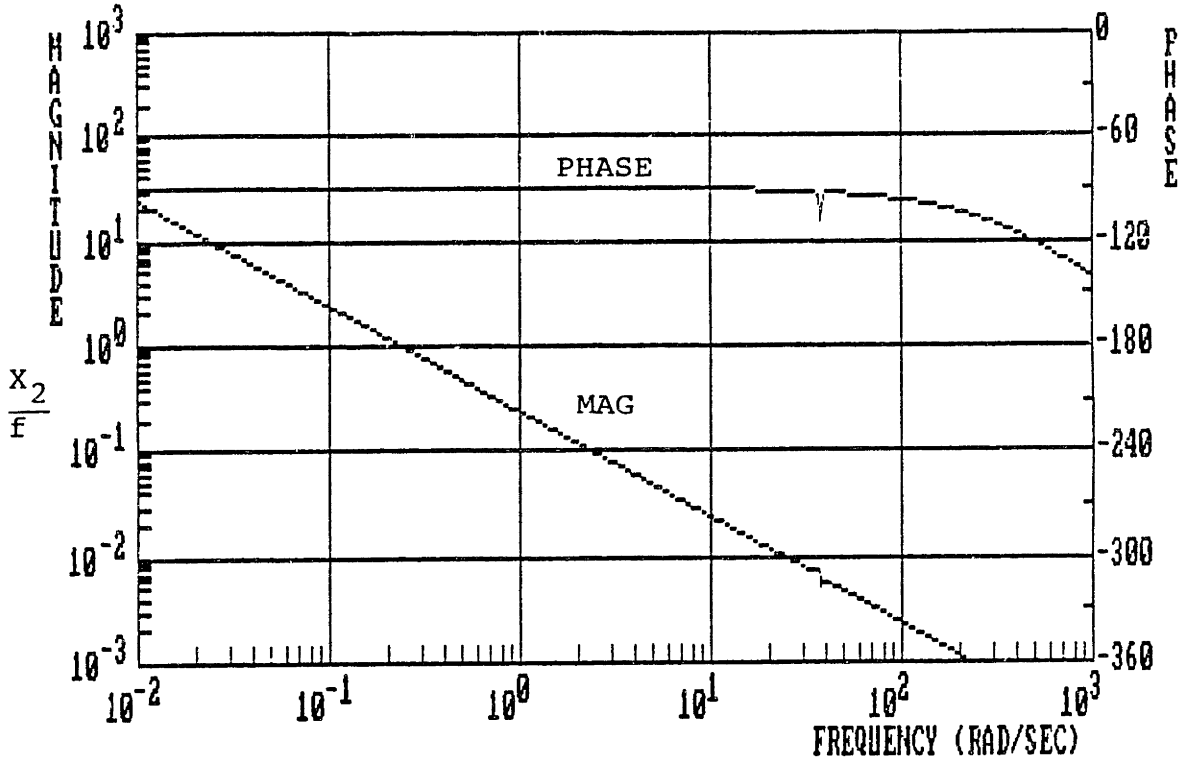

Figure 3.7: Open Loop Bode Plot of Macro/Micro Manipulator in Which Endpoint Velocity Feedback has been Incorporated.

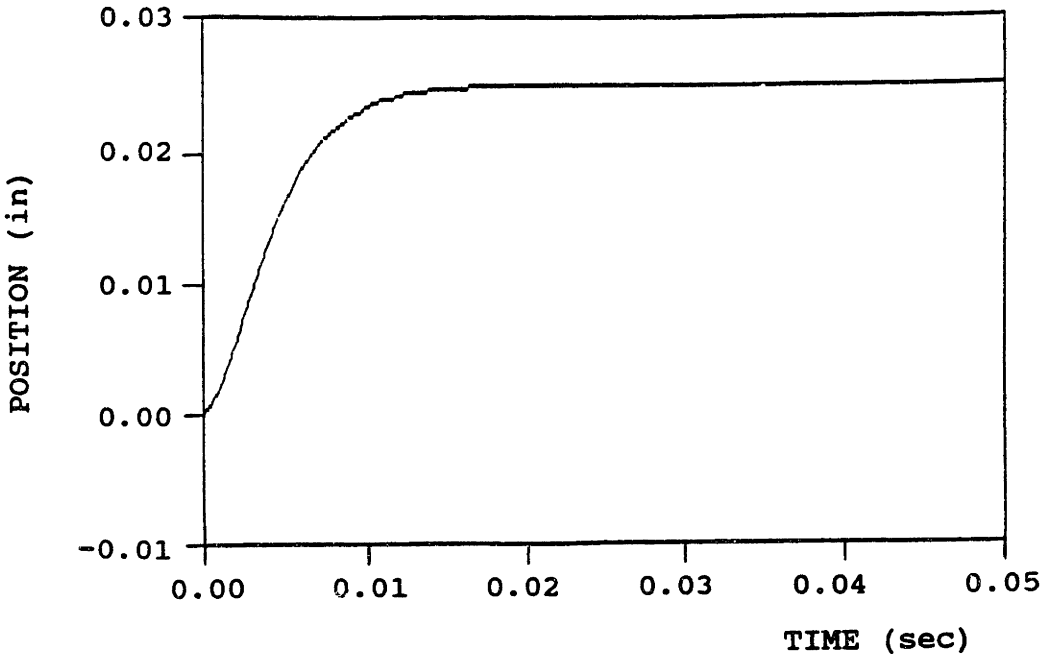

a.

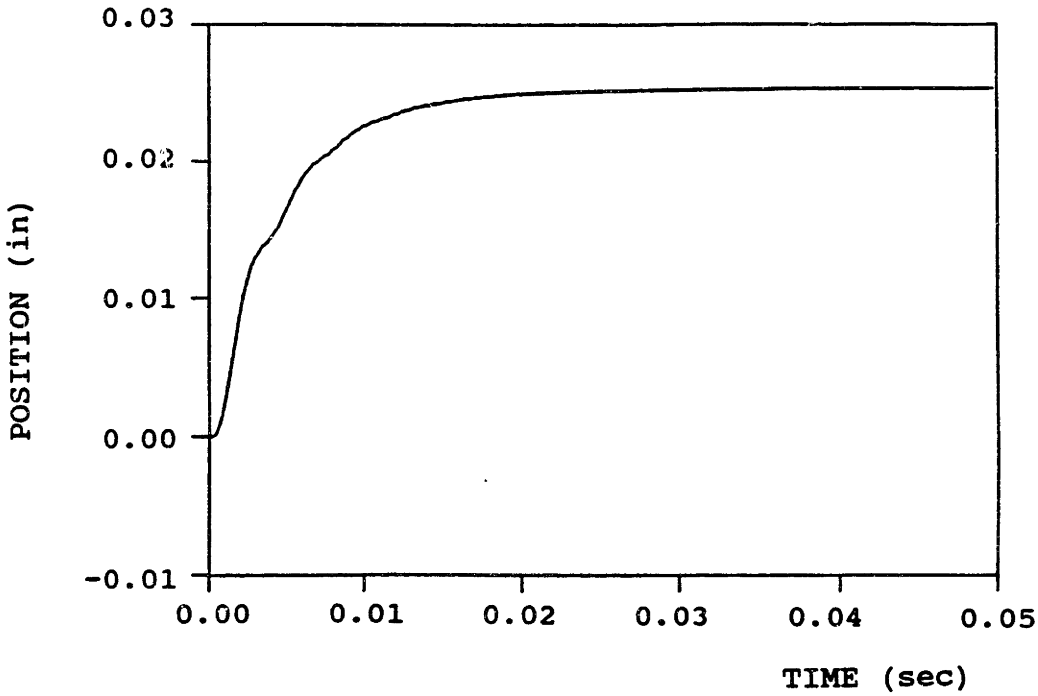

b.

Figure 3.8: a. Response of Macro/Micro Manipulator to a Step Position Input Using Simple Model.
b. Response of Macro/Micro Manipulator to a Step Position Input Using Higher Order Model.

frequency of the macromanipulator can be achieved, as demonstrated in the closed loop Bode plot in Figure 3.9. Furthermore, the proposed controller does not require precise knowledge of the actual system dynamics as does that of Chiang.[19] It is very robust since velocity feedback usually serves as a stabilizing agent.

While the models used in this analysis are admittedly simplistic, they provide a great deal of physical insight. The important system characteristics are clearly brought out. The primary concern in regulating the endpoint position of a macro/micro manipulator is the dynamic coupling between the macro and micro manipulators. More specifically, it is the narrow instability band caused by the structural resonances of the macromanipulator, and the low phase margin at high frequencies. Both of these issues are observed in the Bode plots and root loci obtained from these simple models, and hence are accounted for.

In fact, when the Bode plots and root loci obtained with these models are compared with those obtained from the more detailed model developed specifically for the hydraulic macro/micro manipulator described in reference 8, their validity is confirmed. Furthermore, when the control law proposed above is incorporated in this higher order model that includes servo-valve dynamics and fluid compressibility, the resulting step response is very similar to that obtained with the simple models (see Figure 3.8). The only notable difference is the oscillatory component attributed to the servo-valve dynamics that was included in the higher order model but not in the simple one.

The advantage, on the other hand, of using such simple, yet adequate models, is that a better physical understanding

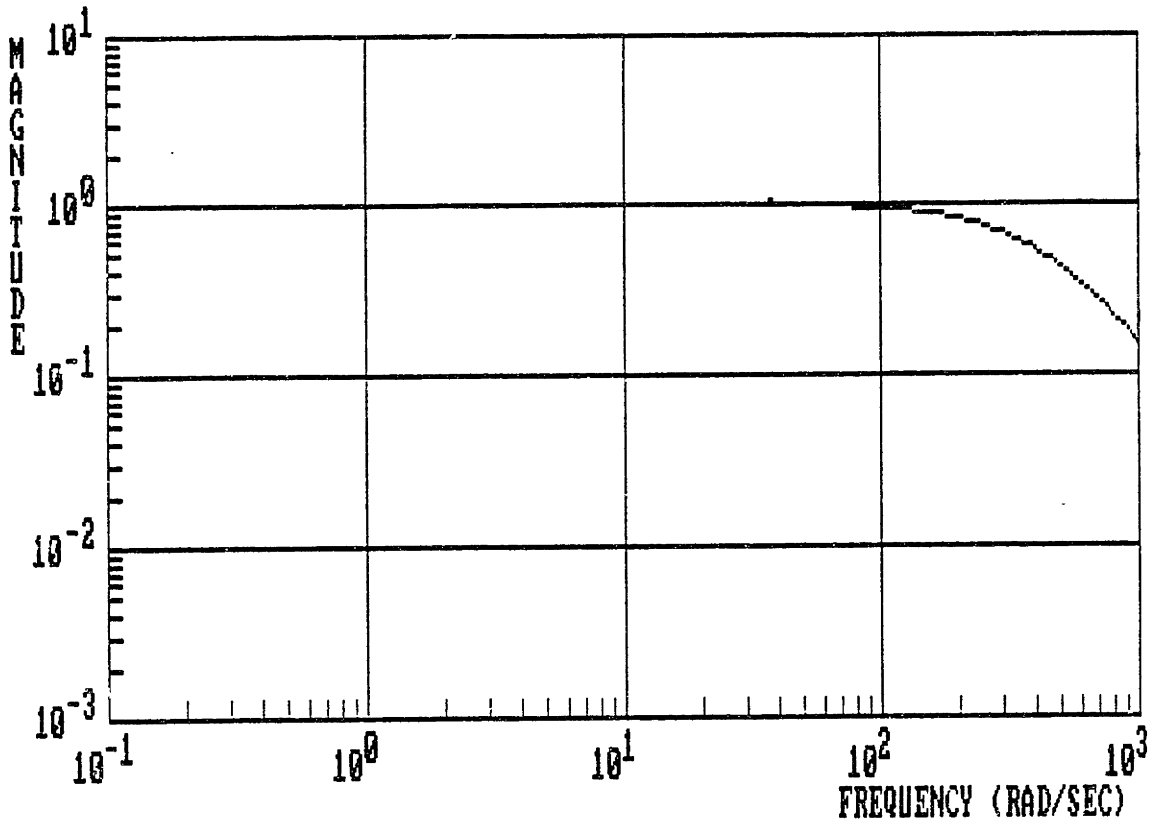

Figure 3.9: Closed Loop Bode Plot of Macro/Micro Manipulator.

of the system is obtained. This provides a better focus on primary problems by not blurring them with secondary details. Having this clear focus led to the proposal of the simple, yet robust controller that was not at all evident when working with the higher order model of the hydraulic macro/micro manipulator.

3.3 Compensation for Settling Time

The time taken by a robot to converge onto its final goal, once that goal is fed to the servo, is governed primarily by its servo settling time. This may have a significant effect on cycle time, especially if there are many short moves that are very common in robotic applications.

Settling time is governed by many factors. These include: inertia, actuator power, control strategy, etc. It is further limited by the structural resonance of the robot, as was pointed out in the previous section.

A micromanipulator attached to the end of a macromanipulator could compensate for this servo settling time by locking in on the target, thus maintaining the endpoint position in the desired location while the macromanipulator is settling. This is demonstrated by simulation in Figure 3.10. A macro/micro manipulator with a structural frequency of 25 Hz, a macromanipulator servo bandwidth of 4 Hz, and an overall endpoint bandwidth of 50 Hz is given a step input of 1 inch. The micromanipulator travel is limited to a maximum of 0.1 inches along each one of its axes. The command given to the micromanipulator is either the final goal (1 inch) when in range, or otherwise, the instantaneous position of the macro-

manipulator plus 0.1 inches. Thus, it is observed in the simulation of Figure 3.10 how the micromanipulator shoots out much faster than the macromanipulator. It soon reaches its travel limit and then attempts to travel at the same rate as the macromanipulator (dashed trace) on which it is attached. When the micromanipulator reaches the final destination, it locks in on it and maintains the endpoint stationary while the macromanipulator is settling. Total response time is cut in half. The response of a stand-alone macromanipulator (without a micromanipulator attached to it) is also included for comparison.

Since the macro/micro manipulator is a type I system (one free integrator) and there is no integral action in the controller, the system cannot track an accelerating input. Since the input to the micromanipulator is the instantaneous position of the macromanipulator plus a constant, and since the macromanipulator accelerates in responding to a step command, the micromanipulator may diverge from the macromanipulator path and may actually fall behind (see Figure 3.11a,b). Nevertheless, as the macromanipulator begins to decelerate, the micromanipulator catches up, overtakes the macromanipulator, and locks in on the final goal. Furthermore, if the move command given to the system is not a step, but rather a ramp, the motion of the macromanipulator and hence the input to the micromanipulator will be a ramp that a type I system can track (see Figure 3.12). Such ramp inputs are actually much more representative of real robot inputs.

If the commanded move is within the travel range of the micromanipulator, the response time is greatly reduced since the micromanipulator motion is not limited by that of the macromanipulator (see Figure 3.13).

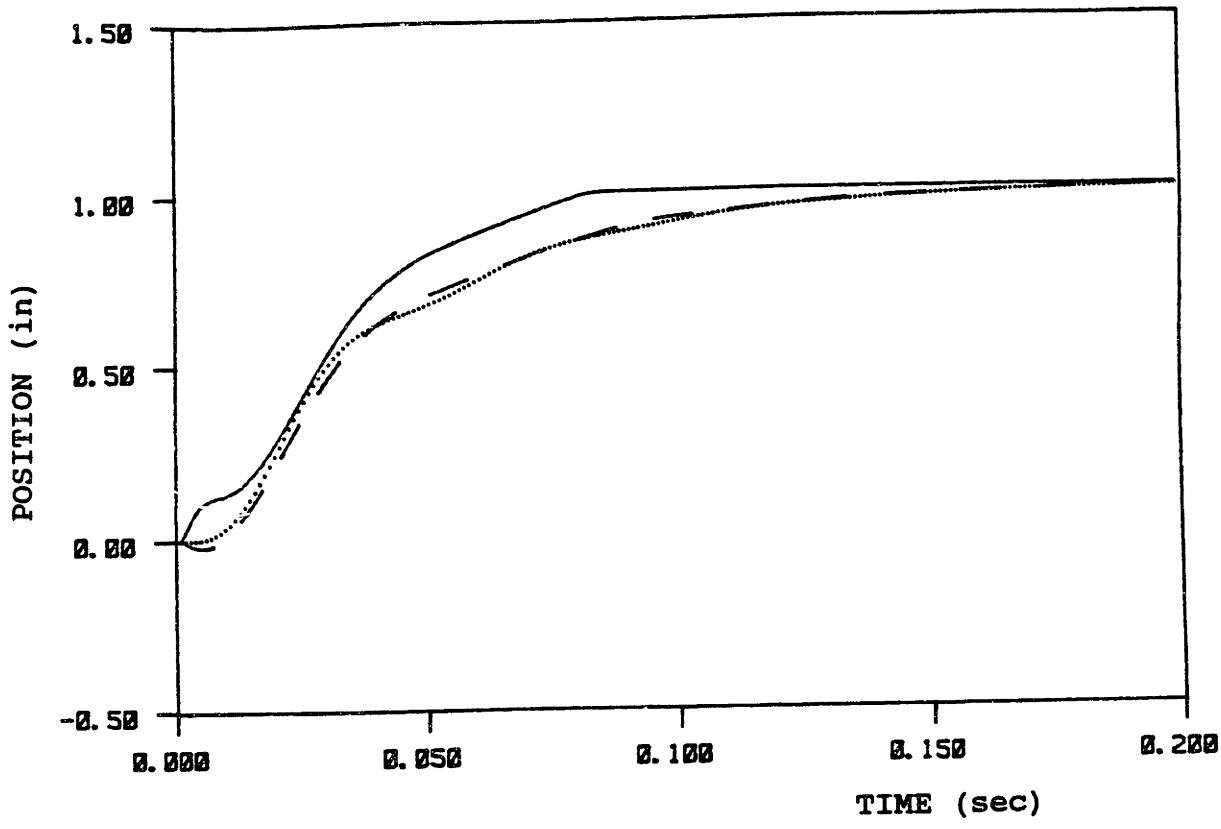

———— Endpoint of Micromanipulator

– – – – – Endpoint of Macromanipulator on which Micromanipulator is Attached

..... Endpoint of Macromanipulator Without Micromanipulator Attached

Figure 3.10: Response to a 1 Inch Step in Position Input.

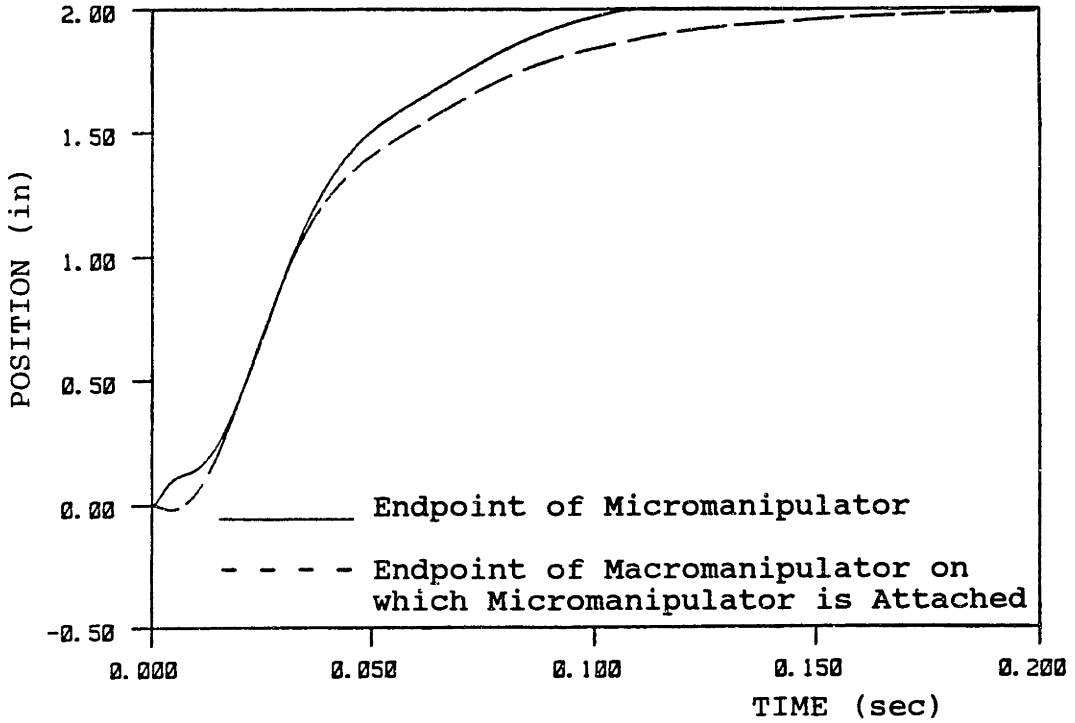

a.

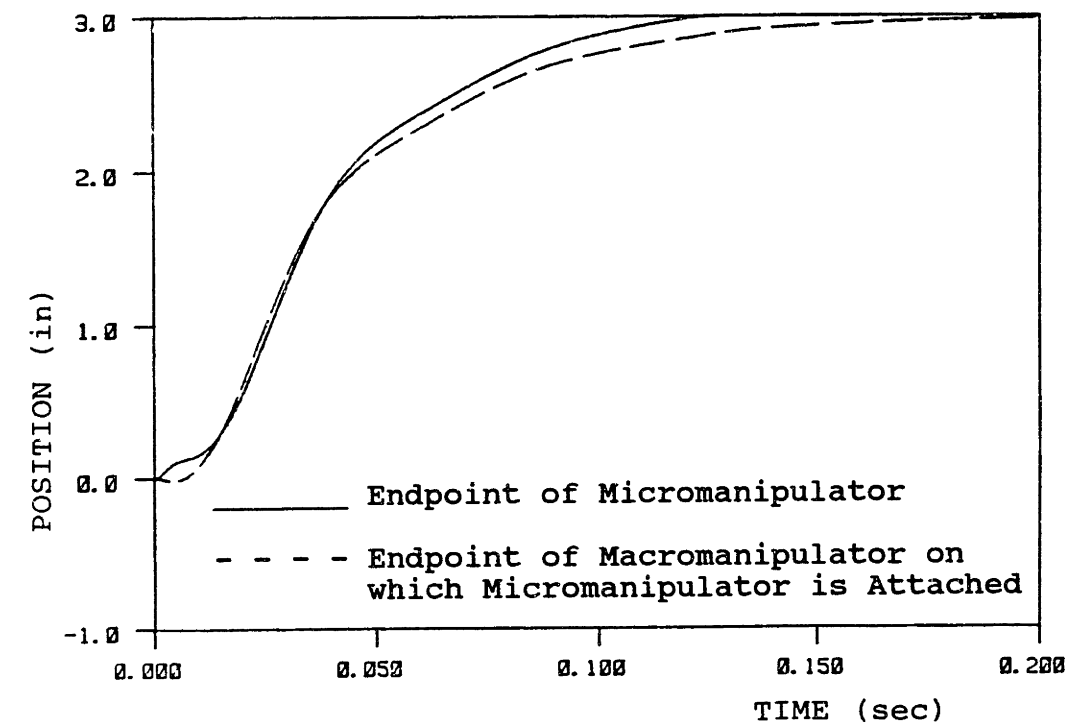

b.

Figure 3.11: a. Response to a 2 Inch Step in Position Input.
b. Response to a 3 Inch Step in Position Input.

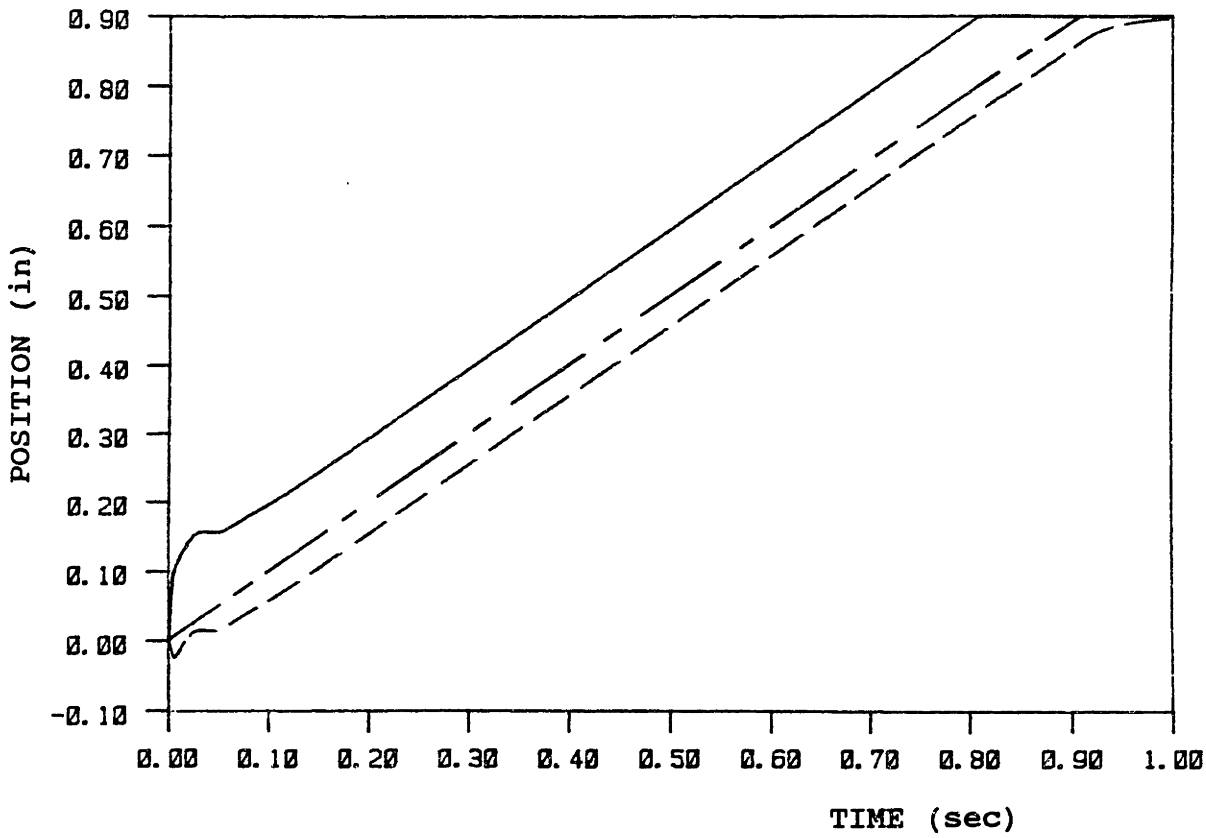

———— Endpoint of Micromanipulator

– – – – – Endpoint of Macromanipulator on which Micromanipulator is Attached

—— – —— Input to Macromanipulator

Figure 3.12: Response to a Ramp Position Input.

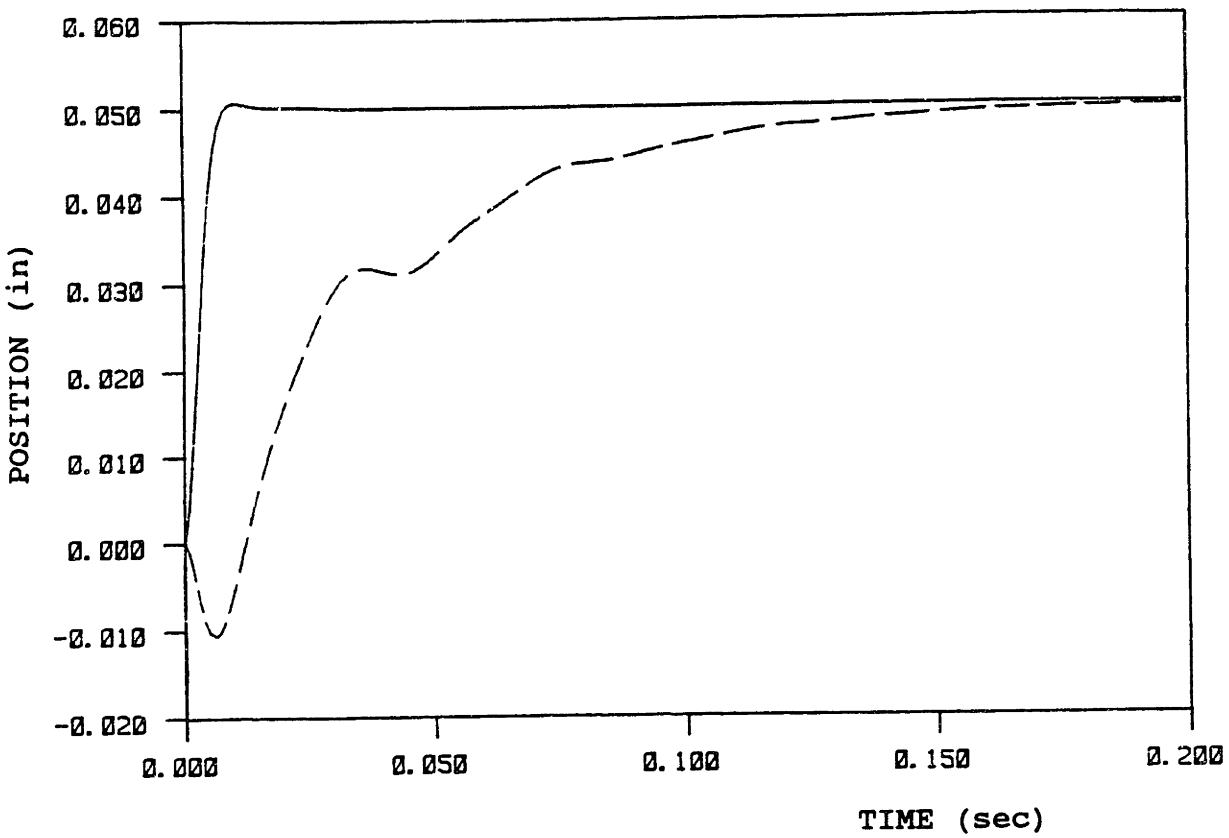

——————— Endpoint of Micromanipulator

– – – – – Endpoint of Macromanipulator on which Micromanipulator is Attached

Figure 3.13: Response of a Step in Position Input that is Within the Travel Range of the Micromanipulator.

3.4 Compensation for Tracking Errors

When a robot is commanded to follow a geometric path at a given velocity profile, each of its joints may have to respond with a different velocity and acceleration in order to maintain the endpoint on the desired trajectory. In fact, one or more of the joints may have to respond with an infinite acceleration to keep the endpoint from deviating from the desired motion. An example of this phenomenon is observed when a robot tries to go around a sharp corner without stopping, thus having to instantaneously stop some of its joints, while instantaneously accelerating others. This is a major problem in applications such as seam welding, seam caulking, spray painting, etc., where quality depends on maintaining a constant velocity.

However, as described previously, a robot servo cannot be made very quick, and certainly not of infinite bandwidth. If, on the other hand, a high bandwidth micromanipulator is mounted on the end of the macromanipulator, it can compensate for these tracking errors. Of course a micromanipulator cannot provide infinite bandwidth either, but it can improve the performance significantly.

In evaluating this claim, a two-axis macro/micro manipulator is analyzed. The reason for the two axes is to enable tracking of an arbitrary path along a given plane, and also to see if the conclusions derived from the one-axis model would apply to more degrees of freedom. In order to focus on the issues relevant to the introduction of the micromanipulator, the kinematics of the system were kept as simple as possible. Thus, translational degrees of freedom were chosen for both the macro and the micro manipulators. However, in order to

introduce coupling between the degrees of freedom, the micromanipulator axes were oriented at a forty-five degree angle from those of the macromanipulator (see Figure 3.14). Each mass is constrained such that it can only translate along one axis. It is thus noted that activation of any of the horizontal actuators would produce motion in the vertical members as well, and vice versa.

The equations of motion are derived (see Appendix A) and a controller is designed independently for each axis using the techniques developed for the single axis case.

In evaluating the tracking performance of such a macro/micro manipulator, the bandwidth of the macromanipulator was kept at about 4 Hz, while a 50 Hz bandwidth was taken for the micromanipulator. This is twice as high as the structural frequency of the macromanipulator which was taken to be at about 25 Hz. Once again, the micromanipulator travel is limited to .1 inch relative to the macro manipulator. The improvement in tracking performance is observed in Figure 3.15, where the system is commanded to track a short linear path in the X-Y plane.

Next, it is investigated how the micromanipulator could improve tracking performance in cases where a high acceleration is necessary to maintain the endpoint from deviating. The macro/micro manipulator is commanded to follow the perimeter of a square at a constant velocity of 1 inch/sec. Maintaining a desired velocity is crucial in applications such as welding, for example. The improvement in tracking with regard to both position and velocity is demonstrated in Figure 3.16. The performance is greatly increased in both respects, but is most evident in the velocity profile.

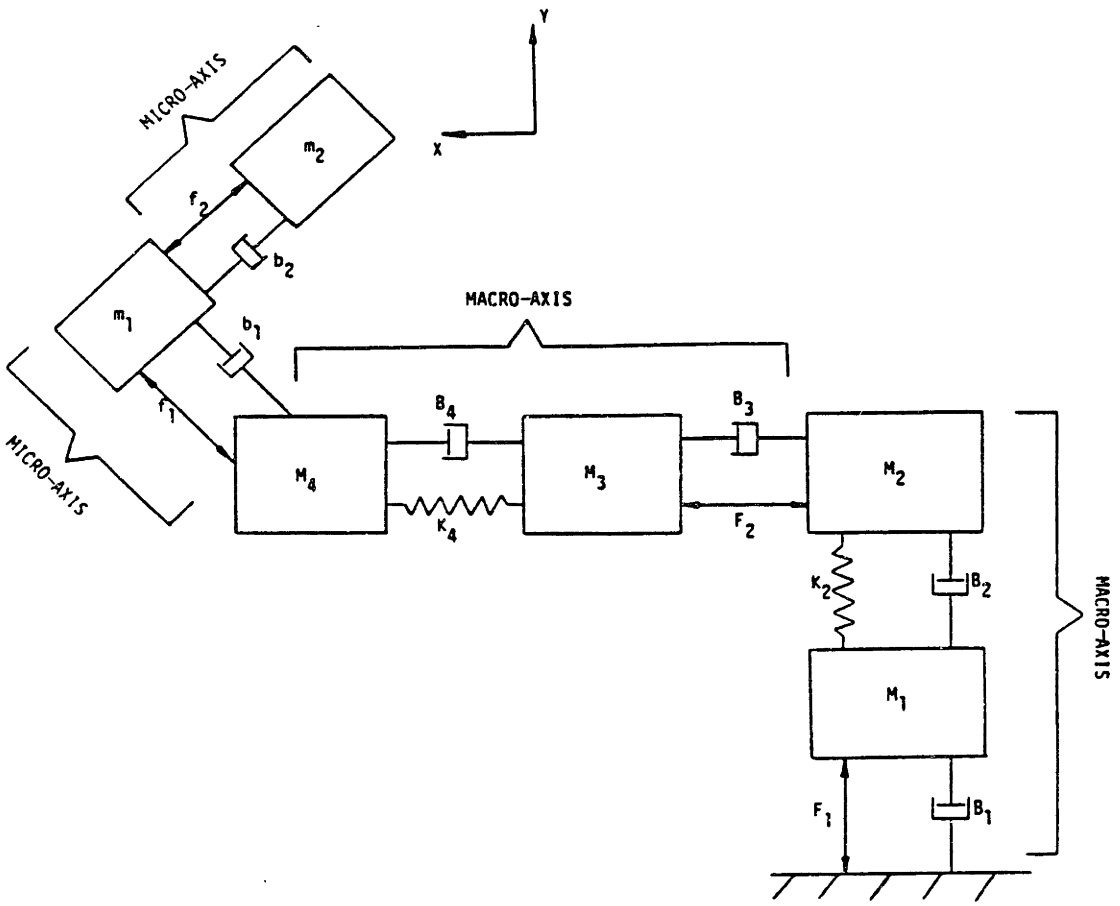

Figure 3.14: Model of a Two-Axis Macro/Micro Manipulator.

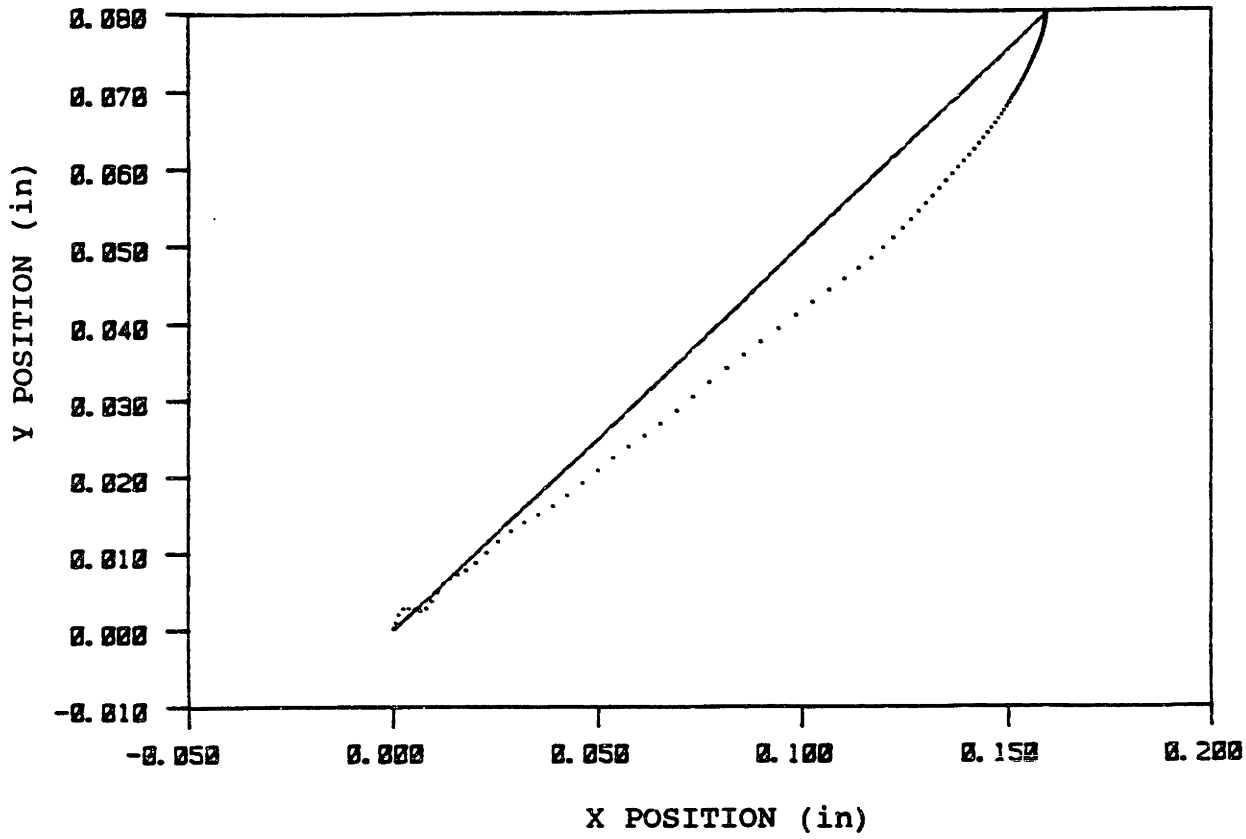

——— Response of Macro/Micro Manipulator

..... Response of Conventional Macromanipulator

Figure 3.15: Comparison Between a Macro/Micro Manipulator and a Conventional Macromanipulator in Tracking a Straight Line in the X-Y Plane.

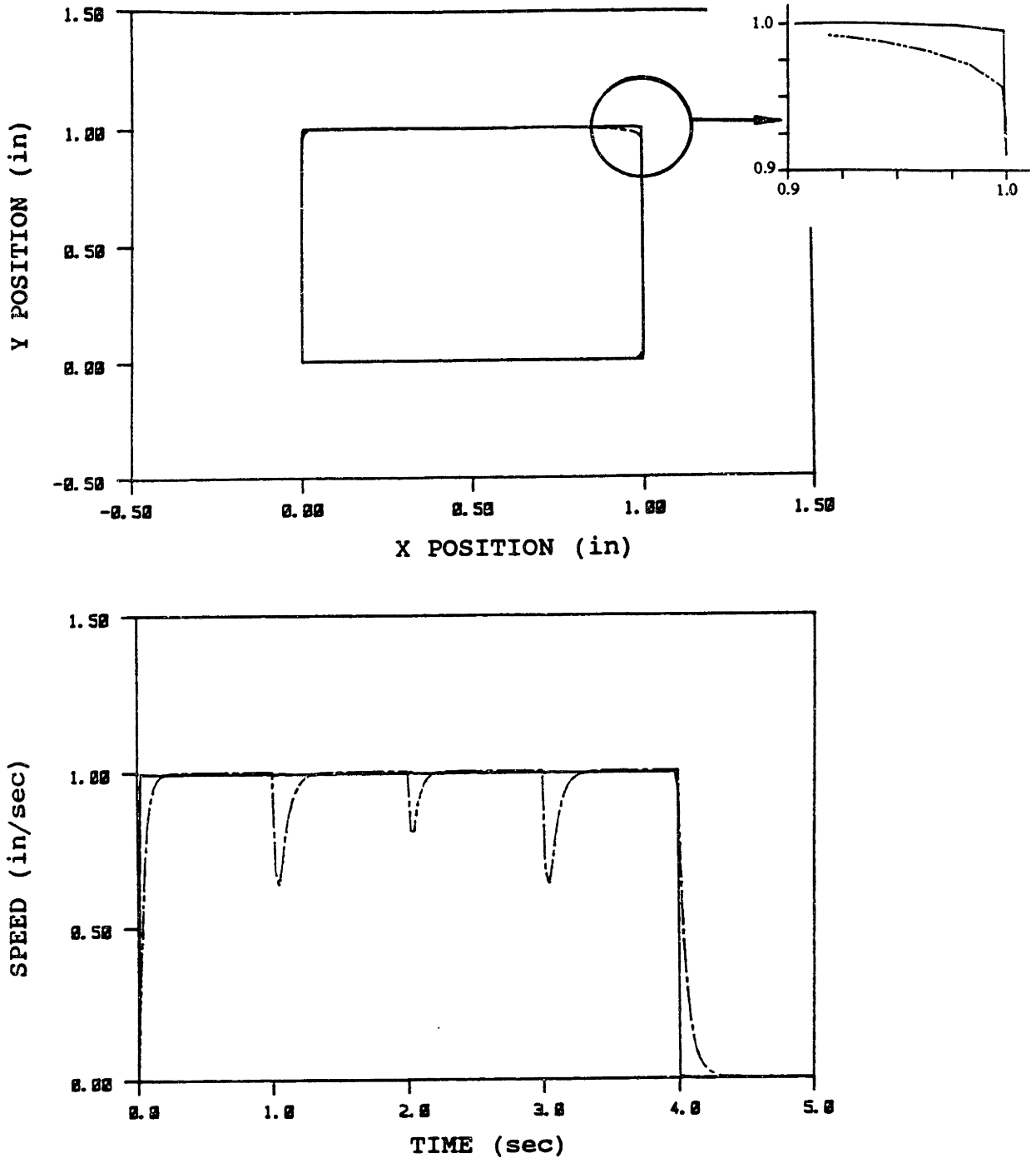

Figure 3.16: Comparison Between a Macro/Micro Manipulator and a Conventional Macromanipulator in Tracking the Perimeter of a Square in the X-Y Plane.

3.5 Chapter Summary

The research presented in this chapter demonstrates the potential advantages of the macro/micro manipulator over conventional manipulators in unconstrained operations. It was shown that a macro/micro manipulator is inherently more stable when endpoint sensing is required. It was also illustrated that the system can easily be controlled above the fundamental structural frequency of the macromanipulator if absolute endpoint velocity is incorporated in the control law.

The macro/micro manipulator was shown to be very advantageous in compensating for tracking errors and settling time of the macromanipulator. This is very important in applications where path control is required. Furthermore, there are cases in tracking a path, where the entire robot must slow down because one of the joints cannot quite keep up. The addition of the micromanipulator would nullify the requirement of all the joints being able to keep up at all times, thus reducing cycle time.

The theory developed with a one axis model was shown to be adequate for more degrees of freedom. The coupling between the macromanipulator's and micromanipulator's respective degrees of freedom (their own) was not detrimental to the performance. Had the micromanipulator's controller been model-sensitive, the addition of more degrees of freedom, each with its own dynamics, might have been detrimental.

Experimental verification of the analytical predictions is presented in Chapter 6.

Chapter 4

THE FORCE CONTROL PROBLEM

4.1 Impedance Control vs. Force Control

Many potential robot applications require the manipulator to be mechanically coupled to other objects during some phase of the operation. If the operation performed during the coupled phase results in either motion with no resisting forces or vice versa along any one axis, then there is no dynamic interaction, along that axis, between the robot and the object it is coupled to. An example of this would be a robot washing a window. There is negligible motion in the normal direction (assuming the glass does not break) while there is negligible resisting force in the tangential direction (assuming low friction). It is thus sufficient to regulate force in the normal direction and position in the tangential direction.[22] Both the position controller and the force controller, therefore, attempt to track a desired input. The higher the bandwidth of the controller, the better its tracking ability.

In general, however, there are cases in which there is a net power transfer between the robot and its environment. These include grinding, drilling, engraving, metal bending, etc. The dynamic interaction is clearly not negligible and force or position control alone no longer suffices. Instead, the dynamic interaction between the robot and the environment must be controlled. Impedance Control has been proposed as a unified approach to this problem.[23]

A general impedance consists of at least a stiffness,

a damping, and an inertia component. Force feedback is a means of modulating the apparent impedance and especially the inertia component.[24] Positive force feedback approximates an increased apparent inertia, while negative force feedback approximates a decreased apparent inertia. A high inertia tends to keep the robot on its planned path regardless of the encountered motion constraints (high dynamic disturbance rejection). A low inertia tends to minimize interface forces by allowing the robot to quickly accept any motion dictated by the environment (low dynamic disturbance rejection). In this perspective, force feedback is incorporated in order to change the apparent dynamics of a system, and not necessarily to track a desired force input.

Thus, whether for modulating impedance purposes, or for interface force regulation, high bandwidth negative force feedback is desirable.

4.2 Problems Encountered in Force Control

For the last fifteen years or so, many researchers attempted to achieve force control of robots. Most experienced great difficulty in just achieving stability let alone good performance. A very common problem was that the robot would begin chattering (losing contact with the environment). Thus, the primary issue became that of stabilizing the system, while performance was neglected. In fact, stability and performance were often confused. Until recently, dynamic performance levels achieved in force control have been no where near those achieved in position control.

The major causes of force control problems are listed below. Immediately following is their description.

I. Instability due to non-collocated actuators and sensor.

II. Initial impact.

III. Low interface damping.

IV. Actuator and/or drive non-linearities.

4.2.1 The Non-collocation Problem

In order to regulate tip forces or modulate the endpoint impedance of a robot, the force sensor used in force feedback would yield the most accurate information when placed at the tip or endpoint of the robot. The actuators, however, are located at the base of the links (see Figure 4.1). This gives rise to a situation of non-collocated actuation and measurement, suggesting the possibility for instability.[7] Interestingly enough, positive force feedback (approximating increased apparent inertia) is inherently stable.[24] Nevertheless, negative force feedback proves to be unstable at high bandwidths because of the interaction between sensor dynamics and structural dynamics of the robot.[24,25,26,27]

Consider the simple model of a one-axis manipulator coupled to a rigid environment through a force transducer (K_t, B_t) as shown in Figure 4.2. This system is actuated at the base as are most conventional robots. The actuator force is denoted by F, while the joint dynamics are lumped into B_1 and M_1. The structural dynamics of the manipulator are lumped into B_2, K_2, and M_2. It is desired to control the interface force F_t (force in spring K_t) in a closed loop fashion ($F=-GF_t$).

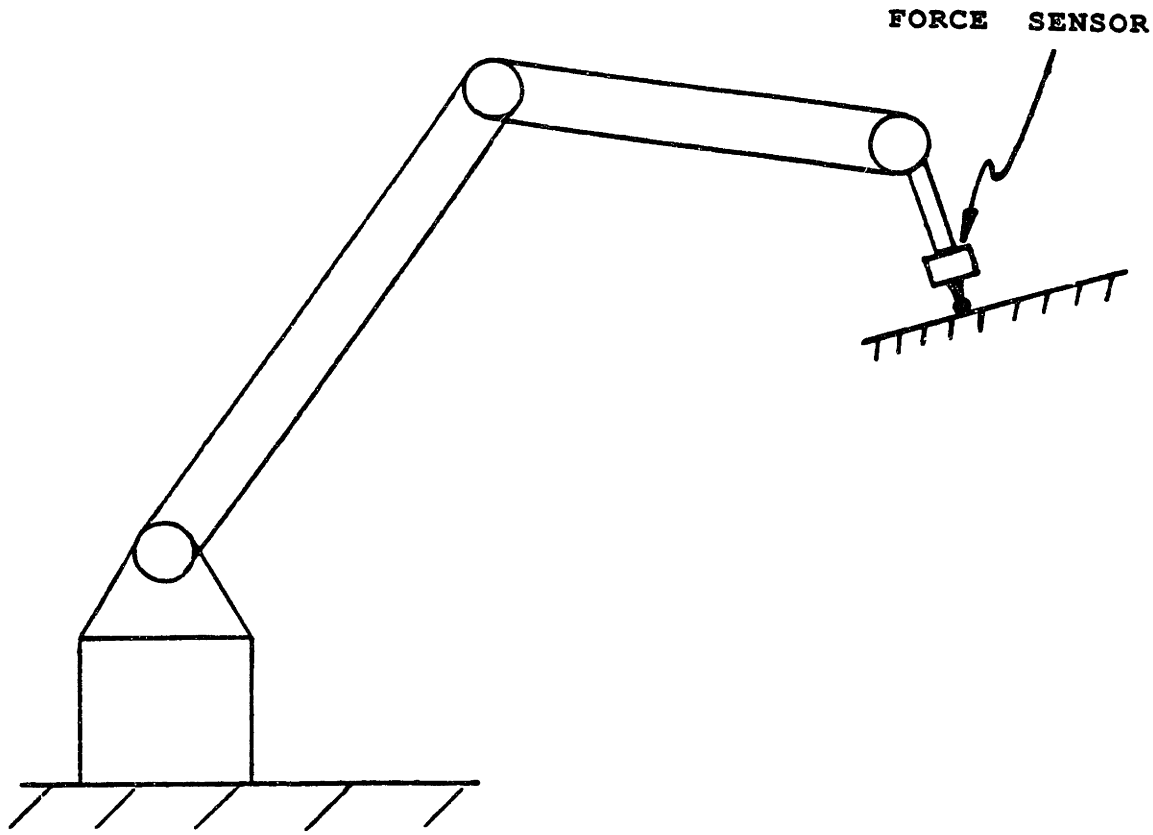

Figure 4.1: Non-collocated Force Control of a Conventional Robot.

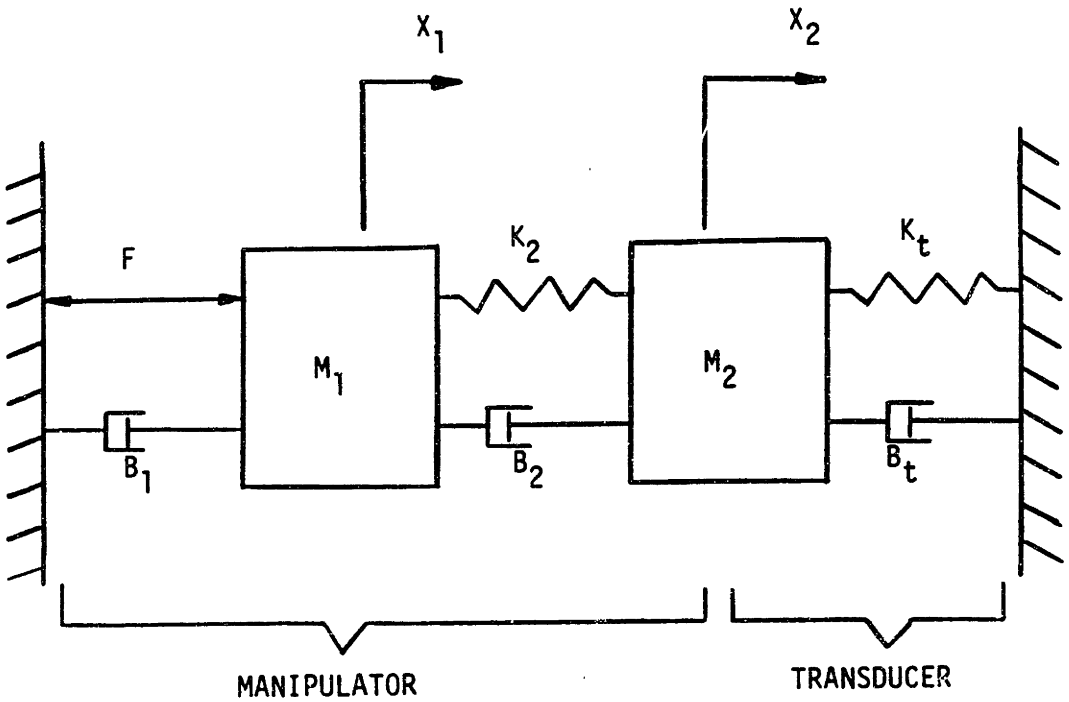

Figure 4.2: Model of a One-Axis Manipulator Coupled to a Rigid Environment.

Deriving the equations of motion of this system (see Appendix B) and using the following parameter values:

$$
\begin{aligned}
M_1 &= 0.0169 \text{ lb}\cdot\text{sec}^2/\text{in} \\
M_2 &= 0.005 \text{ lb}\cdot\text{sec}^2/\text{in} \\
B_1 &= 0.13 \text{ lb}\cdot\text{sec/in} \\
B_2 &= 0.013 \text{ lb}\cdot\text{sec/in} \\
K_2 &= 24 \text{ lb/in} \\
K_t &= 150 \text{ lb/in} \\
B_t &= 0.16 \text{ lb}\cdot\text{sec/in}
\end{aligned}
$$

results in the root locus plot shown in Figure 4.3. The parameter values used here are representative of the system described in reference 8. The transducer parameter values were assumed to be those of a low-quality force transducer.

Examining the root locus in Figure 4.3, it is seen that instability quickly results as the gain is increased. This is caused by the fact that the actuator and force transducer are not collocated, resulting in an interaction between the transducer dynamics and the structural dynamics of the manipulator. This problem can be somewhat alleviated by selecting a transducer significantly softer than the structural stiffness of the manipulator,[25,26] or significantly stiffer.[24] Nevertheless, the system is inherently unstable at high bandwidths.

4.2.2 The Initial Impact Problem

When a robot first comes in contact with the environment, an impact occurs if the normal approach velocity is not zero. It often causes the robot to bounce off the surface one or more times. The force generated by an impact with a rigid environment is experienced too quickly to be controlled by the actuator. In fact, it would probably be best if the controller was disabled until the impact was over. This would avoid

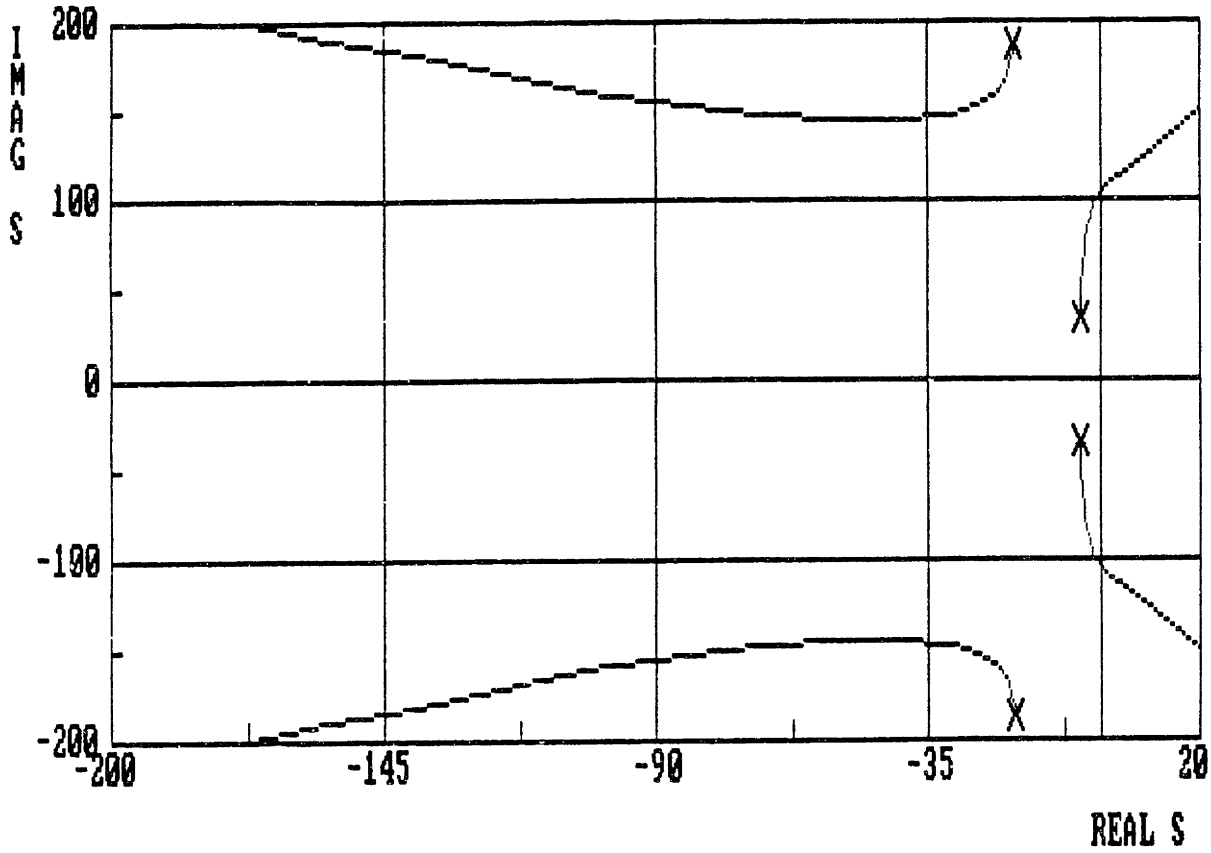

Figure 4.3: Root Locus of Force Control ($F=-KF_t$) on a Conventional Manipulator.

a delayed, counter-productive reaction.

The impact force is a function of the stiffness and damping of the interface between the robot and the environment. It is also a function of the approach velocity and effective endpoint inertia of the robot. If the environment and approach velocity cannot be altered for a given application, the impact force can be reduced by decreasing the endpoint inertia of the robot.

A great deal of physical insight can be gained by examining a very simple example of this phenomenon. Consider a mass (M) being propelled by an actuator (f) into contact with an environment consisting of a spring (K) and damper (B). Note that this is not meant to be an accurate model of a real robot.

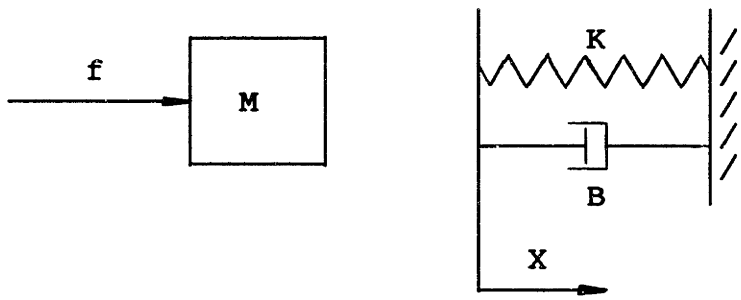

For simulation purposes, the parameters are taken arbitrarily as follows:

$$M = .01 \text{ lb}\cdot\text{sec}^2/\text{in}$$
$$K = 1000 \text{ lb/in}$$
$$B = 1 \text{ lb}\cdot\text{sec/in}$$

The open loop transfer function of the system above, while in contact with the environment, is simply:

$$\frac{F_K}{f} = \frac{K}{MS^2 + BS + K} \qquad (4.1)$$

Hence, the system is always stable, providing more insight into performance issues.

If the mass is out of contact with the environment at time zero, then the effects of impact can be seen. Assume the mass at time zero is at X = -0.1 inches. No force feedback is incorporated (open loop). It is desired to achieve a force (F_K) of 1 pound. Hence, f is set equal to 1. The simulations in Figure 4.4 show both position response (X) of the mass, as well as the achieved force (F_K) for various values of M. As might be expected, reducing the mass results in lower force peaks and less bouncing.

It is also interesting to note that the higher the desired force, the less severe the bouncing problem becomes. In fact, if the desired force is high enough, there will not be any bouncing exhibited (see Figure 4.5).

If negative force feedback ($f = F_D - GF_K$) is incorporated, it is seen in Figure 4.6 that as the gain is increased, the bouncing problem becomes more severe. In fact, open loop force control seems to yield the best results.

If negative force feedback is used, but the mass starts out in contact with the spring-damper environment, it is seen in Figure 4.7 that while the response is quite oscillatory, there is no bouncing and the system is stable even at high gain. Again open loop force control seems to yield the best results.

Finally, if the environmental damper is increased by a factor of ten, negative force feedback achieves a very good response. This is illustrated in Figure 4.8, where a gain of 2 was used.

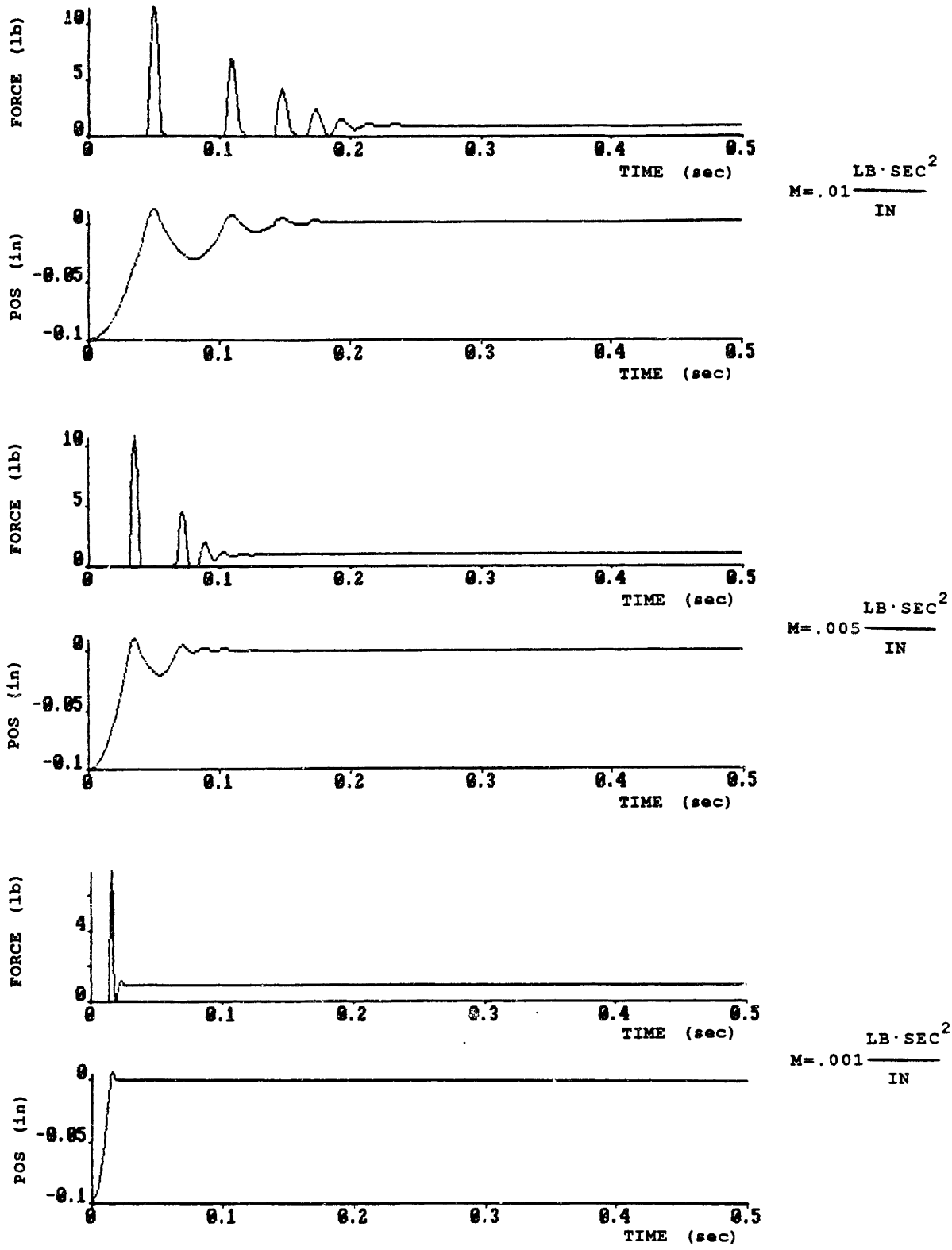

Figure 4.4: The Effect of Inertia on Open Loop Force Control With Initial Impact.

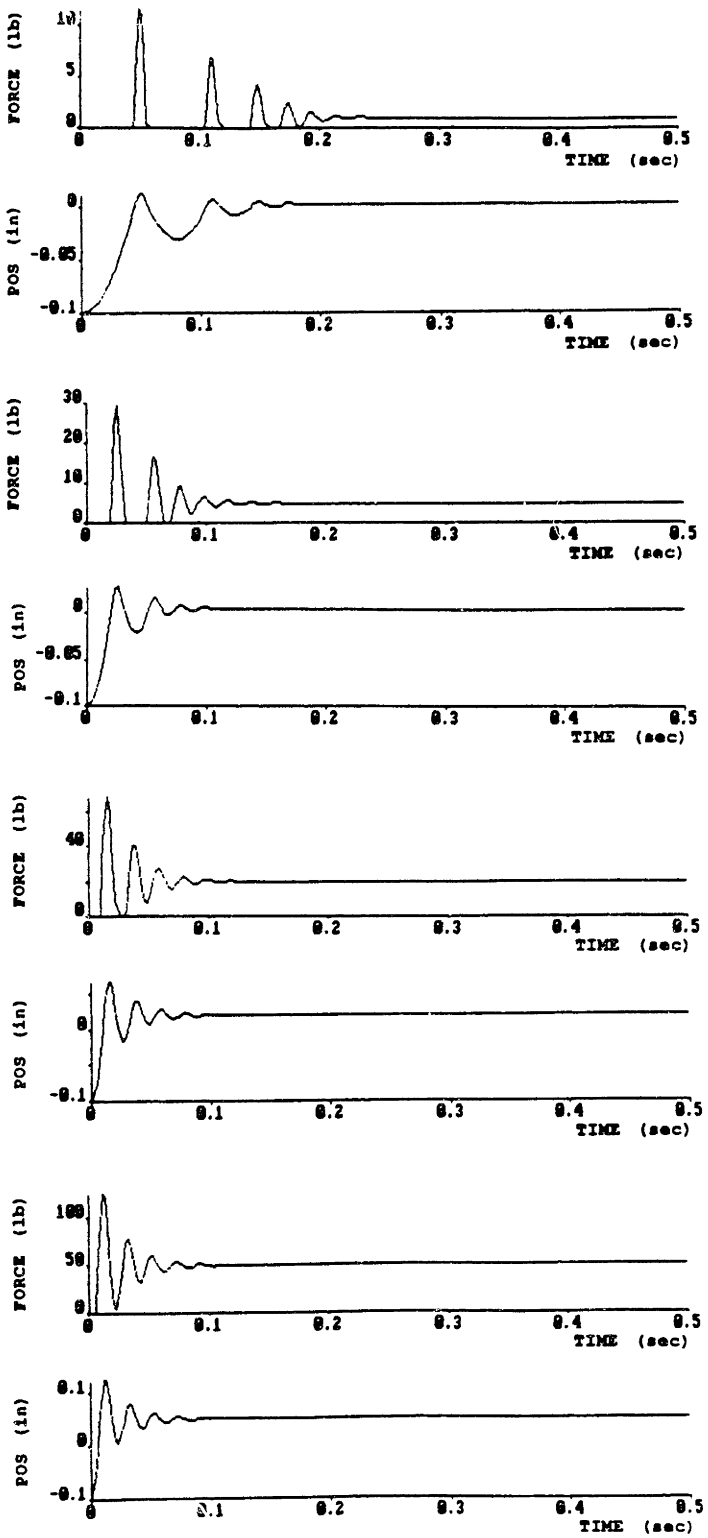

Figure 4.5: The Effect of Desired Force on Open Loop Force Control With Initial Impact.

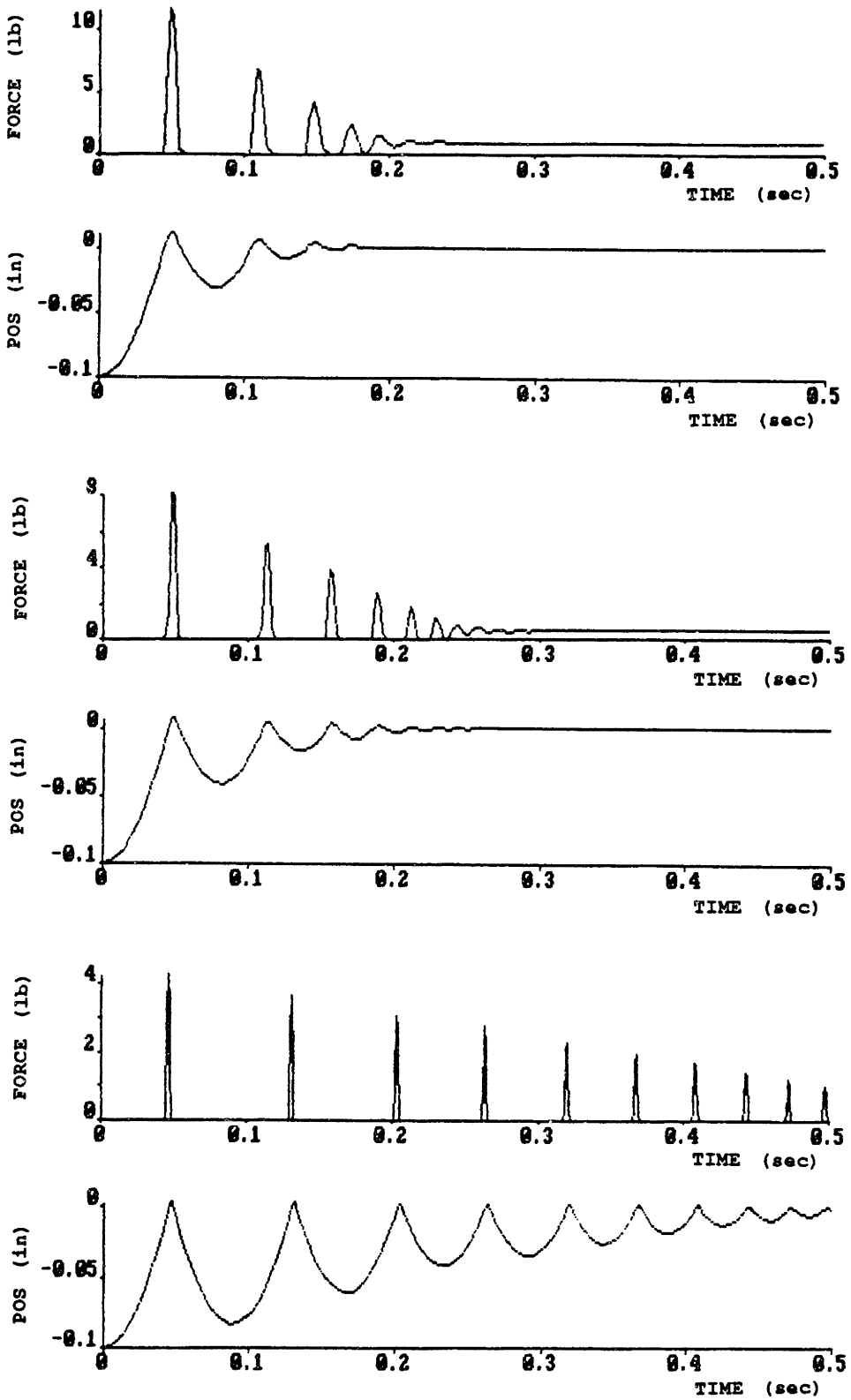

Figure 4.6: The Effect of Gain (G) on Negative Force Feedback ($f=F_D-GF_K$) With Initial Impact.

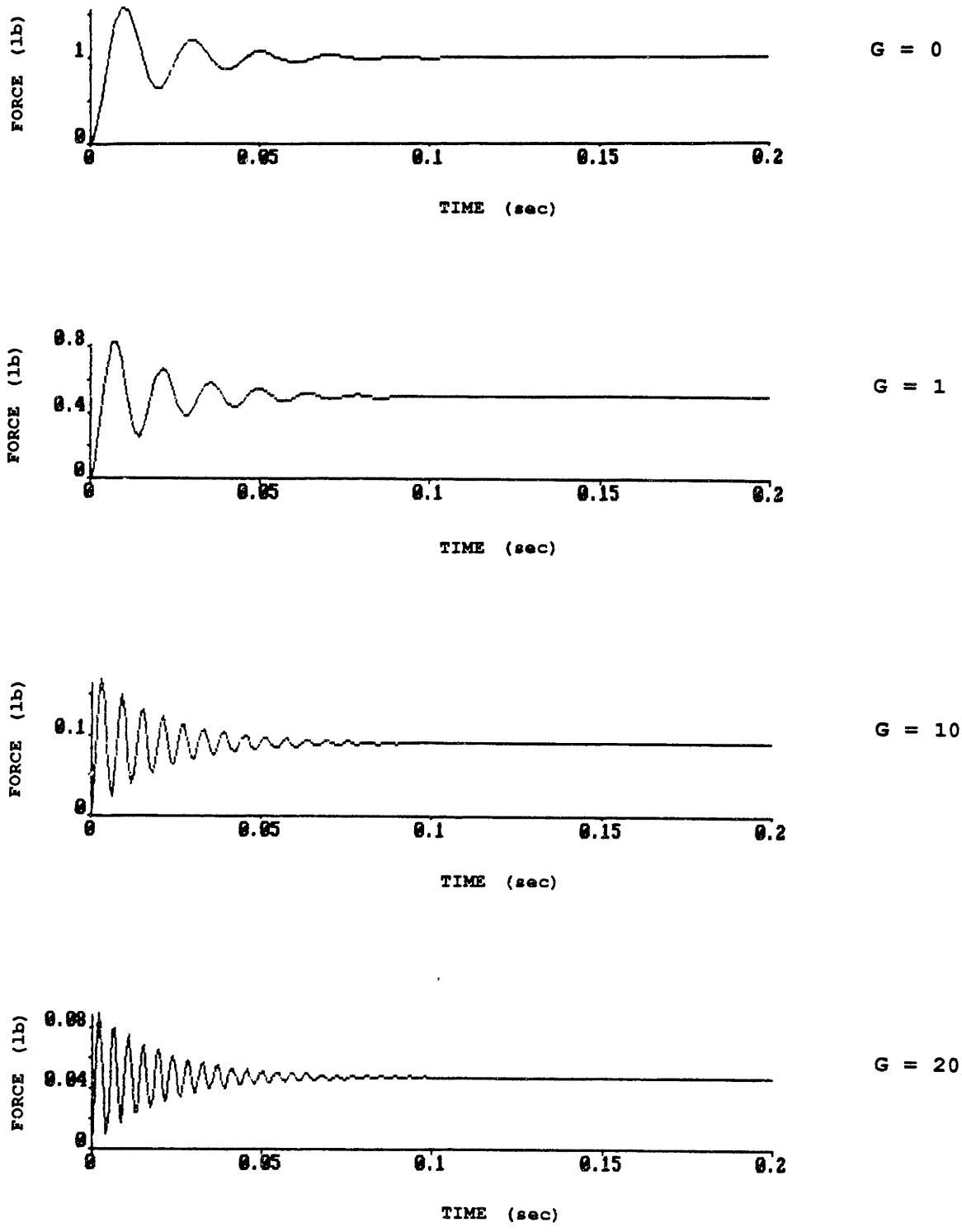

Figure 4.7: The Effect of Gain (G) on Negative Force Feedback ($f=F_D-GF_K$) Without Initial Impact.

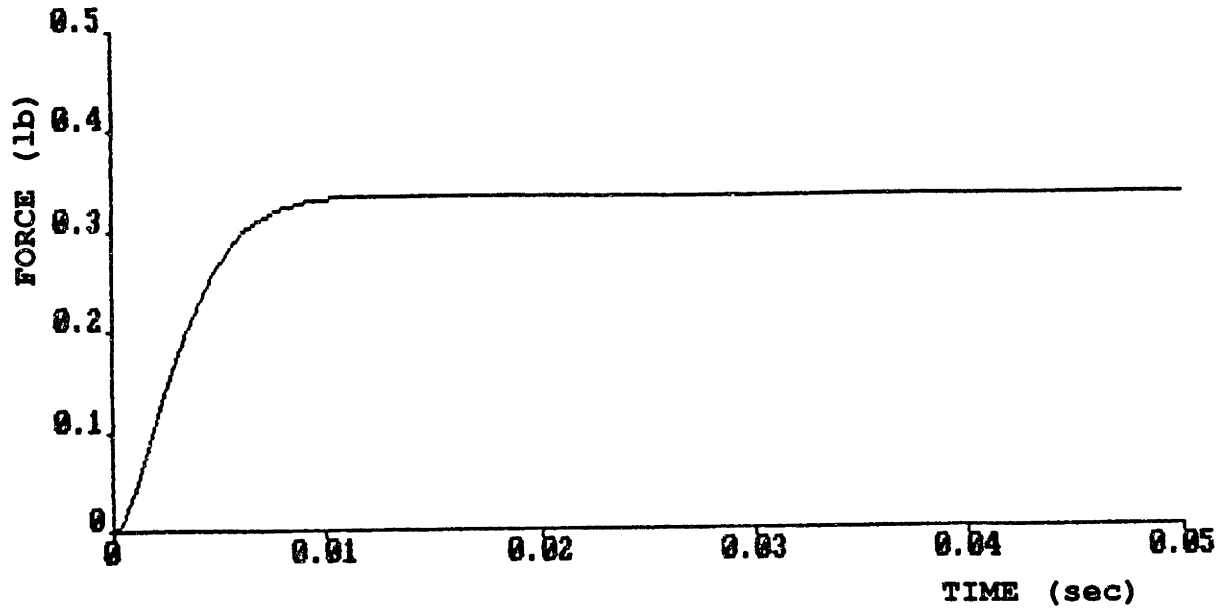

GAIN = 2 DAMPING = 10 $\frac{\text{LB}\cdot\text{SEC}}{\text{IN}}$

Figure 4.8: Negative Force Feedback ($f=F_D-GF_K$) With Increased Endpoint Damping.

4.2.3 The Low Interface Damping Problem

Many environments, such as metallic ones, are rigid and very lightly damped. As illustrated in the previous section, however, if the environmental damping is increased, response is greatly improved. Actually, the benefit arises from the fact that the damping ratio (ζ) of the system is increased as the damping is increased. Recall that the transfer function of the simple system in the previous section is:

$$\frac{F_K}{f} = \frac{K}{MS^2 + BS + K} \tag{4.1}$$

The damping ratio (ζ) of this system is derived to be:

$$\zeta = \frac{B}{2}\sqrt{\frac{1}{MK}} \tag{4.2}$$

Obviously, as damping (B) is increased, the damping ratio becomes higher. Thus, working against a well-damped environment, or placing a well-damped interface between the robot and the environment enhances performance. This may or may not be practical, depending on the application. Also note, however, that the damping ratio can be increased by reducing the mass (M). Thus, reducing the endpoint mass helps in two ways: it reduces the impact force, as stated earlier, while it also increases the damping ratio.

It should be noted that reducing K in this simple example also results in a higher damping ratio. Altering the environmental or work-piece stiffness, however, is often impractical. In a real robot system, one can attempt to place a soft, well-damped interface between the force transducer and tool. This

may increase the damping ratio, but due to the inertia of the tool, the force measurement from the transducer would not accurately describe the interface force between the tool and the work-piece at high frequencies.

4.2.4 The Actuator/Drive Non-linearities Problem:

No real actuators behave like ideal torque sources. They all exhibit some degree of non-linearity such as dead-band, resolution limitations, ripple, etc. Stiction causes some of these non-linearities and can be detrimental in force control.[28] If a robot is commanded to exert a certain desired force on a rigid environment, chatter can occur if that desired force is within the range of the actuator's non-linearities. This is independent of the non-collocation problem previously discussed. If it is desired, for example, to apply a force of one ounce while the actuator output contains a "noise" of two ounces, then the robot would lose contact with the environment and chatter. If under the same conditions, a force of five pounds is applied, then the force will not be perfectly constant but no bouncing will occur. High resolution direct drive actuators may alleviate these problems, at least for low frequency range.

Consider now actuators that behave more like flow sources than torque sources. Examples are motors with high reduction transmissions (non-backdrivable) and hydraulics. These actuators attempt to control force through position. In other words, if it is desired to apply a force of F pounds on an environment with a stiffness of K lb/in, then the robot must be displaced F/K inches "into" the environment. Assume now

that the actuator has an optimistic resolution of 0.00001 inches, or there is an uncontrollable "noise" of that same value. Assume also that a force is to be applied to a rigid environment with a stiffness of 10,000,000 lb/in. It is easily seen that a resolution or noise of 0.00001 inches corresponds to a force (F=KX) of 100 pounds. This obviously presents a big problem if the forces to be controlled are well below 100 pounds. It should be noted that if the environmental stiffness (K) is reduced to 100 lb/in, or an interface with a 100 lb/in stiffness is placed between the robot and the environment, then the force corresponding to 0.00001 inches is only 0.001 pounds.

Since most commercial robots possess non-backdrivable actuator-transmission systems that behave like flow sources, it has often been stated that in order to achieve stability, the interface stiffness must be made low. While this alleviates the problem caused by actuator-drive imperfections, it does not solve the non-collocation problem. Hence, low interface stiffness yields stability, but only at low bandwidth.

This is illustrated in Table 4.1 which lists the force control performance (in terms of bandwidth) achieved by others using base actuation - endpoint feedback. It is seen in Table 4.1a that performance of conventional robots is not very good. The non-collocation problem still limits achievable bandwidth, regardless of the interface characteristics. Table 4.1b lists some of the achievements in force control using a one-axis, specially designed apparatus. These apparatus generally consist of high performance motors that resemble ideal torque sources, and very short and stiff structural members to reduce the non-collocation problem.

RESEARCHERS	BANDWIDTH*
Whitney (1976)	2-3 Hz
Raibert and Craig (1981)	2-3 Hz
Khatib and Burdick (1986)	2-3 Hz
Maples and Becker (1986)	2-3 Hz

a.

Jilani (1974)	6 Hz
An (1986)	20 Hz
Youcef-Toumi and Nagano (1987)	15 Hz
Kazerooni (1988)	20 Hz

b.

* Estimated from reported force step responses when bandwidth was not explicitly given.

Table 4.1: Reported Achievements of Force Control using Base actuation - Endpoint sensing.
a. Implementations on Conventional Robots.
b. Implementations on High Performance Apparatus.

Hence, high performance force control can be achieved with the proper hardware. Use of short and stiff links may often not be a practical solution, especially if dexterity is necessary. Furthermore, when multiple degrees of freedom are introduced, the non-collocation problem is further aggravated. Of course if structural stiffness could be increased without increasing mass or having to reduce length, performance would benefit.

4.3 Chapter Summary

The simple model used in this chapter is not an accurate model of a robot, yet it gives a great deal of insight into the force control problem. It is very difficult to concentrate on performance issues of force control when working with a real robot, or an accurate model of a robot. This is because the stability problem overshadows performance. By using a simple model that does not exhibit instability, we are able to concentrate on performance and come up with some design criteria for better force control.

Force control can be improved through better hardware design. More specifically, robots should be designed with the following characteristics:

a. Stiffer, but not heavier, links to alleviate the non-collocation problem.

b. Reduced endpoint inertia. This diminishes the impact force and also increases the effective endpoint damping ratio.

c. Actuators/drives that come as close to ideal torque sources as possible (direct drive).

The macro/micro manipulator concept is beneficial in alleviating the problems of force control described in this chapter. It reduces the effect of the initial impact since the endpoint inertia (that of the micromanipulator) is very low. The low endpoint inertia also reduces the problem of low interface damping since the effective endpoint damping ratio is higher. The problem of actuator-drive imperfections is also alleviated since it is generally easier to achieve a micro-actuator that resembles a torque source, than one that must provide a large range of motion as well. Finally, as will be shown in the next chapter, the macro/micro manipulator alleviates the problem due to non-collocation of actuators and sensor.

Chapter 5

CONSTRAINED MOTION OF A MACRO/MICRO MANIPULATOR

In the last chapter, we concentrated on performance issues of force control by using a simple model that is always stable. A higher order model, however, illustrated that conventional robots are inherently unstable architectures for high bandwidth force control. The scope of this chapter is to characterize both the stability and performance of a macro/micro manipulator under force control.

5.1 Stability of a Macro/Micro Manipulator in Constrained Motion

Consider a macro/micro manipulator system attached to a rigid environment through a force transducer (see Figure 5.1). The micromanipulator is denoted by f along with some corresponding damping and inertia, B_3 and M_3. Again, it is desired to regulate the interface force F_t in a closed loop fashion. In this case, however, we have two actuators (F and f) to work with. First, we will investigate if and how the micromanipulator (f) alone can regulate the interface force, while the macromanipulator actuator (F) is just used to close a position loop around the macromanipulator ($F = -GX_1$). Then, we will investigate how the macromanipulator can be used in conjunction with the micromanipulator to better regulate the interface forces.

Deriving the equations of motion (see Appendix C) and

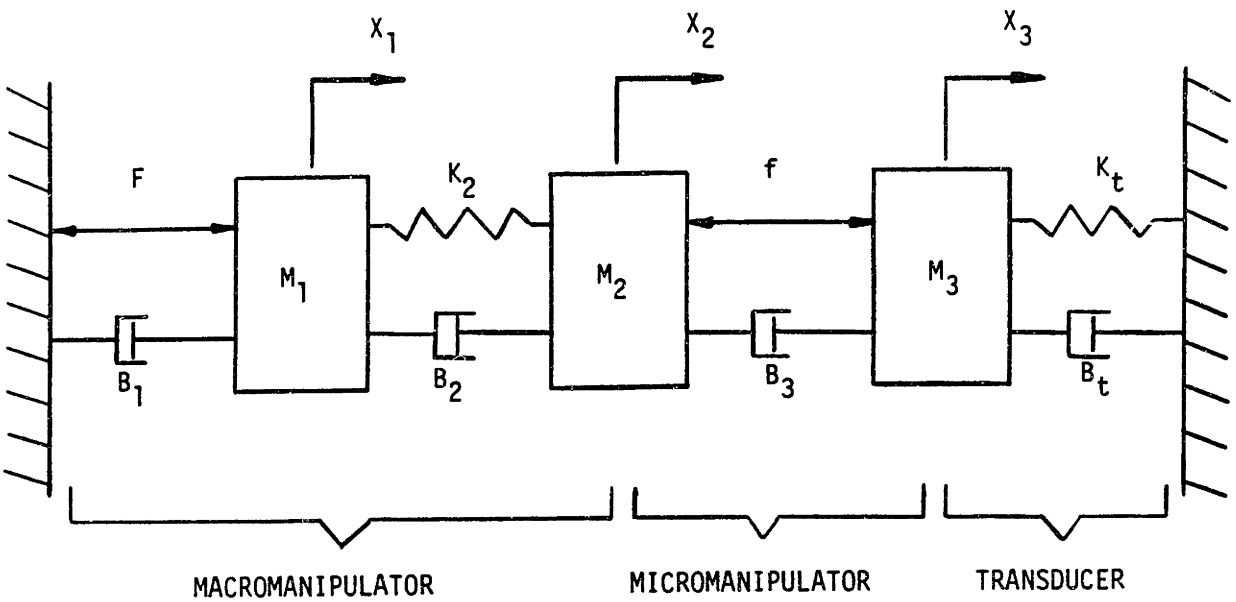

Figure 5.1: Model of a One-Axis Macro/Micro Manipulator Coupled to a Rigid Environment.

using the following parameter values:

$M_1 = 0.0169$ lb·sec^2/in
$M_2 = 0.0169$ lb·sec^2/in
$B_1 = 0.13$ lb·sec/in
$B_2 = 0.013$ lb·sec/in
$K_2 = 24$ lb/in
$K_t = 150$ lb/in
$B_t = 0.16$ lb·sec/in
$B_3 = 0.13$ lb·sec/in
$M_3 = 0.005$ lb·sec^2/in

results in the Bode plot of Figure 5.2 and root locus plot of Figure 5.3. The parameter values used here are representative of the macro/micro manipulator system described in reference 8. Once again, the transducer parameter values used were assumed to be those of a low-quality force transducer. It is seen that the system remains stable at all frequencies, although there are some resonances and anti-resonances caused by the force transducer and structural dynamics. Nevertheless, the analysis shows that a macro/micro manipulator system is an inherently stable physical configuration for high bandwidth force control. This is in contrast to conventional robot architectures that are inherently unstable at high bandwidth force control, as was illustrated in Figure 4.3.

While simple, proportional negative force feedback implemented on the micromanipulator ($f = -GF_t$) proves to be stable, performance could be further improved. The low phase margin at high frequencies, and the observed resonance must be dealt with.

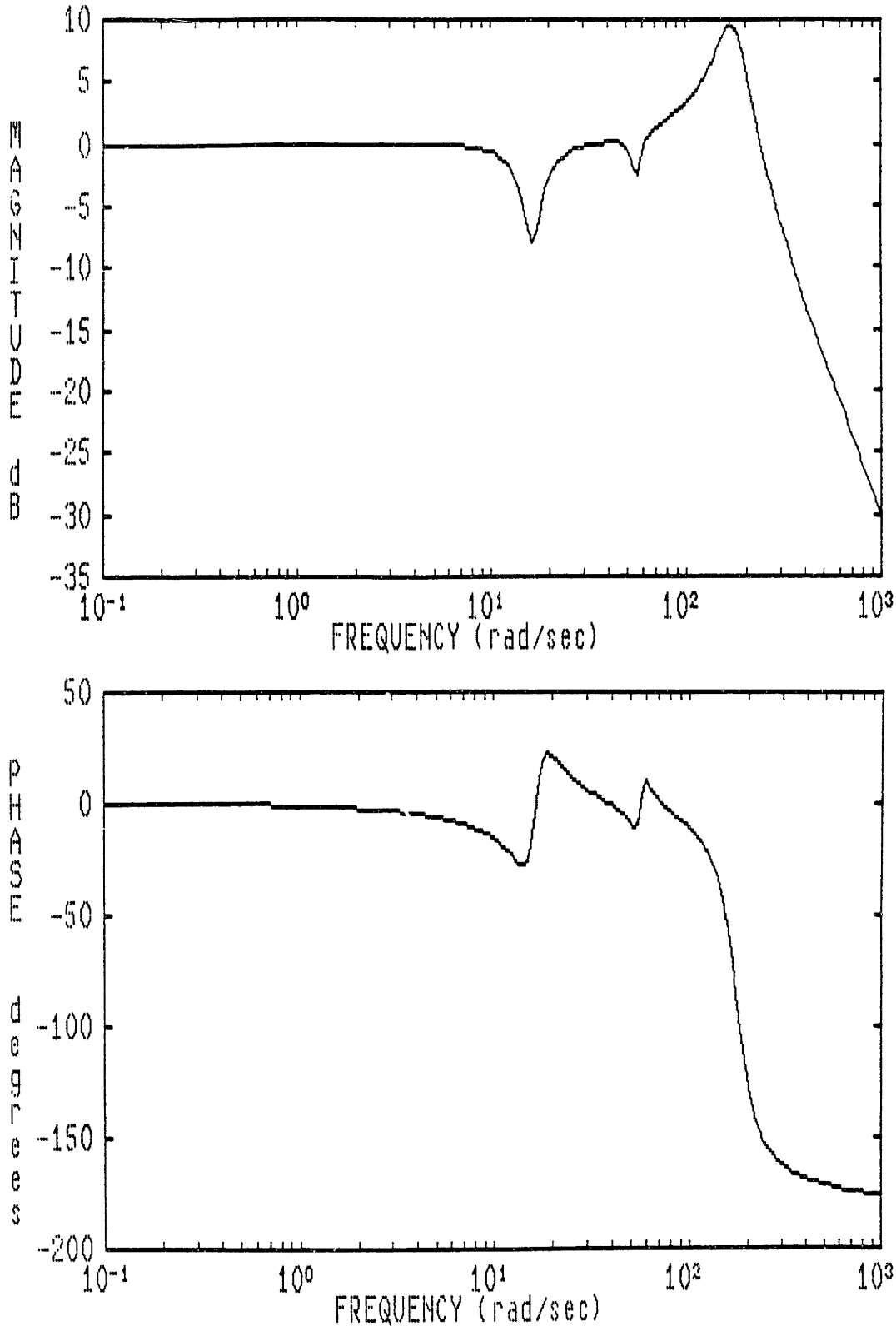

Figure 5.2: Bode Plot of Force Control (F_t/f) on a Macro/Micro Manipulator.

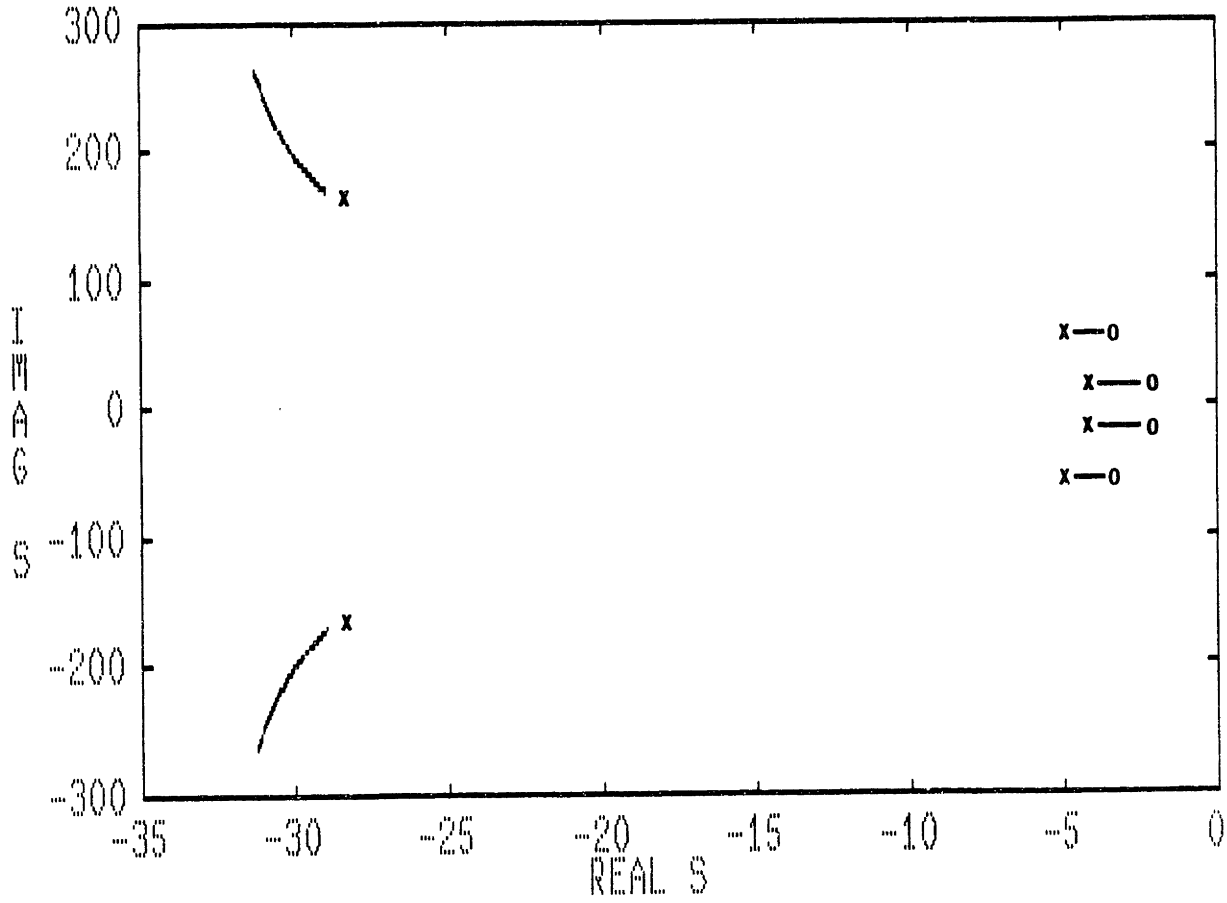

Figure 5.3: Root Locus of Force Control ($f=-KF_t$) on a Macro/Micro Manipulator.

5.2 High Bandwidth Force Regulation and Inertia Reduction

5.2.1 Controller Design in the Physical Domain

Designing a simple, yet robust controller based on the Bode plot and root locus of the macro/micro manipulator is very difficult. While the S-Plane provides a great deal of information about stability, natural frequencies, etc., physical insight is lost. After all, if the control action is neglected for a moment, the model of the macro/micro manipulator in Figure 5.1 represents a physical system composed of masses, springs and dampers. Why not design a controller in the physical domain then, where there is more insight into the real system? In order to do that, however, we must convince ourselves that the complete controlled system can be described as a physical system as well.

Hogan[23] postulates (without proof) that "it is impossible to devise a controller which will cause a physical system to present an apparent behavior to its environment which is distinguishable from that of a purely physical system." In other words, no controller can make a physical system disobey the laws of physics. Although this postulate is not proved, it does make a great deal of sense. For example, regardless of what command a controller might issue to a mass, that mass will not be able to change its position instantaneously. If the controller issued a step position command, the mass will respond with a finite acceleration and not in a step fashion. Hence, if the above postulate is correct, it implies that the complete controlled system can be described as an equivalent physical system. Consequently, a control system could be designed that approximates the robust behavior of a target

physical system composed only of masses, springs and dampers, through proper location of actuators and sensors. The resulting controlled system could meet design specifications and be extremely robust.

Although designing controllers in the physical domain makes good sense, a detailed procedure has not yet been developed. The approach, however, is based on the following postulate:

Given ideal (no dynamics) actuators and sensors,

any physical system can be made to emulate the dynamic behavior of any other physical system, provided that actuators and sensors can be placed at any point in that system.

Of course, this is usually not feasible in practice. The "art" of designing in the physical domain becomes that of wisely locating the available actuators and sensors, and selecting a target physical system that can be approximated with the achievable actuation and sensing. More will be said about this subject in Chapter 7.

5.2.2 Raising the Impedance of the Macromanipulator

Examining the model of the macro/micro manipulator system in Figure 5.1, it is observed that if the impedance seen by the micromanipulator base (that of the macromanipulator) is increased enough, then the effect of the structural dynamics seen in the Bode plot of Figure 5.2 would decrease. In the limit, raising the impedance to infinity is the same as

placing the micromanipulator sitting on ground, so there would be no structural dynamics to worry about. This is shown in the Bode plot of Figure 5.4a, where the impedance (stiffness, damping, inertia) of the macromanipulator was increased by a factor of 100. Note that the structural anti-resonance exhibited in Figure 5.2 is greatly diminished.

If the impedance of the macromanipulator could be physically increased by a factor of 100, then the problem is solved. Since that is not a practical solution in this case, it must be determined whether it can be approximated with achievable actuation and sensing.

Given that there exists an actuator at the base of the macromanipulator, the question becomes: what to sense and where to sense it in order to approximate a higher impedance? Since positive force feedback tends to amplify impedance, it is attempted to sense the force that the micromanipulator inflicts on M_2 and feed it back to the macromanipulator actuator in a positive fashion ($F = +Gf$).

Examining the Bode plot of Figure 5.4b, it seen that the proposed positive force feedback scheme did not help matters. This makes sense since the actuator (F) is transmitting force to M_2 through a dynamic system. There is no way for F to make M_2 appear to the micromanipulator to be anything other than M_2 at high frequencies.

If, on the other hand, an actuator F_g is placed between M_2 and ground, then M_2 can indeed be made to appear very large through positive force feedback ($F_g = +Gf$). This is seen in the Bode plot of Figure 5.4c, where the structural dynamics are greatly attenuated. Such actuation can be achieved by having several actuators placed at key locations in the workspace, to which the macromanipulator would clamp its endpoint.

a.

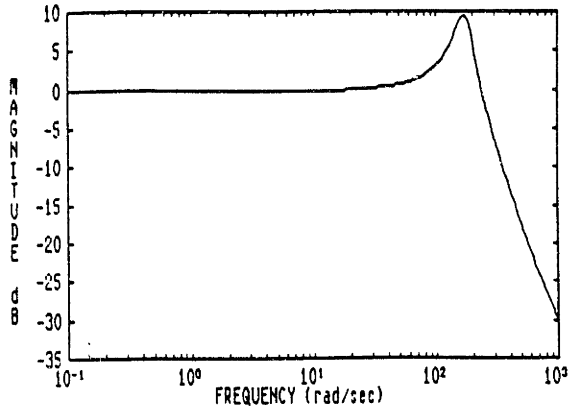

b.

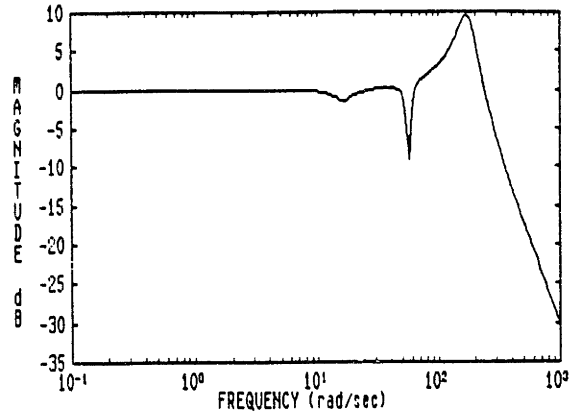

c.

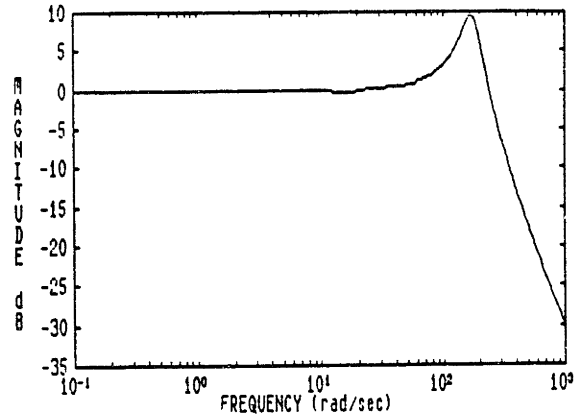

Figure 5.4: Bode Plot (Mag) of Force Control (F_t/f) on Macro/Micro Manipulator With Increased Macromanipulator Impedance.
a. Impedance Physically Increased.
b. Impedance Increased Through Control: F=+Kf.
c. Impedance Increased Through Control: F_g=+Kf.

This would be an extension of Asada's and West's Braced Manipulation Concept,[4] but with their proposed passive braces replaced by active ones.

Although possible, this approach would be very costly. Furthermore, it would reduce the flexibility of the system, which is one of the main reasons for the introduction of robots in the first place. Thus, a more easily achievable target physical system must be chosen.

5.2.3 Active Impedance Matching

Further examination of the macro/micro manipulator model of Figure 5.1 reveals the reason why the macromanipulator structural dynamics is excited. Since there is very little dissipation capability in the structure (B_2 is very small), much of the energy transferred from the micromanipulator to the macromanipulator is reflected back through the structure, exciting structural modes. One way of alleviating this problem would be to increase the structural damping (B_2). This is mechanically difficult to achieve, although not impossible.[21] Another alternative is to increase B_2 through control action. However, in order to achieve that, an actuator (F_r) must be placed between M_1 and M_2, with a control action:

$$F_r = -G(\dot{X}_2 - \dot{X}_1)$$

Such an actuator, though, would be impractical.

Another means of enhancing the capability of dissipating energy transferred by the micromanipulator to the macromanipulator is by increasing B_1. However, arbitrarily increasing B_1

may not help, as can be seen when B_1 is raised to infinity (Figure 5.5). In this case, M_1 becomes a ground and no energy is dissipated through B_1, leaving the structural dynamics present. There should be, however, some value of B_1, between zero and infinity, that maximizes dissipation.

The structural dynamics of the macromanipulator can be viewed as a mechanical transmission line, where the micromanipulator is the source input and B_1 is the load. Then, the energy transferred from the source to the load can be maximized if the load's impedance is matched to the characteristic impedance of the transmission line.[29] This issue has been addressed by various disciplines including Electromagnetic Wave Theory.

The characteristic impedance of a uniform, non-dissipative transmission line is given[29] as:

$$Z_o = \sqrt{\frac{L_o}{C_o}} \qquad (5.1)$$

where L_o is the inductance per unit length and C_o is the capacitance per unit length. The reflection coefficient (R_I), quantifying the ratio of wave reflection back to the source, is given[29] as:

$$R_I = \frac{Z_o - Z_L}{Z_o + Z_L} \qquad (5.2)$$

where Z_L is the impedance of the load. Note that if the impedance of the load is matched to the characteristic impedance of the line ($Z_L = Z_o$), R_I becomes zero and there is no reflection. In other words, all the energy input by the

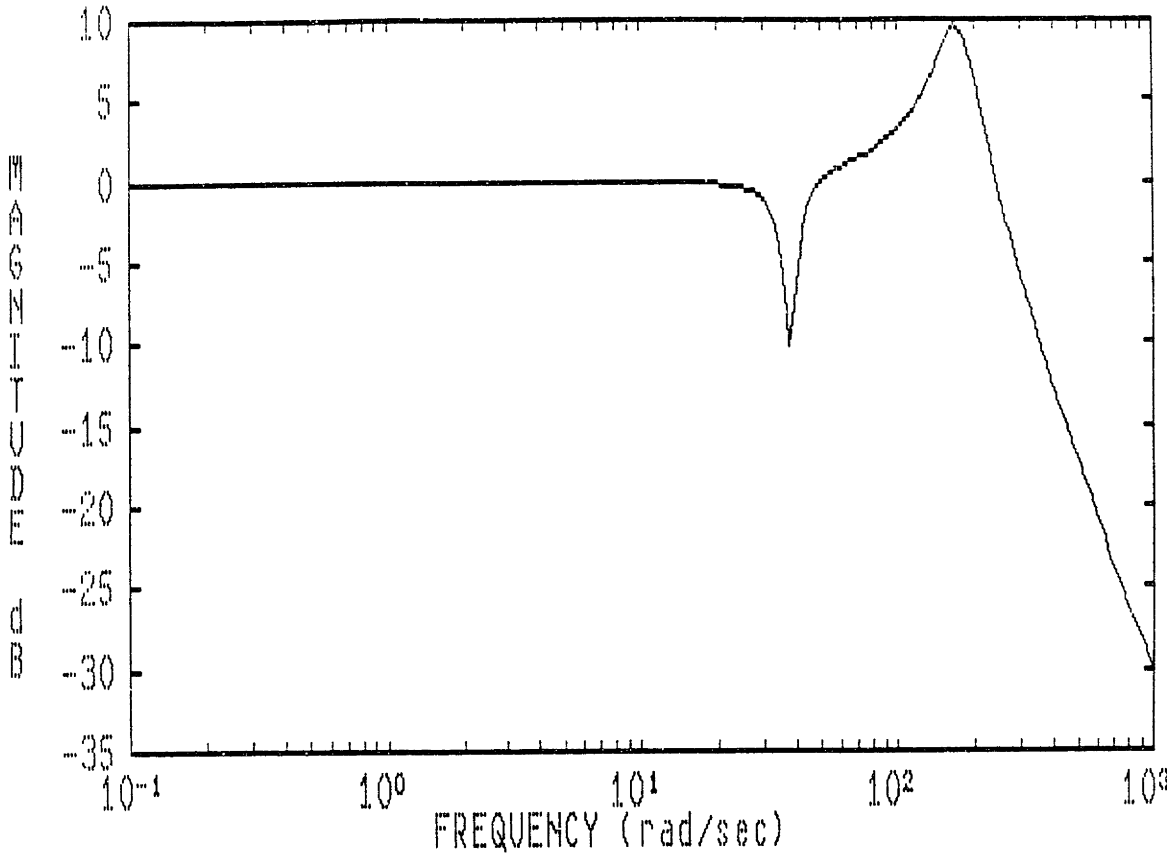

Figure 5.5: Bode Plot (Mag) of Force Control (F_t/f) on Macro/Micro Manipulator With High B_1.

source gets absorbed by the load. Such impedance matching tends to make a finite length transmission line appear to be infinitely long, eliminating reflection. If Z_L is zero or infinity, then there is no energy absorbed by the load, since the load experiences flow with no effort or effort with no flow, respectively.

Taking the mechanical equivalence, where force and voltage are viewed as efforts, while velocity and current are viewed as flows, yields:

$$Z_o = \sqrt{M \cdot K} \tag{5.3}$$

for the characteristic impedance of a non-dissipative mechanical transmission line. Referring to the macro/micro manipulator model of Figure 4.3 and neglecting the structural damping (B_2), the characteristic impedance of the macromanipulator structure can be approximated as:

$$Z_o \approx \sqrt{(M_1 + M_2) \cdot K_2} \tag{5.4}$$

Replacing the parameters above with actual values yields:

$$Z_o \approx 0.9 \text{ lb} \cdot \text{sec/in} \tag{5.5}$$

Thus, if we match the load (B_1) to this characteristic impedance, most of the energy transferred to the macromanipulator structure should be dissipated through B_1, reducing the amount of reflection and hence structural modes excitation (see Figure 5.6). The value of B_1 can be modulated by actually placing a mechanical damper on the joint axis or through control action.

Modulating B_1 through control action is easily achieved since there already exists an actuator (F) between ground and

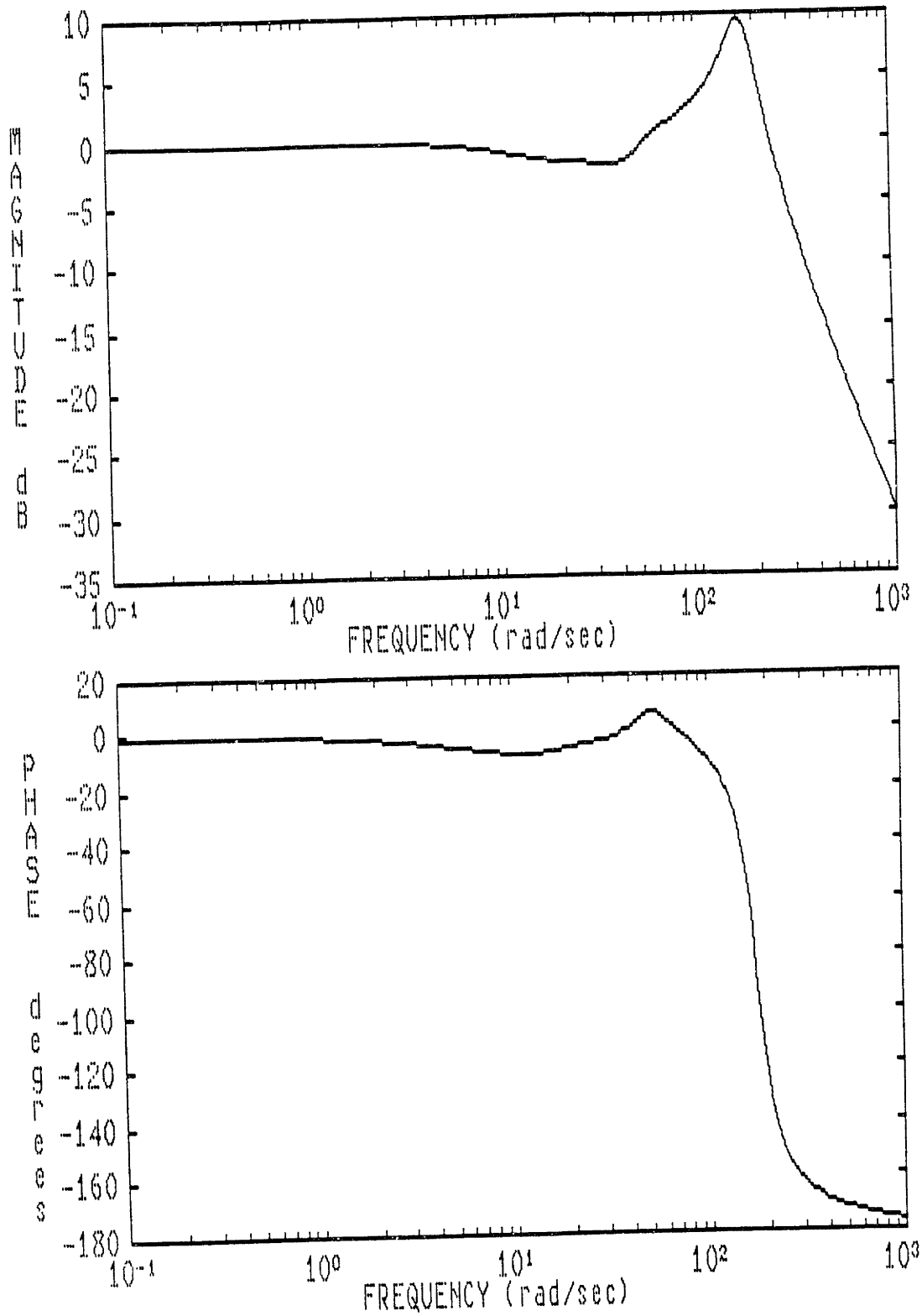

Figure 5.6: Bode Plot of Force Control (F_t/f) on Macro/Micro Manipulator With B1 Chosen Through Impedance Matching.

M_1. The control law for the actuator would simply be:

$$F = -G\dot{X}_1$$

In other words, closing a velocity loop around the macromanipulator joint achieves the desired dissipation.

It should be noted, though, that there is also a spring action (position loop: $F = -KX_1$) in parallel with B_1. If K is taken to be very large, then M_1 effectively becomes a ground and there is no dissipation through B_1. If K is not very large, however, then its effect on the impedance matching technique is negligible. This is confirmed in Figure 5.6, where the value of K was taken to be 10.

Although it is not clear which way energy is flowing in an active control system, by using the concept of physical equivalence we are able to describe the control action as a dissipator.

The control scheme proposed above is very simple. With the proper amount of velocity feedback around the macromanipulator joint, its structural dynamics are attenuated, allowing the micromanipulator to treat the macromanipulator as a low frequency disturbance. The control law for the micromanipulator can now be designed neglecting the dynamics of the macromanipulator. Also, we did not introduce a model-sensitive compensator, as did Tilley,[20] that would require precise knowledge of the real system. Even if we are off by as much as 50% from the correct amount of velocity feedback, the system remains well behaved (see Figure 5.7a,b). Even if the determined amount of velocity feedback is completely wrong due to modeling errors, performance would be hurt but stability would not be jeopardized. Furthermore, since we did not introduce any additional dynamics through compensation, our resulting controller is very robust.

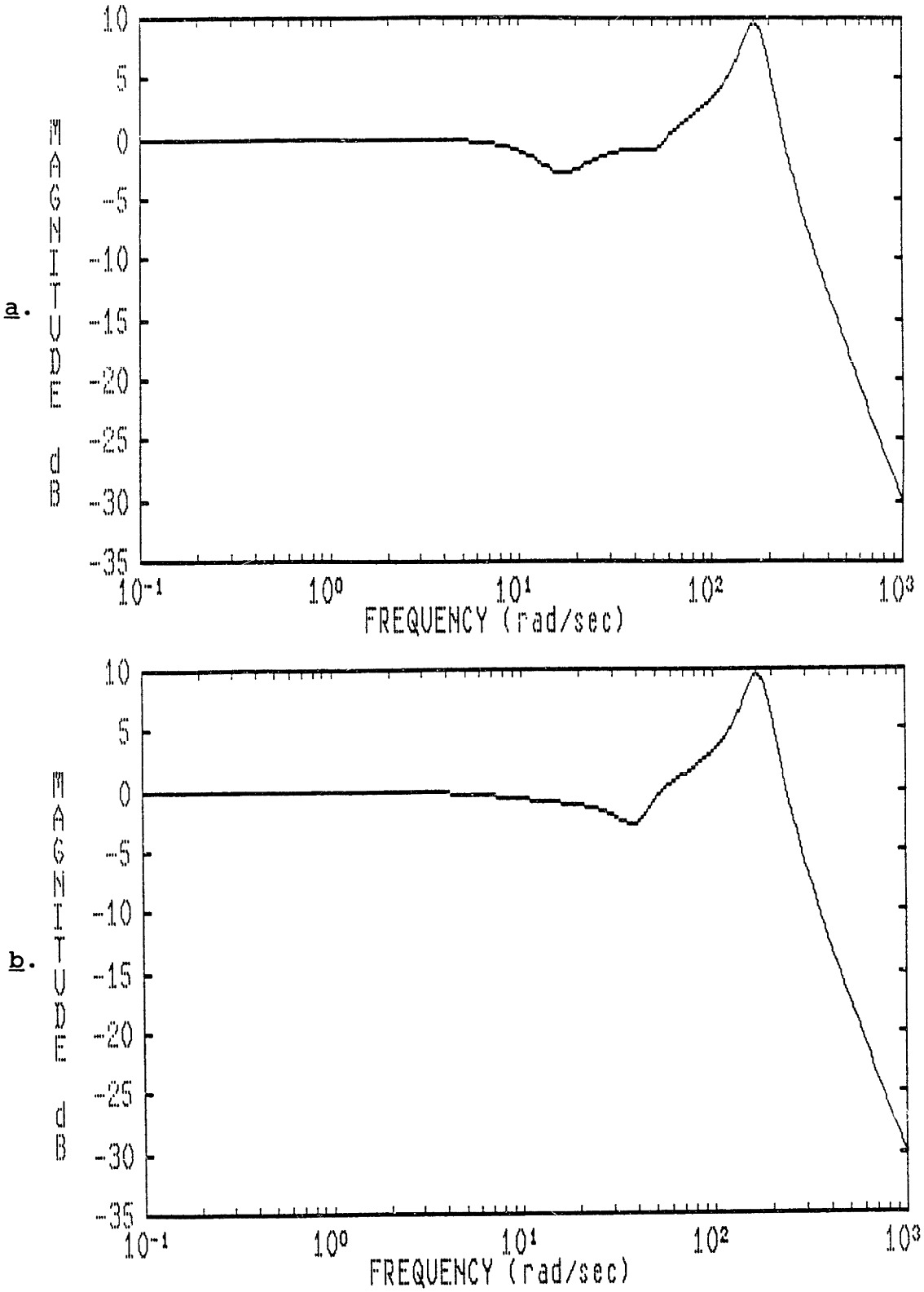

Figure 5.7: Bode Plot (Mag) of Force Control (F_t/f) on Macro/micro Manipulator With Miscalculated B_1.
a. B_1 50% Lower than Ideal.
b. B_1 50% Higher than Ideal.

Finally, this impedance matching technique also works with the unconstrained macro/micro manipulator of Figure 3.2, as is observed in the Bode plot of Figure 5.8. It is seen that through proper selection of B_1 stability is achieved at all frequencies. This is a very useful result, indicating that the controller structure does not have to be changed during the transition between unconstrained and constrained motion.

It is now seen why taking B_1 in Figure 3.2 to be infinity, and hence collapsing the system to that of Figure 3.1b, is actually the worst case scenario.

5.2.4 Increasing Force Transducer Damping

Examining the Bode plot of Figure 5.6, it is observed that while the structural dynamics of the macromanipulator were attenuated through impedance matching, the force transducer resonance is still present. This resonance is caused by the light damping (low B_t) of the transducer, as observed in the low phase margin at high frequency. This problem can be eliminated if a force transducer with intrinsic high damping is used (see Figure 5.9). Such transducers, that still provide high stiffness, may or may not be readily available. An alternative approach is to increase B_t through control action.

Strictly speaking, increasing B_t through control action would require an actuator between M_3 and ground. However, since the macromanipulator dynamics were attenuated through impedance matching, the micromanipulator treats the macromanipulator as a low frequency disturbance. This gives rise

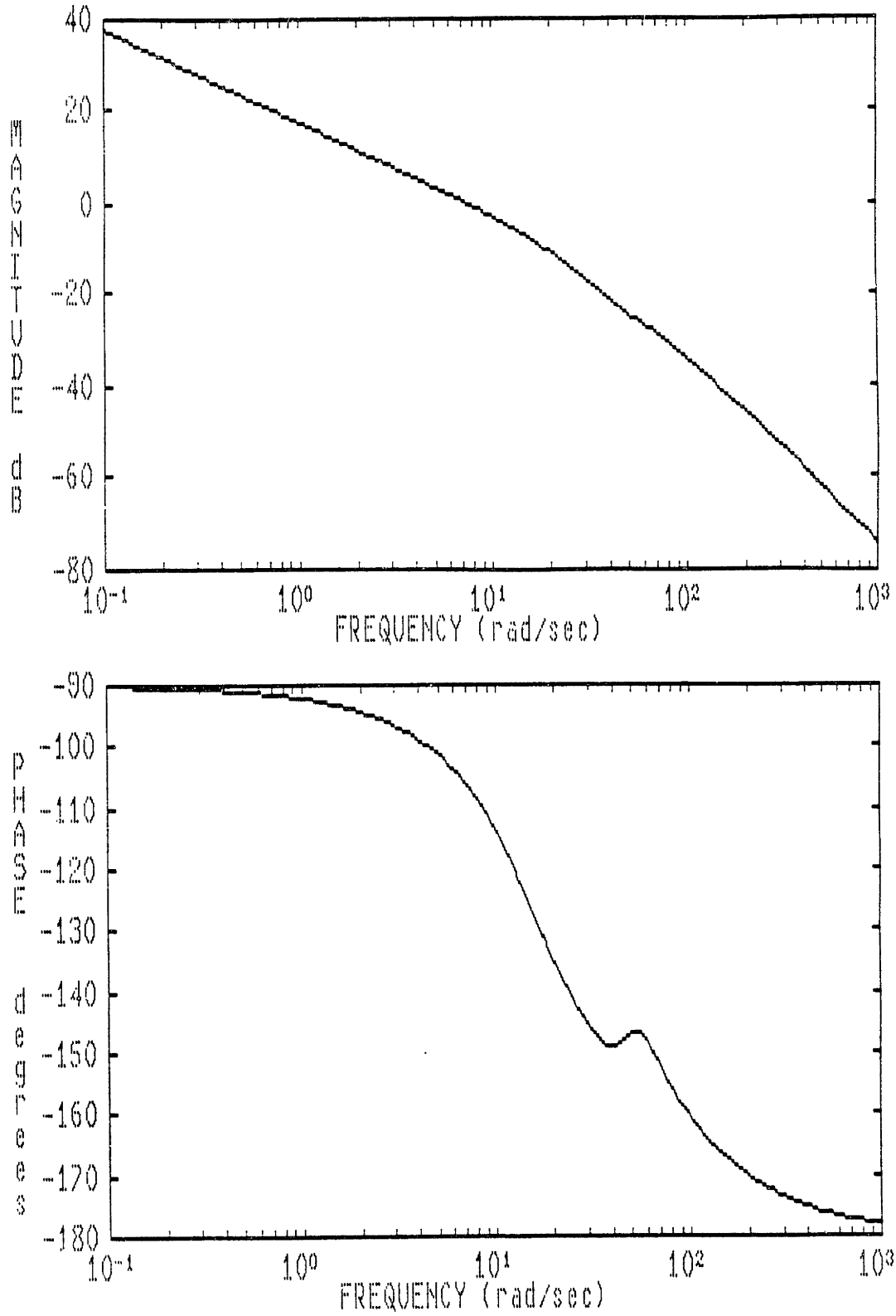

Figure 5.8: Bode Plot of Endpoint Position Control on Unconstrained Macro/Micro Manipulator Using Impedance Matching Technique.

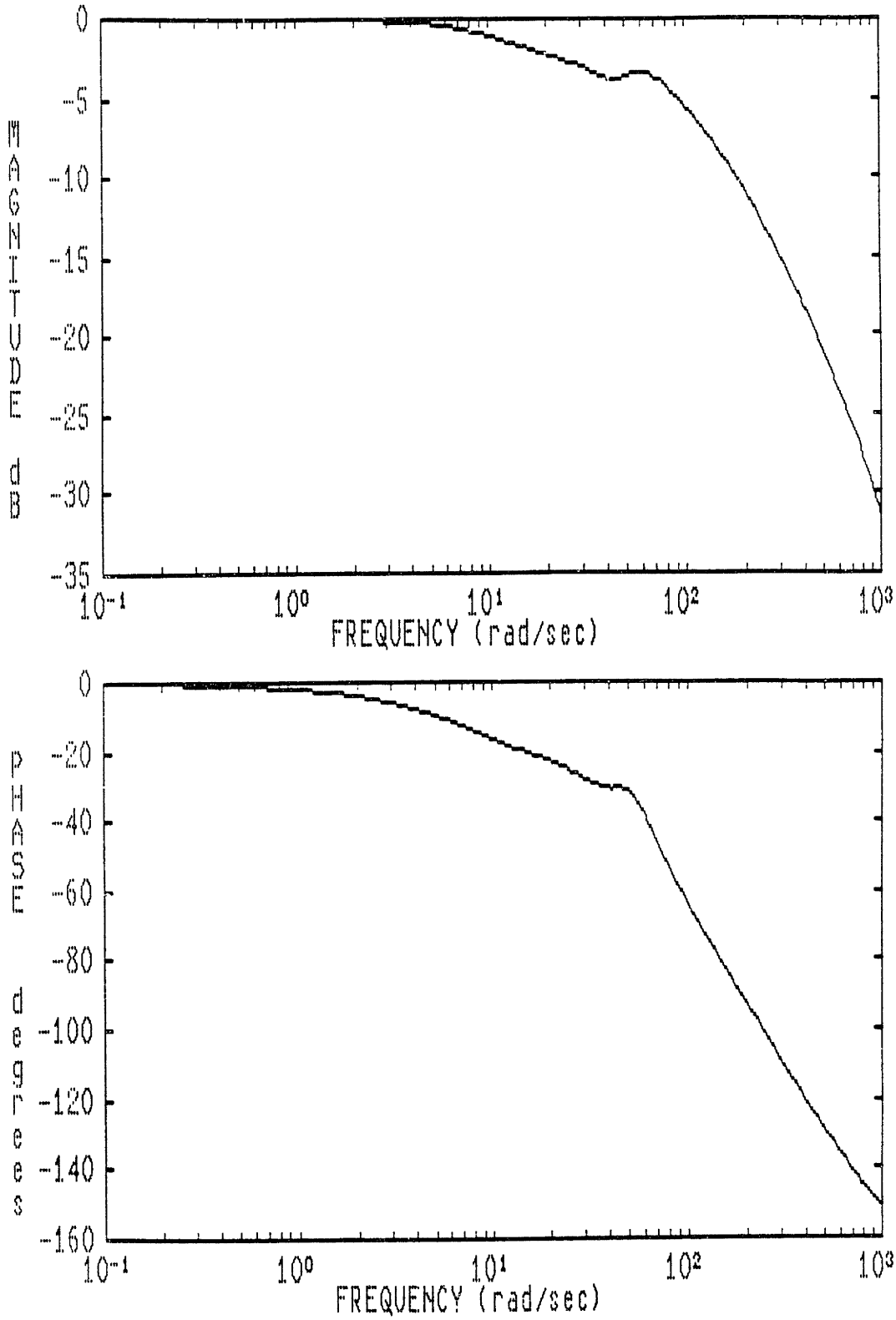

Figure 5.9: Bode Plot of Force Control (F_t/f) on Macro/Micro Manipulator With Increased Transducer Damping.

to a situation very similar to having the micromanipulator attached to ground. Thus, incorporating negative endpoint velocity feedback in the micromanipulator:

$$f = -G\dot{X}_3$$

results in a system response very similar to that of actually raising the transducer damping (see Figure 5.10).

Once the transducer resonance is attenuated, simple proportional force feedback performed by the micromanipulator actuator (f), of the form:

$$f = -GF_t$$

enables interface force regulation at bandwidths higher than the structural frequencies of the system. This can be seen in the closed loop Bode plot of Figure 5.11a, and the response to a step input in desired interface force (Figure 5.11b).

5.3 Chapter Summary

The research presented in this chapter suggests that a macro/micro manipulator is inherently more stable in regulating interface forces than a conventional robot system. The additional actuator introduced by the macro/micro manipulator allows the approximation of a robust target physical system composed only of masses, springs and dampers. The system controller designed based on physical equivalence is simple, yet very robust.

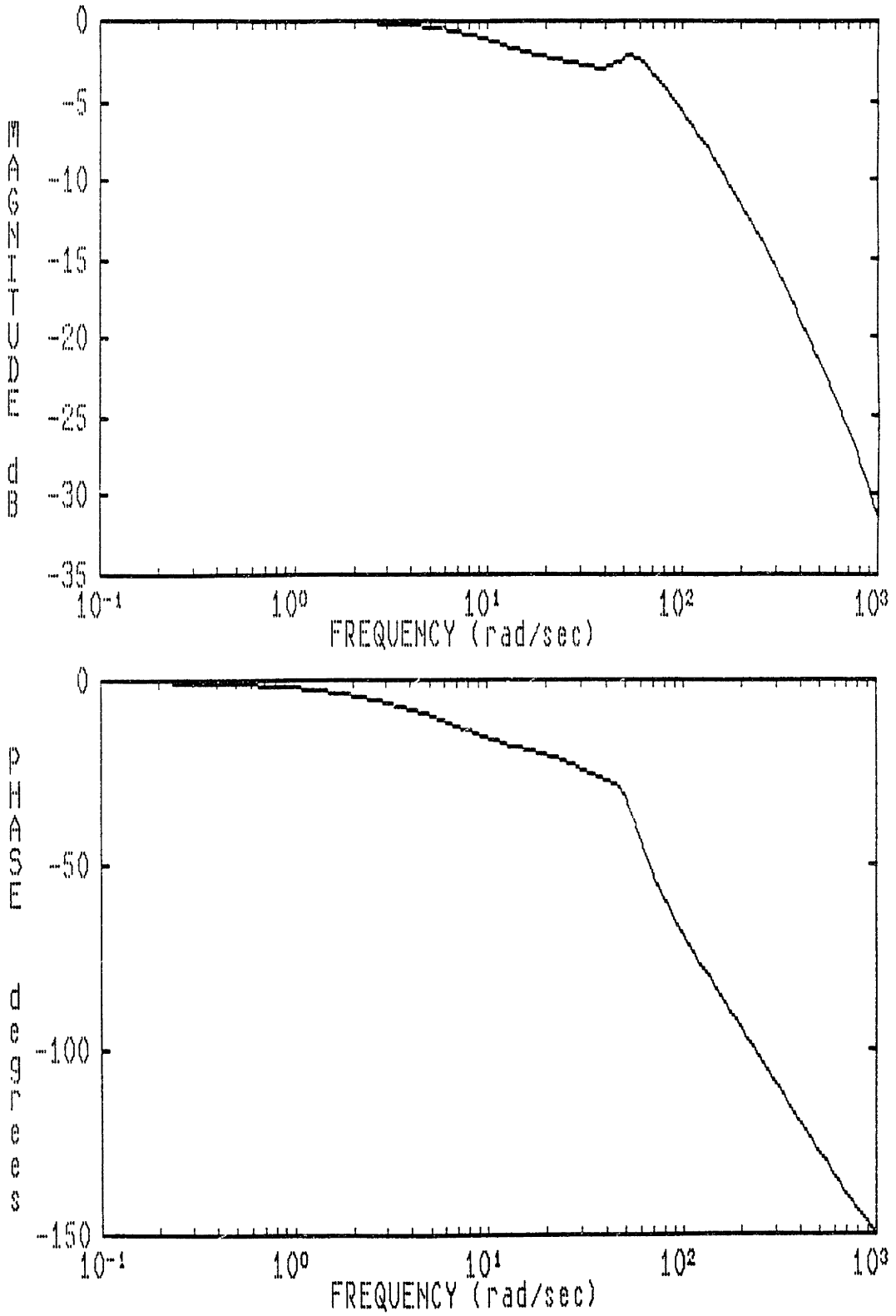

Figure 5.10: Bode Plot of Force Control (F_t/f) on Macro/Micro Manipulator Using Endpoint Velocity Feedback.

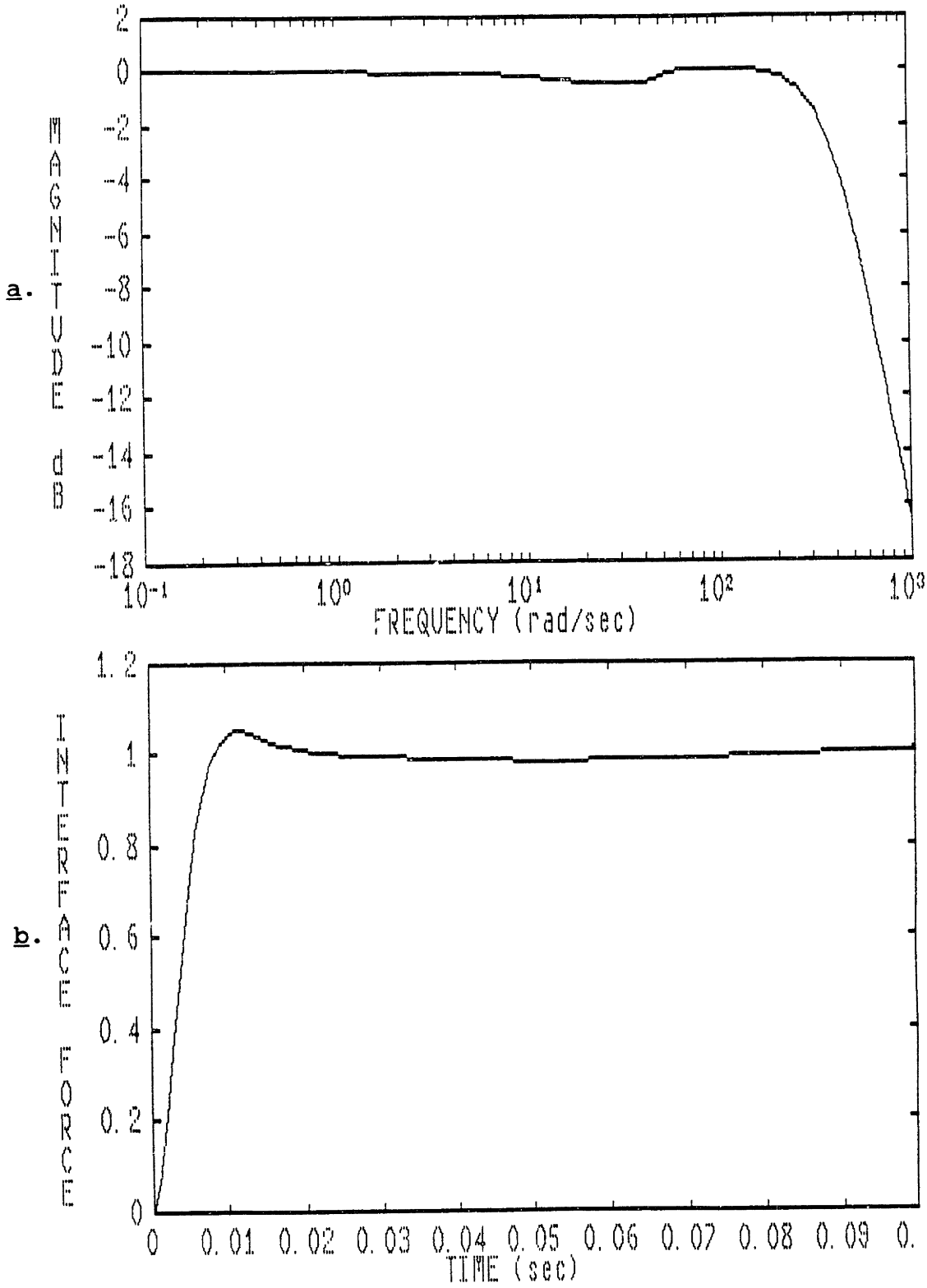

Figure 5.11: a. Closed Loop Bode Plot of Force Control (F_t/f) on Controlled Macro/Micro Manipulator.
b. Response of Macro/Micro Manipulator to a Step Input in Desired Interface Force.

A control action by the macromanipulator of the form:

$$F = -G_1 X_1 \; -G_2 \dot{X}_1$$

along with the control action by the micromanipulator:

$$f = -G_3 F_t \; -G_4 \dot{X}_3$$

is sufficient to achieve force regulation at bandwidths much higher than the fundamental structural frequency of the macromanipulator. The value of G_2 was chosen based on impedance matching, while the values of G_1, G_3, and G_4 were chosen based on frequency domain analysis of Classical Control.

Finally, the fact that the macromanipulator joint impedance had to be matched to the characteristic impedance of the structure confirms that there are indeed cases when neither position control (infinite impedance), nor force control (zero impedance) suffices. It is in these cases that impedance control is beneficial.

Chapter 6

EXPERIMENTAL PERFORMANCE CHARACTERIZATION

6.1 Scope of Experiments

The experiments described in this chapter were performed for two reasons: to determine whether a macro/micro manipulator system is indeed inherently more stable and well suited for endpoint control, as the the analysis predicts, and to characterize how much of a performance improvement a macro/micro manipulator might provide over a conventional robot.

Regardless of how elaborate a model is used to describe a real system, it cannot completely characterize that system. There are always some approximations and assumptions made at one level or another in modelling. Increasing the information content of a model may improve its accuracy. However, increasing the complexity may lead to loss of physical insight into the system. Furthermore, the primary issues of importance will be blurred by secondary ones. Thus, the best model is the simplest model that still describes the relevant behavior of the system being analyzed.

Since no model completely characterizes a physical system, there is always the possibility that some important issues were omitted in the analysis. Hence, experimental verification is necessary to truly characterize the behavior of a system. It is generally impossible, however, to perform an exhaustive set of experiments. Nevertheless, experimentation can verify some aspects of the system, and it also increases the confidence in the analytical predictions that

could not be experimentally confirmed. This chapter attempts to do just that.

6.2 Prototype Micromanipulator

The micromanipulator used in this research is shown in Figures 6.1 and 6.2. It was designed by the author and is fully described in reference 8. It is hydraulic with the following specifications:

- Degrees of freedom:	5 (3 in translation, 2 in rotation)
- Payload:	50 pounds
- Bandwidth:	50 Hz at maximum displacement
- Maximum displacement:	0.1 inch translation, 4° rotation
- Size:	6 inch cube
- Weight	7.5 pounds (not including servo-valves)

The micromanipulator is controlled via hydraulic servo-valves and can accelerate 50 pounds at 45G's. It was designed for use in heavy industries such as automotive and aerospace.

There are 5 piston-pairs integrated into the package (one pair for each degree of freedom). Hence, all actuation is done through push-push action and not push-pull. This eliminates backlash. Furthermore, it allows for equal area on both sides of the pistons, which is beneficial for control. Each piston is 1 inch in diameter, and can apply 2300 pounds with an operating hydraulic pressure of 3000 PSI. The force to weight ratio is 300:1.

It is not meant to imply that the macro/micro manipulator

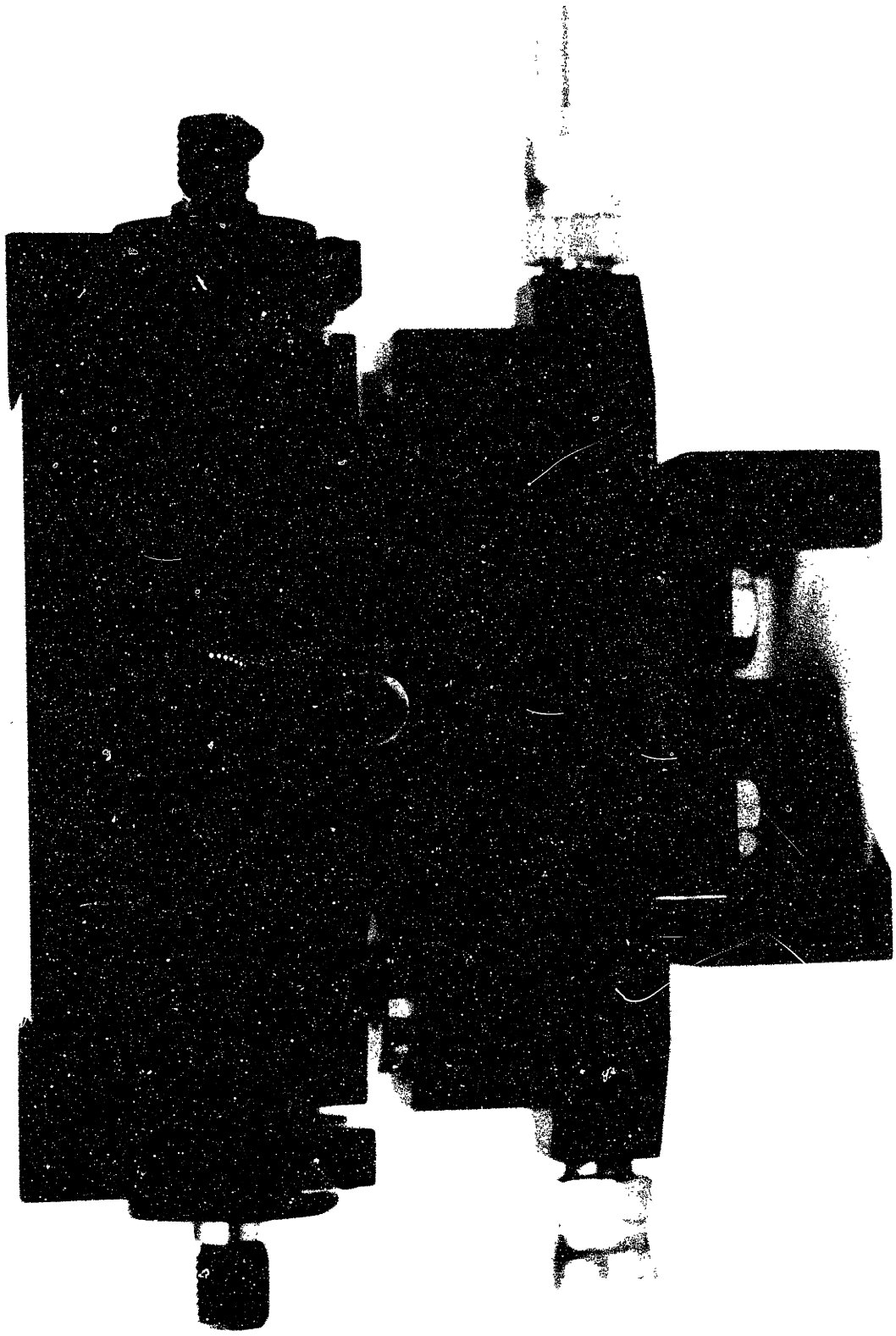

Figure 6.1: Prototype Micromanipulator.

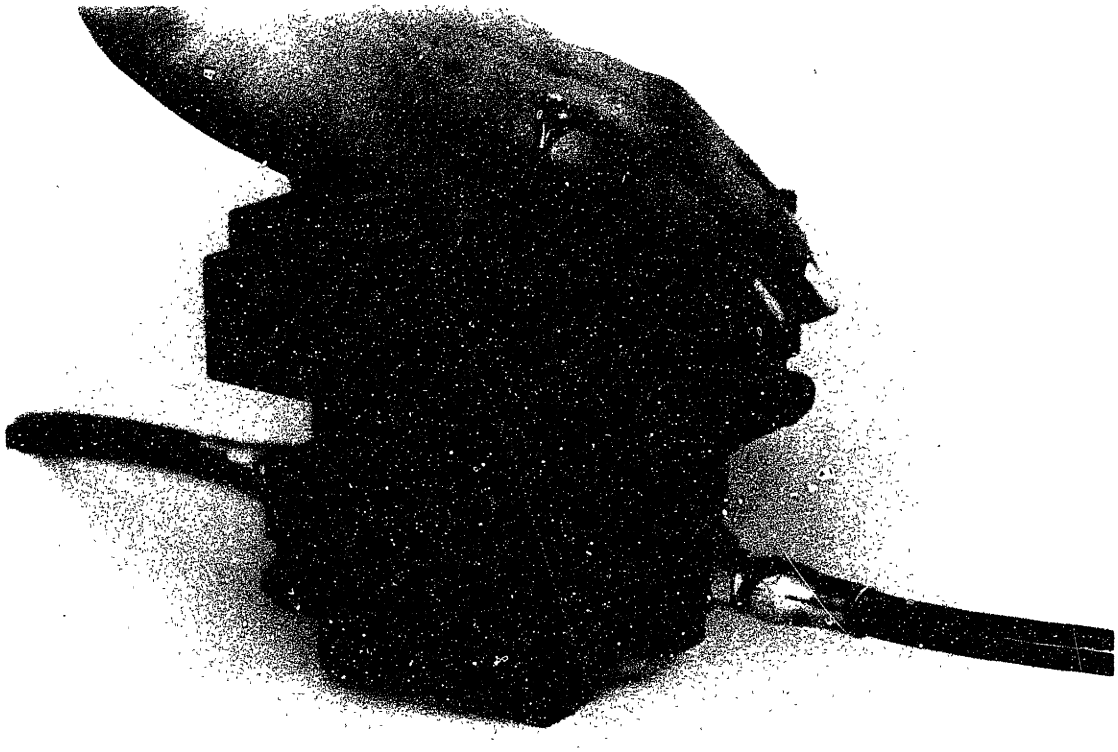

Figure 6.2: Relative Size of Prototype Micromanipulator.

concept is only applicable to heavy industries. In designing the first prototype, it was desired to determine the feasibility of a very powerful, high performance, and compact micromanipulator. The macro/micro manipulator is applicable to light industries as well. Hydraulics, of course, may no longer be the appropriate means of actuation. Electromagnetics may be an alternative.

6.3 Implementation on an Industrial Robot

The experiment described in this section is a qualitative one. The prototype micromanipulator described in the previous section was attached to a Hitachi robot (see Figure 6.3). The purpose was to see if the micromanipulator could indeed compensate for the settling time of the Hitachi robot and hence reduce cycle time. There was no access into the Hitachi controller and little was known about the robot structure. The micromanipulator was controlled independently using endpoint feedback from an optical sensor. Only one of its degrees of freedom was used.

The complete system was commanded to move 1/4 inch along an axis aligned with one of the micromanipulator's axes. Note that the travel range of the micromanipulator was limited to 0.1 inches. Hence, completion of the move would require motion of both the micromanipulator and macromanipulator (Hitachi).

The input to the Hitachi servos was a position ramp. The input to the micromanipulator was the instantaneous position of the macromanipulator + 0.1 inches. If the command amounted to the final goal plus or minus 0.1 inches, then the micro-

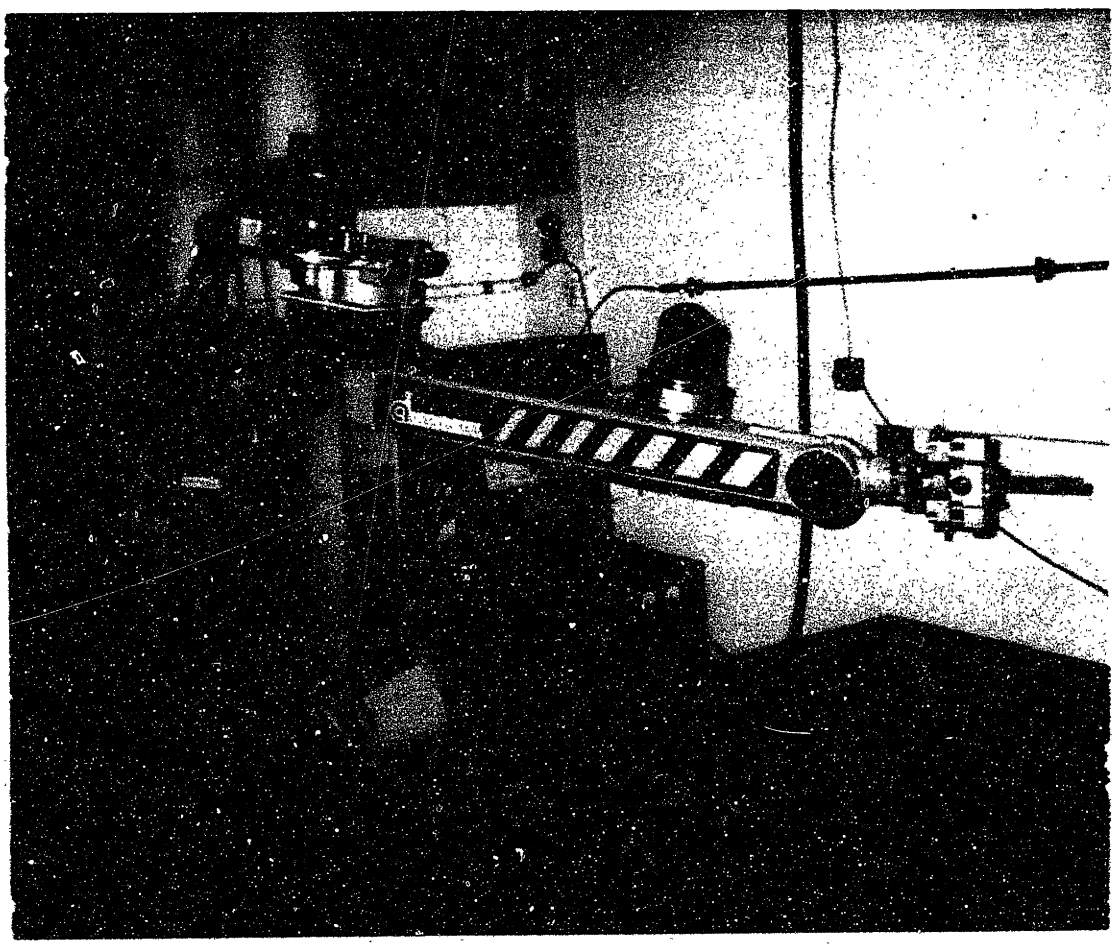

Figure 6.3: Micromanipulator Attached to an Industrial Robot.

manipulator was commanded to move to the final goal. In other words, in order to prevent the micromanipulator from exceeding its travel range, it was always kept (by software) within its travel range of the macromanipulator.

The response of the system is shown in Figure 6.4. It is observed that the micromanipulator shoots out much faster than the macromanipulator. It then runs out of travel range and has to wait for the macromanipulator to catch up. When the system gets close to the final destination, the micromanipulator locks in on it and compensates for the remaining motion of the macromanipulator. Note that the tool or endpoint completes the move in about one half the time it takes the macromanipulator in this particular move. This experimentally obtained response qualitatively agrees with the simulated response of Figure 3.12. The parameter values used in that simulation are not representative of the Hitachi robot, hence a quantitative agreement was not expected.

6.4 One-Axis Macro/Micro Manipulator Test-Bed

In order to validate the analytical prediction that a macro/micro manipulator is inherently more stable and better suited for endpoint control than a conventional robot, an experimental test bed was designed and constructed. The prototype micromanipulator described in section 6.2 was attached to a very flexible (first structural mode at 1.8 Hz), one-axis macromanipulator (see Figure 6.5). The reason for using such a flexible structure is to accentuate the stability problems by examining an extreme case. It is not meant to imply that robots should be constructed with floppy

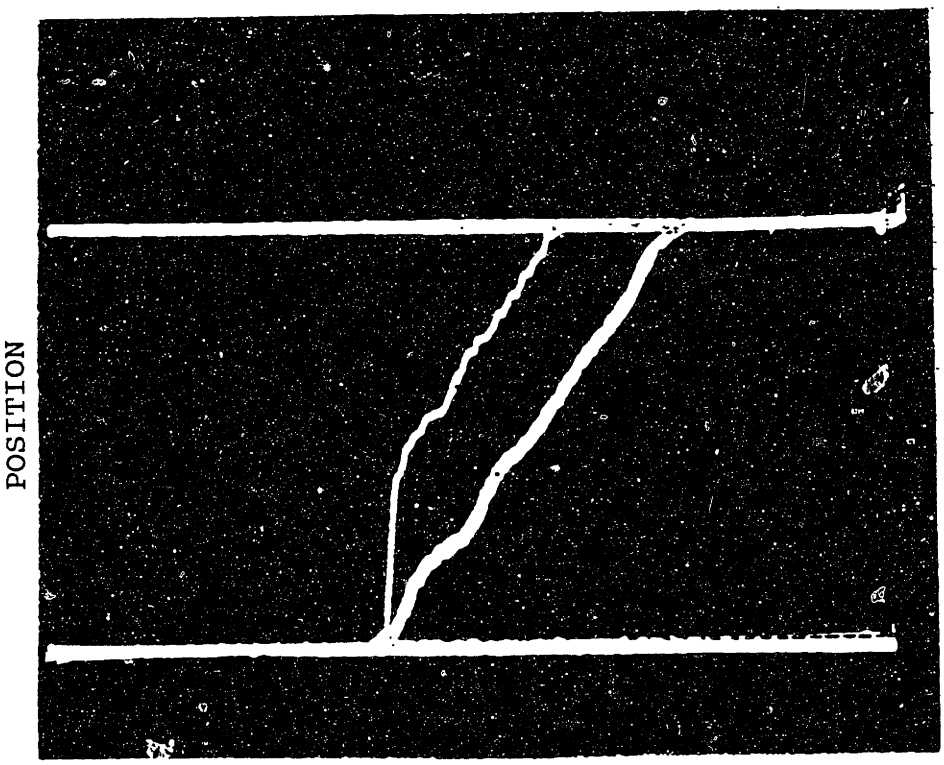

THIN TRACE: MICROMANIPULATOR

THICK TRACE: MACROMANIPULATOR

Figure 6.4: Response of Macro/Micro Manipulator to a 1/4 Inch Position Command.

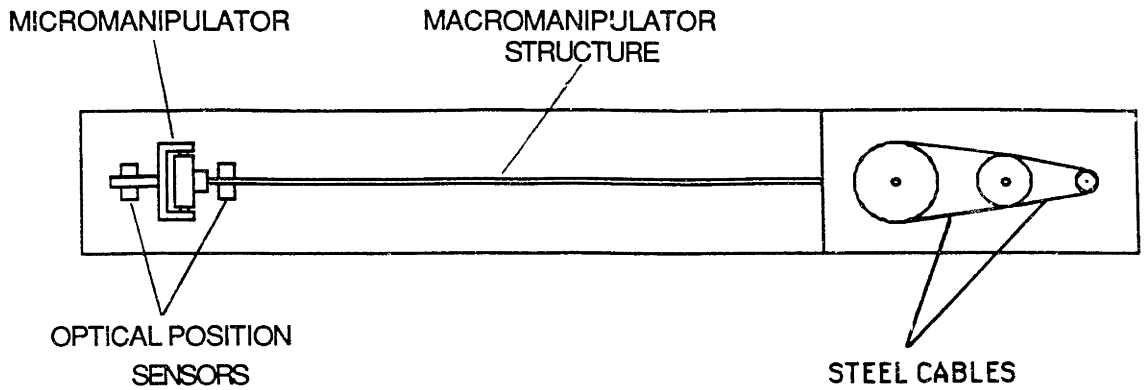

a.

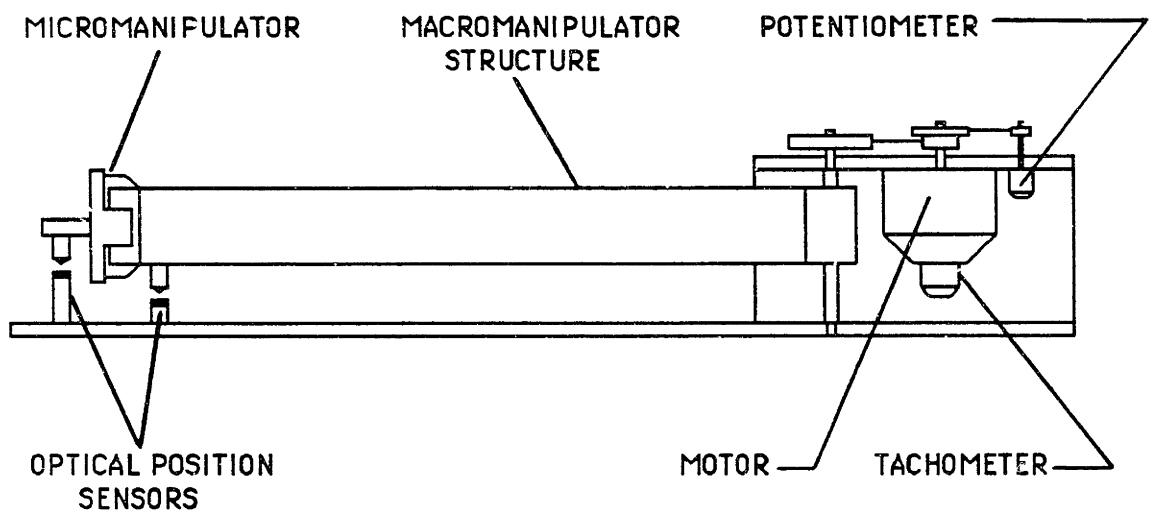

b.

Figure 6.5: a. Top View Schematic of Experimental Apparatus.
b. Front View Schematic of Experimental Apparatus.

structures. On the contrary, stiffer structures are generally easier to control. A flexible structure was used in this experiment to demonstrate how the addition of a micromanipulator would improve performance even in the worst case scenario.

The macromanipulator was actuated at the base by a PMI (model F12M4HA) electric motor. A steel cable with a 3:1 reduction was used to transmit the motor torque to the base of the macromanipulator. The angular velocity of the base was measured by a tachometer integral to the motor. The angular position of the base was measured using a potentiometer driven by the motor through a steel cable with a 4:1 amplification factor. Hence the actual base rotation to potentiometer rotation ratio was 12:1. This was helpful because the maximum angular displacement of the macromanipulator was only about .3 degrees. The macromanipulator was controlled by an Aerotech (model 3010) voltage to current amplifier.

The micromanipulator was controlled by a Moog hydraulic servo-valve (series 30), along with a Moog (model 121A132) voltage to current amplifier. Only one axis of the micromanipulator was used to compensate for lateral motion of the macromanipulator. The endpoint position of the micromanipulator and macromanipulator was measured using United Detector optical sensors (PIN-LSC30D) with the corresponding 301B-AC amplifiers. The endpoint velocity of the micromanipulator was measured using a Schaevitz Engineering velocity transducer (model 6L3VT-Z). Front and top view photographs of the apparatus are shown in Figures 6.6 and 6.7 respectively.

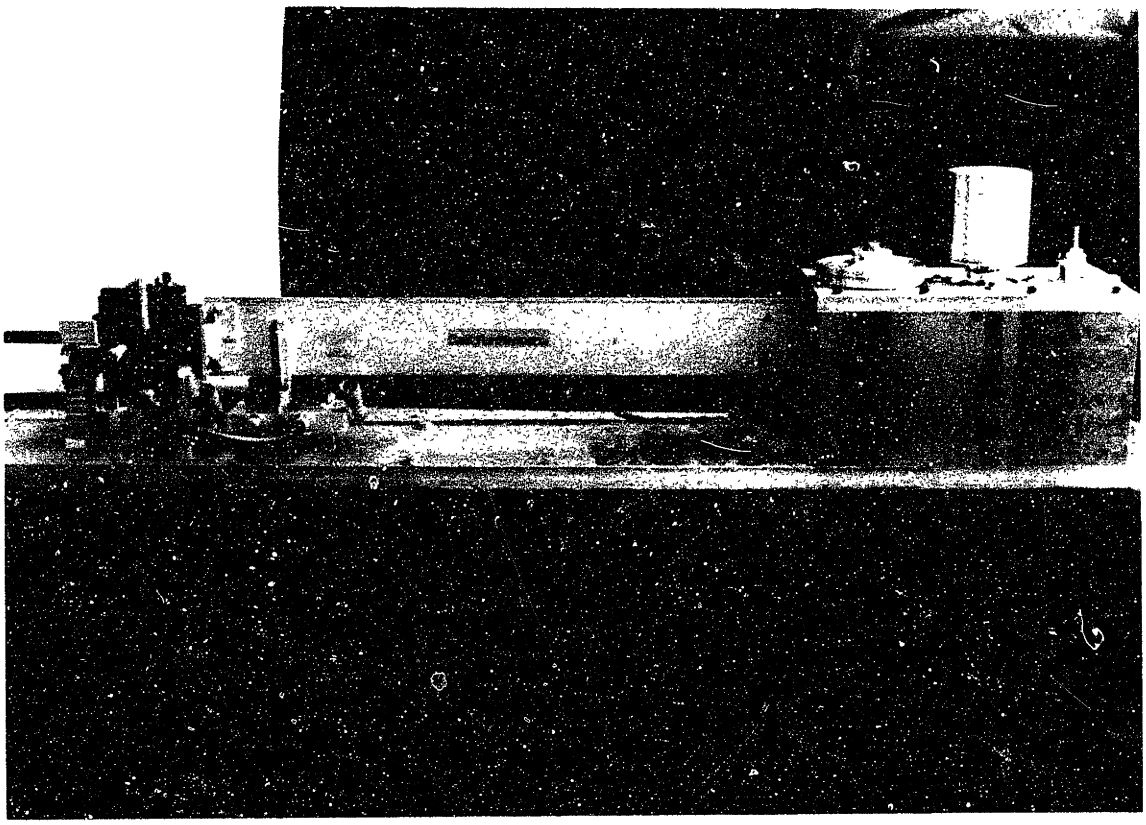

Figure 6.6: Front View Photograph of Experimental Apparatus.

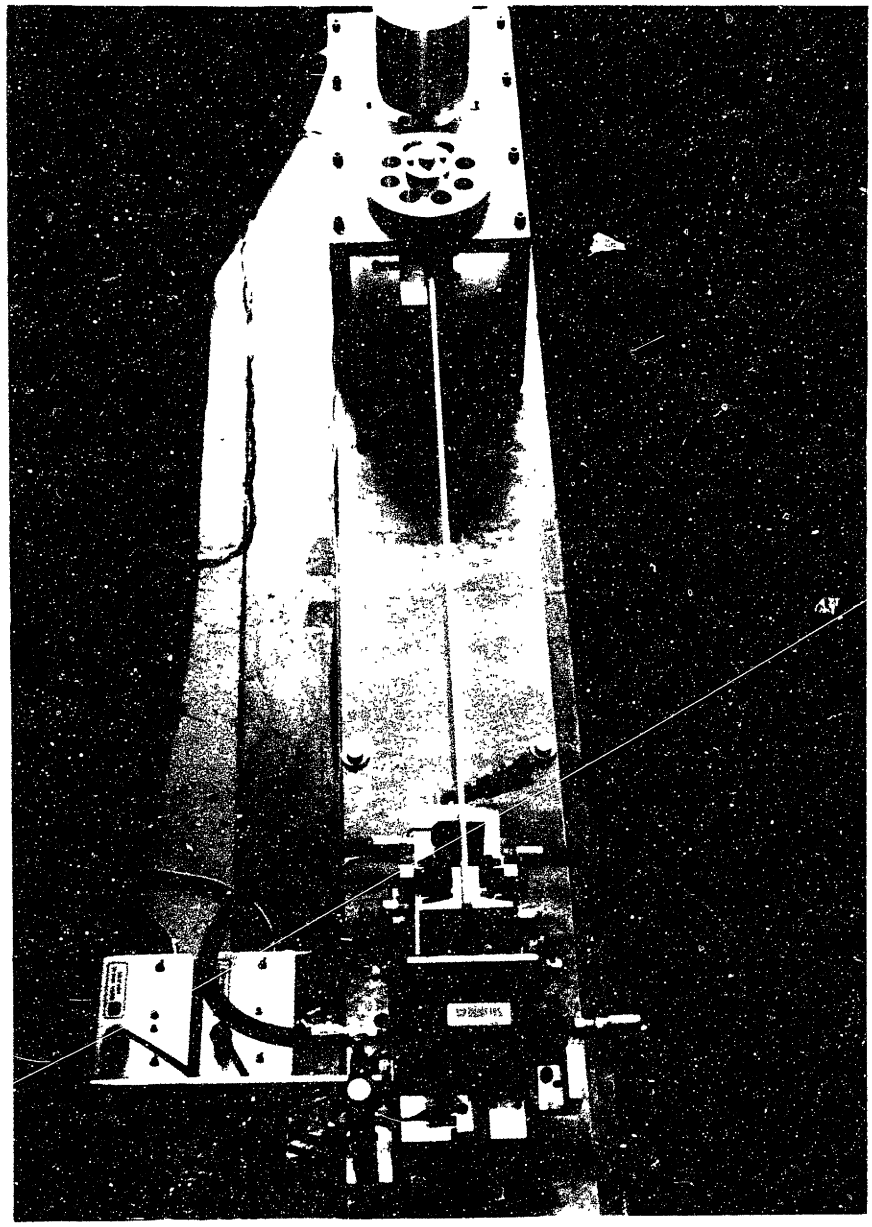

Figure 6.7: Top View Photograph of Experimental Apparatus.

6.5 Unconstrained Motion

6.5.1 Collocated vs. Non-collocated Control

The apparatus described in section 6.4 was used to validate the analytical prediction that collocated control is inherently stable while non-collocated control is inherently unstable. The micromanipulator was turned off during these experiments. The behavior of the macromanipulator alone was studied by subjecting it to a series of step position commands.

In the first experiment, the macromanipulator was actuated by the base motor and controlled using base measurements (collocated control). An oscilloscope picture of the best possible step response obtained with proportional control is shown in Figure 6.8. It is observed that it takes about 1.2 seconds for the macromanipulator to settle. When the gain was increased to the highest possible value obtainable in this apparatus, the response become quite oscillatory, but nevertheless stable (see Figure 6.9a). This result is commensurate with the analytical prediction that collocated control is inherently stable.

In the second experiment, the same apparatus was used, but instead of using base measurements for feedback, the endpoint position of the macromanipulator was used as proportional feedback (non-collocated). The micromanipulator was still turned off, and the macromanipulator was actuated using the base motor. The response of the system to a step position command is given in Figure 6.9b. It is seen that instability occurs even though the gain used in this experiment was five times smaller than that used in the collocated experiment of

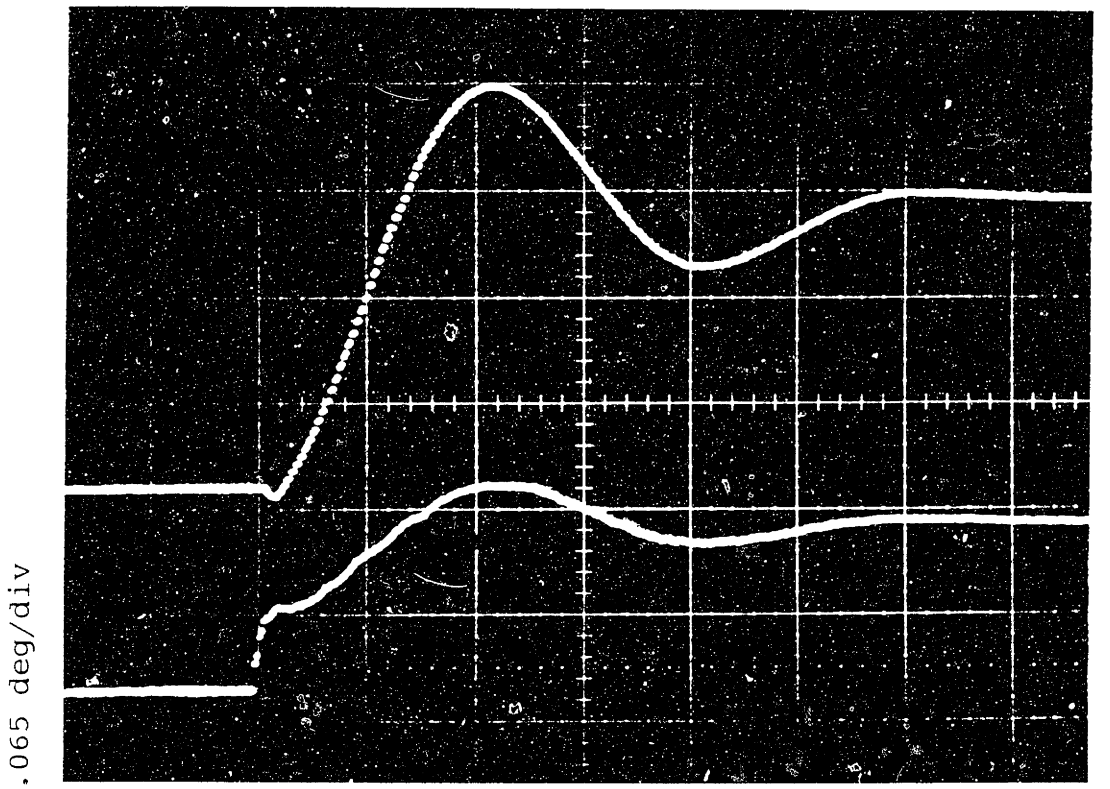

UPPER TRACE: ENDPOINT DISPLACEMENT
LOWER TRACE: BASE ROTATION

Figure 6.8: Best Position Step Response of Macromanipulator With Collocated Control.

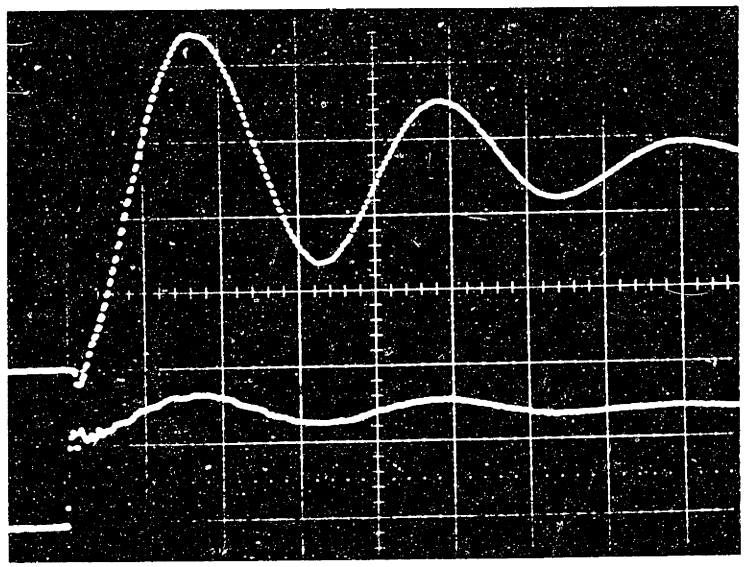

a.

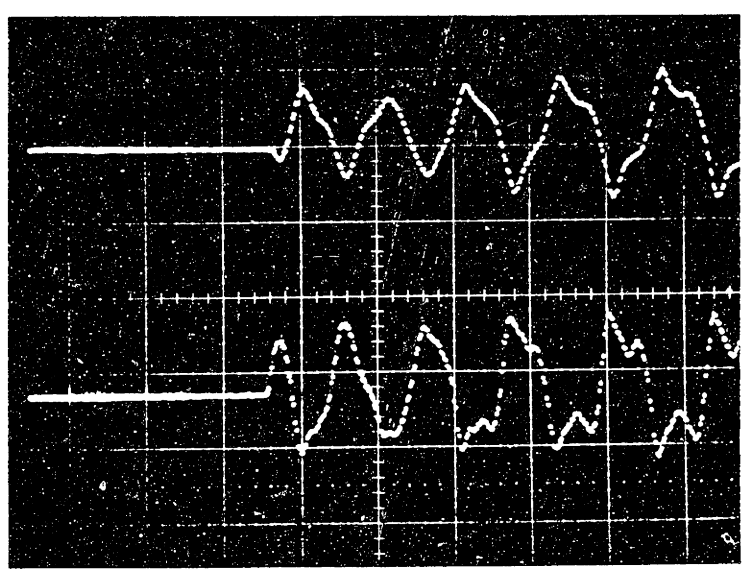

b.

Figure 6.9: a. Collocated Position Control of Macromanipulator With Highest Obtainable Gain.
b. Non-collocated Position Control of Macro-manipulator With 1/5 of Maximum Gain.

Figure 6.9a. This confirms that non-collocated control is inherently unstable at high gain.

6.5.2 Endpoint Position Control of a Macro/Micro Manipulator

The purpose of the experiments described in this section was to validate the analytical prediction that a macro/micro manipulator is inherently more stable and better suited for endpoint control than a conventional robot, and to quantify the improvement in performance. The apparatus described in section 6.4 was used, but this time the micromanipulator was activated as well. The macromanipulator was actuated at the base and controlled using base measurement (collocated control). The micromanipulator was controlled using endpoint measurement.

A step position command was simultaneously issued to both the macro and micro manipulators. The response of the system endpoint (micromanipulator position) as well as that of the macromanipulator is shown in Figure 6.10a. The micromanipulator reaches its target very quickly and locks in on it while the macromanipulator is still moving. Recall that there is no connection between the micromanipulator and ground. It is carried by the macromanipulator, yet it is capable of compensating for the macromanipulator's undesirable motion.

Since the micromanipulator's motion excites the macromanipulator, it would not be fair to evaluate performance improvement by comparing the endpoint response to that of the macromanipulator response while the micromanipulator is active. Instead, it should be compared to the response of the macromanipulator alone. Hence, the best achieved response of

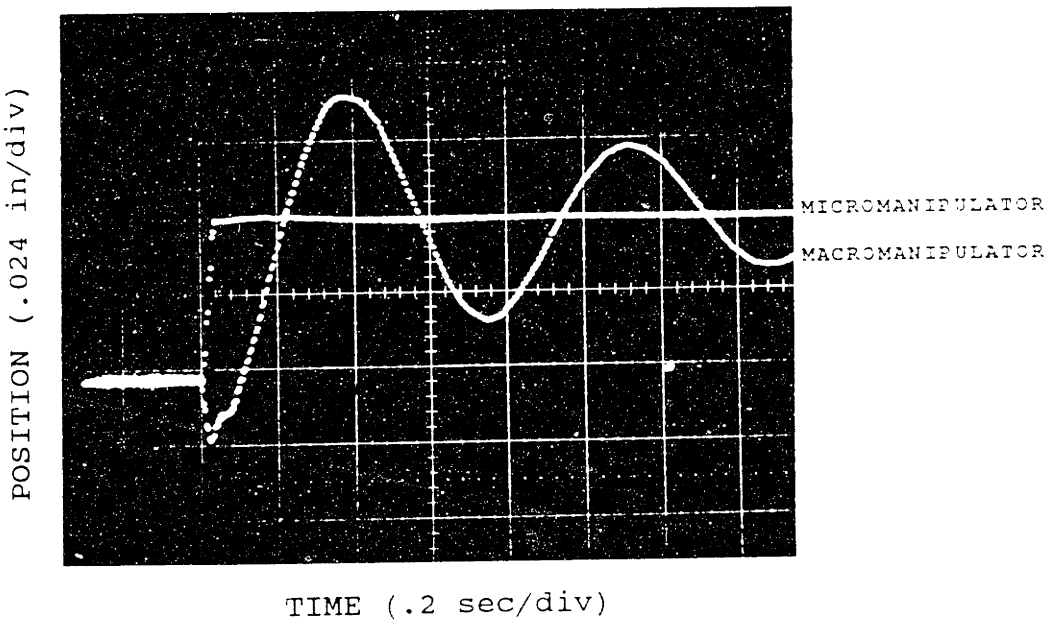

a.

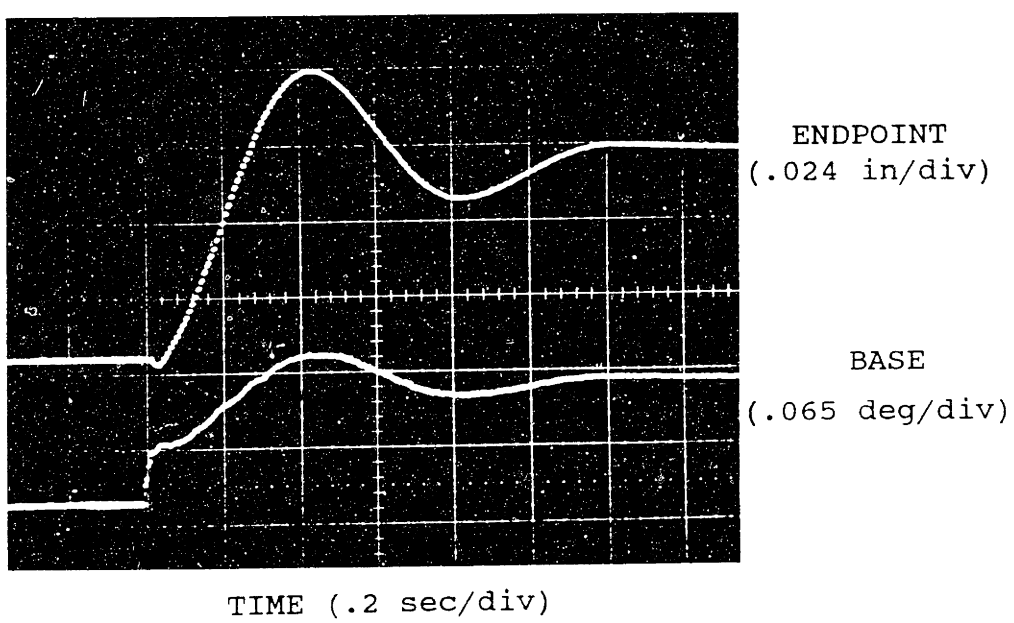

b.

Figure 6.10: a. Response of Macro/Micro Manipulator to a Step Position Command.
b. Best Obtainable Response of Macromanipulator to a Step Position Command.

the macromanipulator (Figure 6.8) is reshown in Figure 6.10b for comparison. It is noted that the macro/micro manipulator settles in 40 milliseconds while the macromanipulator alone settles in 1.2 seconds. The settling time is reduced by a factor of 30. Figure 6.11 illustrates the same response as Figure 6.10a but with a larger time scale, which shows that the macromanipulator does indeed settle and is not continuously excited by the micromanipulator.

Examining Figures 6.10a and 6.11 again, it is seen that the micromanipulator maintains the system endpoint quite stationary. Yet, while it is maintained well within a 5% settling range, it is not perfectly motionless. Relative to the oscillatory motion of the macromanipulator, however, it provides an extraordinary improvement. If the macromanipulator structure was stiffer, the motion of the endpoint after it reached the target would become negligible.

Once stability and improvement in performance was demonstrated, it was desired to determine the actual bandwidth of the macro/micro manipulator. The position of the macromanipulator was regulated about zero, while a sinusoidal command was issued to the micromanipulator. Figure 6.12 illustrates the system endpoint response vs input. At a frequency of 20 Hz the system endpoint tracks the input with no attenuation at all, with a phase-lag of about forty five degrees. A -3 dB bandwidth of 28 Hz is achieved. The corresponding phase-lag is somewhat greater than ninety degrees. This is an order of magnitude higher than the first structural mode (1.8 Hz). It is also higher than the second structural mode (20 Hz) of the macromanipulator. These structural frequencies were determined experimentally by locking the motor shaft and exciting the endpoint of the beam by hand.

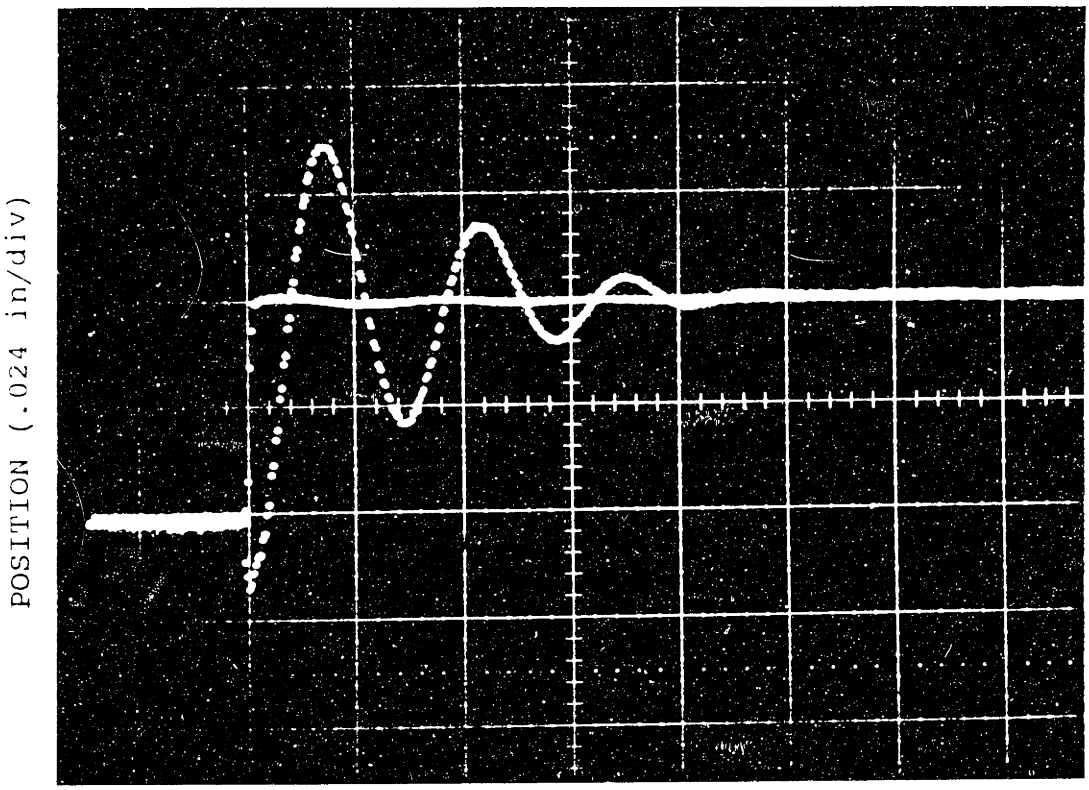

Figure 6.11: Extended Response of Macro/Micro Manipulator to a Step Position Command.

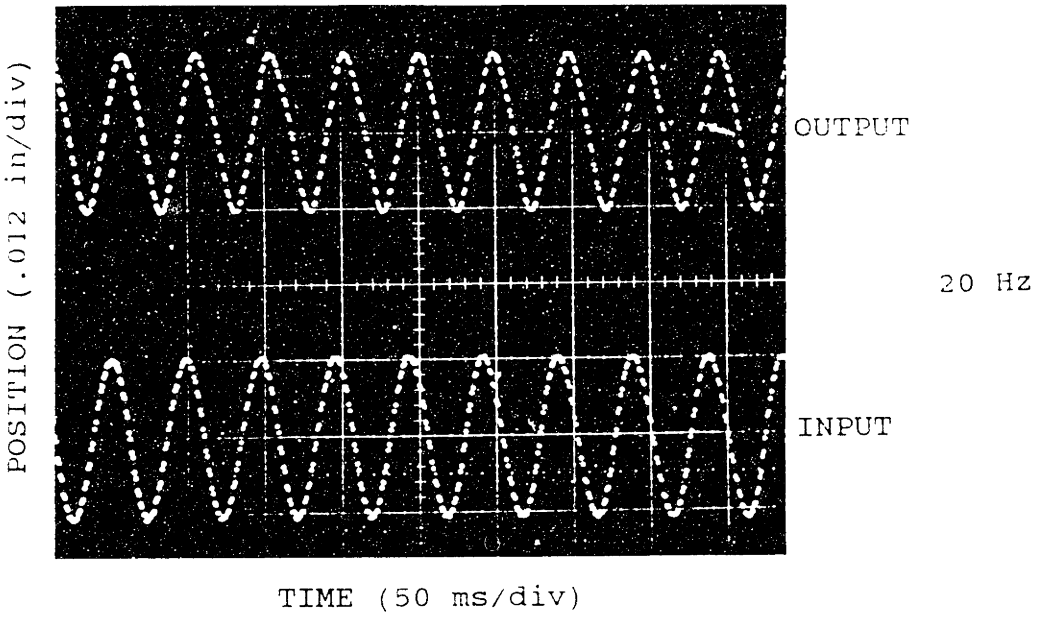

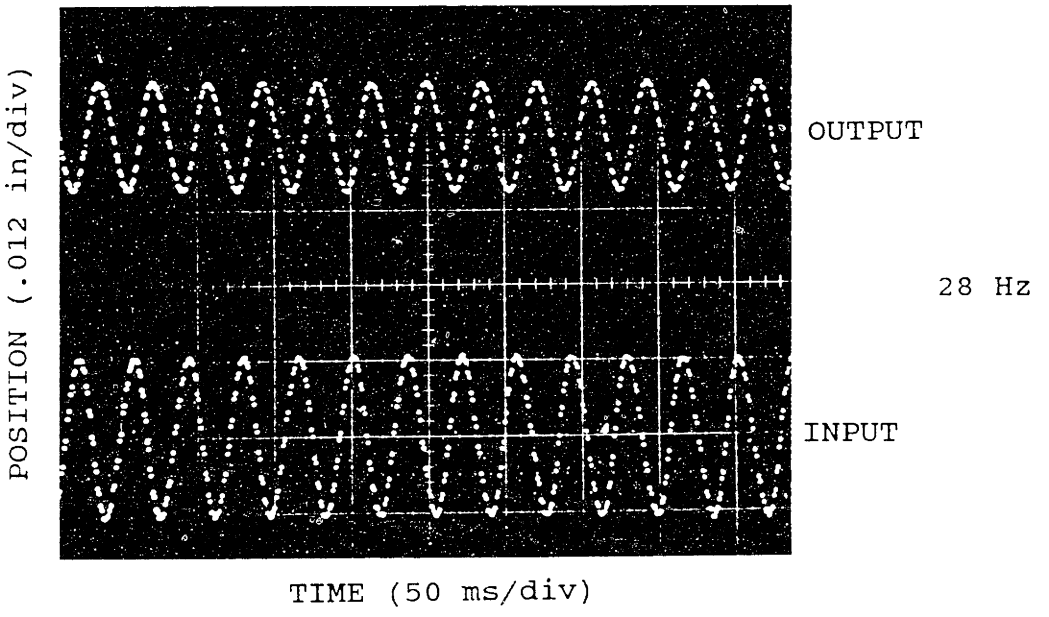

Figure 6.12: Response of Macro/Micro Manipulator to Sinusoidal Position Inputs.

It should be noted that a bandwidth of 28 Hz is only achievable if the micromanipulator does not exceed its travel range. Hence, a design tradeoff must be made in specifying the micromanipulator's travel range. A small range may restrict applicability, while a large range may degrade performance.

6.6 Constrained Motion

The purpose of the experiments described in this section was to validate the analytical predictions that a macro/micro manipulator is inherently more stable and better suited for force control than a conventional robot, and to quantify the improvement in performance.

In principle, the macro/micro manipulator can alleviate all the problems of force control listed in section 4.2. However, the prototype micromanipulator used in this work is hydraulic, and behaves like a flow source rather than a torque source. Hence, as explained in section 4.2, it is not well suited for force control. In order to alleviate this problem, a soft (15 lb/in) interface had to be placed between the force sensor and the rigid environment. Nevertheless, it is shown experimentally that the macro/micro manipulator is beneficial with respect to the other problems of force control: non-collocation, initial impact, and low interface damping. The same soft interface was used for both the macro-manipulator alone as was for the macro/micro manipulator. Hence, the performance of both systems can be compared.

A PCB (model 208A02) piezo-electric force sensor was attached to the endpoint of the system described in section

6.4. This sensor is virtually incompressible (10^7 lb/in stiffness). It was desired to regulate the force applied to a rigid environment through the interface described above.

Recent findings by Colgate[30] indicate that the stiffness of the environment relative to the robot structure is of primary importance, and not necessarily the absolute value. More specifically, using conventional robot architectures, it is extremely difficult to achieve good force control against environments that are as stiff or stiffer than the robot structure. While the interface used in these experiments was fairly soft, it was actually five times stiffer* than the macromanipulator structure. It will be shown in this chapter that the macro/micro manipulator architecture can overcome this restriction.

6.6.1 Force Control of a Macromanipulator.

With the micromanipulator turned off, the macromanipulator was commanded to apply a force of 0.2 pounds to the environment. The force measurement from the transducer was fed back in a negative proportional fashion. The initial position of the macromanipulator was 0.050 inches away from the environment. Hence, the system was out of contact with the environment at time zero. When the step force command was issued, the system impacted the environment and attempted to regulate the applied force. The force response at various gains is given in Figure 6.13.

---

* The structural stiffness of the macromanipulator was determined by locking the motor shaft and measuring the force necessary to deflect the endpoint of the structure by 0.25 inches.

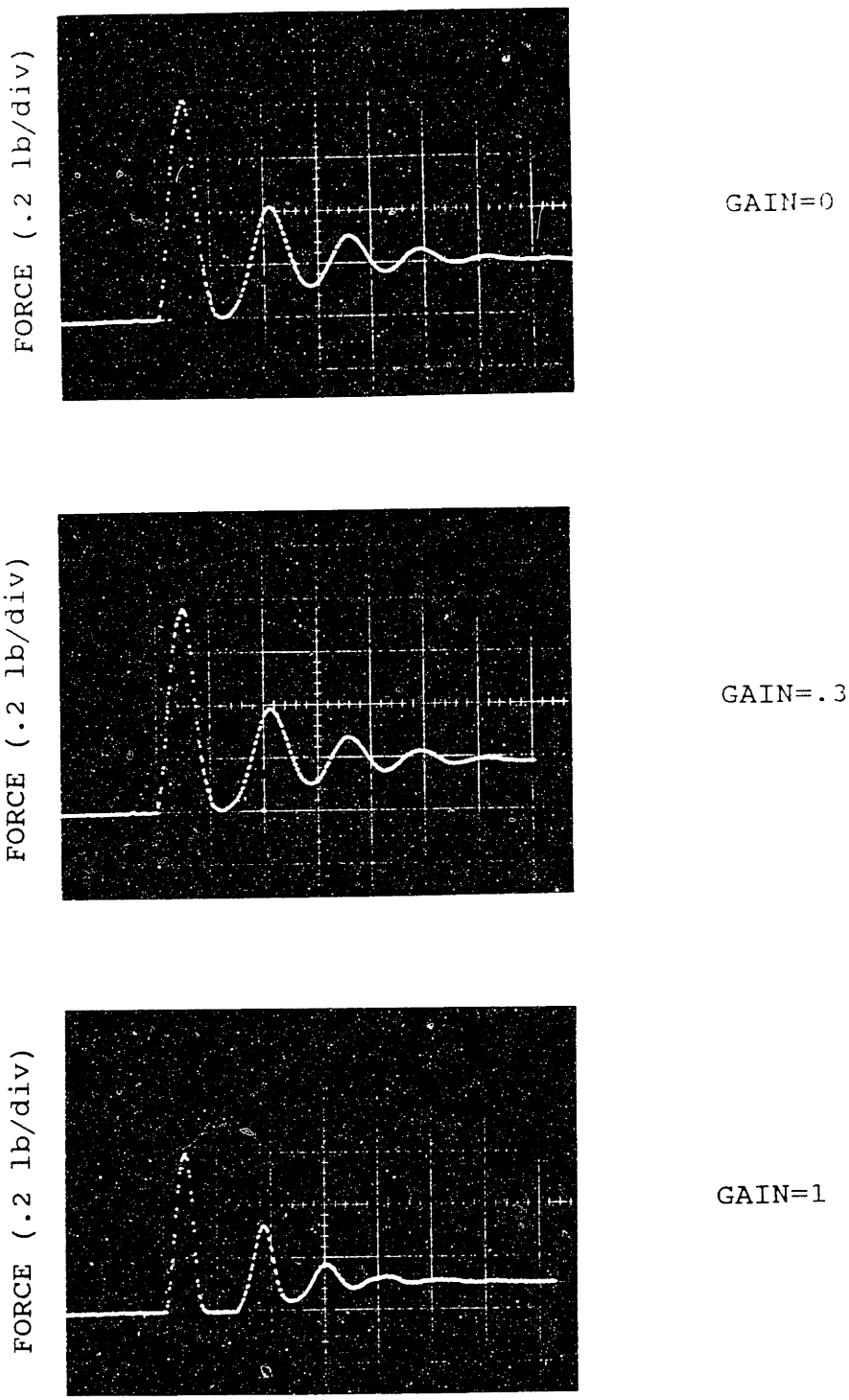

Figure 6.13: Response of Force Controlled Macromanipulator to a Force Step With Initial Impact.

(Cont'd)

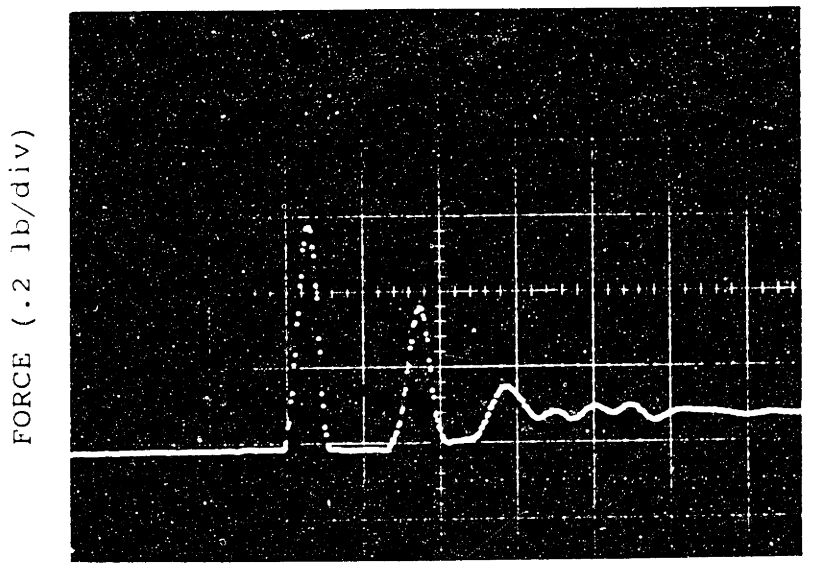

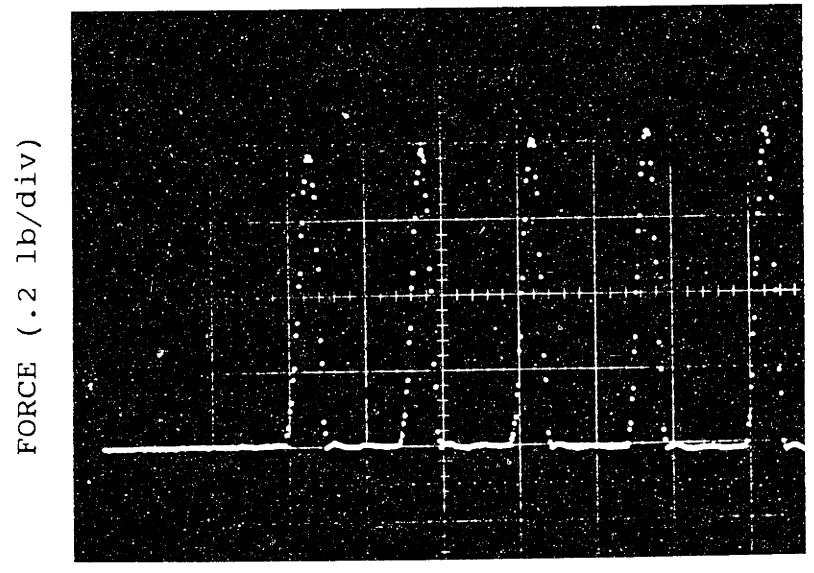

Figure 6.13: (Cont'd)

Examining the open loop case, the system exhibits a force peak due to initial impact, bounces back, almost losing contact, and then settles on the desired force value. It takes about 1.3 seconds from impact for the macromanipulator to settle. As the gain was increased, bouncing became more severe. In fact, at a gain of about 2, the system became unstable. This confirms the analytical prediction that high performance force control on conventional robots is inherently unstable due to non-collocation of actuator and sensor. Note that instability occurred despite the use of a soft interface. The non-collocation problem is present regardless of the interface stiffness.

Comparing this experimental result with the simulation of Figure 4.6, it verified that increasing the gain gives rise to more bouncing. Instability was not exhibited in that simulation, as was in the experiment, because the simple model used was purposely formulated to be stable for all gains. This was done in order to distinguish the performance issues from the stability issues.

6.6.2 Force Control of a Macro/Micro Manipulator

This experiment was similar to the last one, only this time the micromanipulator was activated as well. The position of the macromanipulator was regulated about zero. The micromanipulator was commanded to exert a 0.2 pound force against the same environment as in the last experiment. The micromanipulator was force controlled by feeding back the measurement from the transducer in a negative proportional fashion. The system once again began 0.50 inches away from the

environment, giving rise to an impact. The step response is shown in Figure 6.14a. The best obtained force control response of the macromanipulator alone (open loop) is repeated in Figure 6.14b for comparison purposes.

It is seen in Figure 6.14a that the initial impact no longer produces a large force peak. Furthermore, the large oscillations exhibited by the macromanipulator are greatly suppressed. A magnified view of the first 60 milliseconds (see Figure 6.15) reveals a rise time of only 10 milliseconds, with very little overshoot.

Once it was established that the macro/micro manipulator's performance in force control is highly superior to that of the macromanipulator, it was desired to determine its bandwidth. The macro/micro manipulator's ability to track a sinusoidal force input was characterized. The response at various frequencies is shown in Figure 6.16. It is observed that the macro/micro manipulator can track sinusoidal inputs up to a frequency of 50 Hz with virtually no attenuation, and a phase-lag of about forty five degrees. The -3 dB bandwidth is shown to be 60 Hz, with a corresponding phase-lag that is somewhat greater than ninety degrees. This is 32 times higher than the frequency of the first structural mode of the macromanipulator, establishing that high bandwidth force control can be achieved when using the proper physical architecture.

6.7 Chapter Summary

The experiments described in this chapter confirm the analytical predictions that a macro/micro manipulator is an inherently stable and well suited physical architecture for

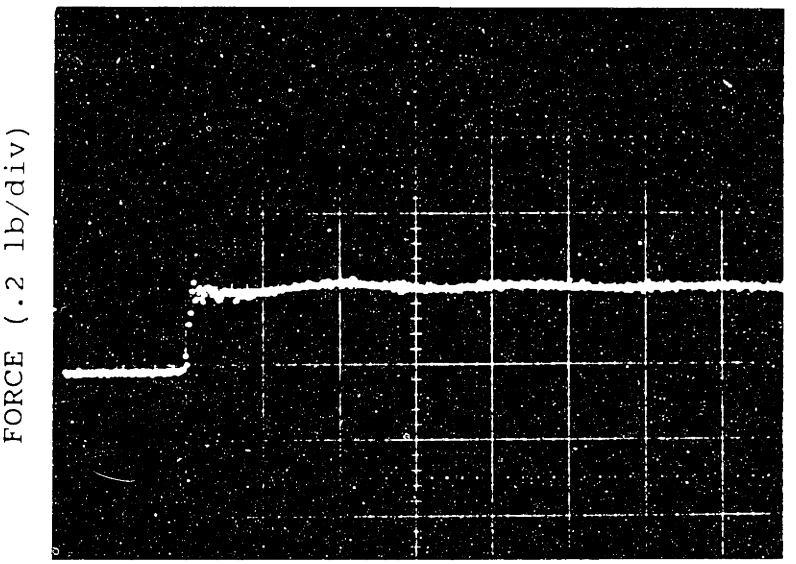

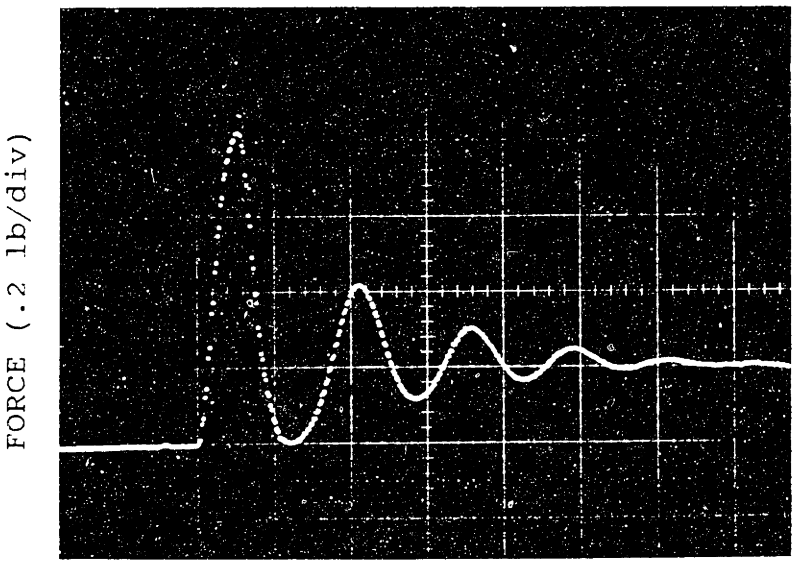

Figure 6.14: a. Response of Force Controlled Macro/Micro Manipulator to a Force Step With Initial Impact.
b. Response of Open Loop Force Controlled Macromanipulator to a Force Step With Initial Impact.

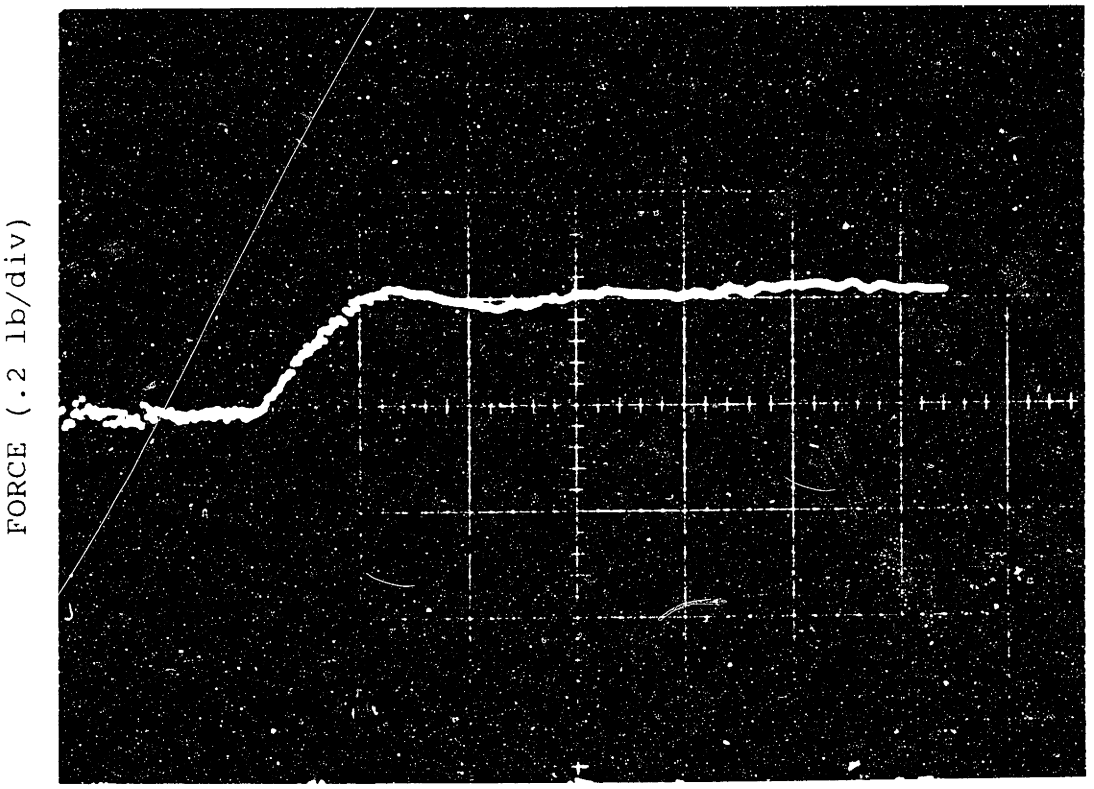

Figure 6.15: Magnified Response of Force Controlled Macro/Micro Manipulator to a Step Force With Initial Impact.

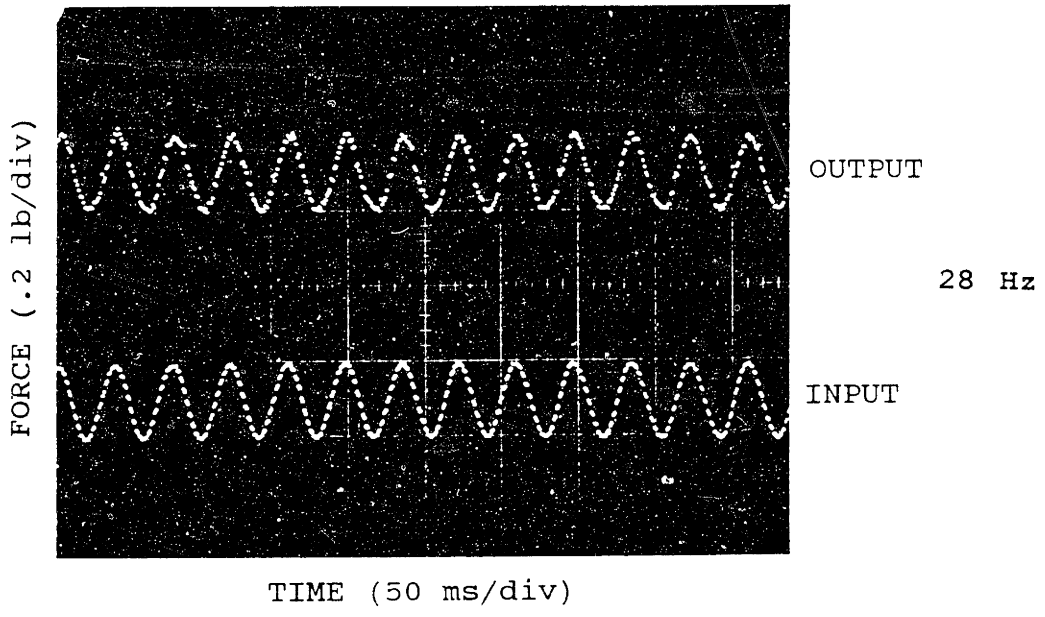

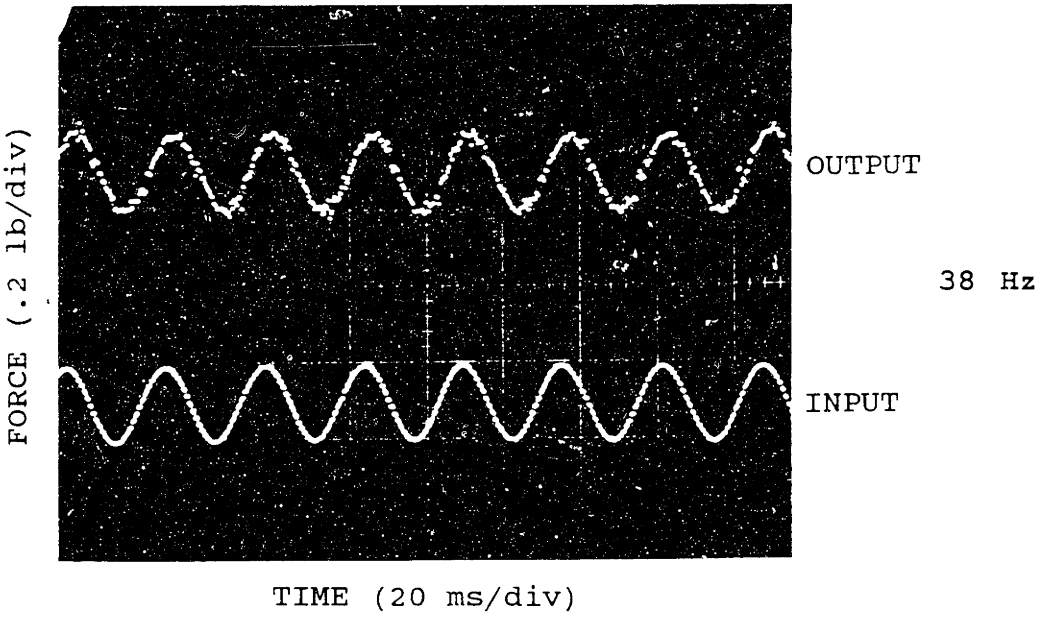

Figure 6.16: Response of Force Controlled Macro/Micro Manipulator to Sinusoidal Force Inputs.

(Cont'd)

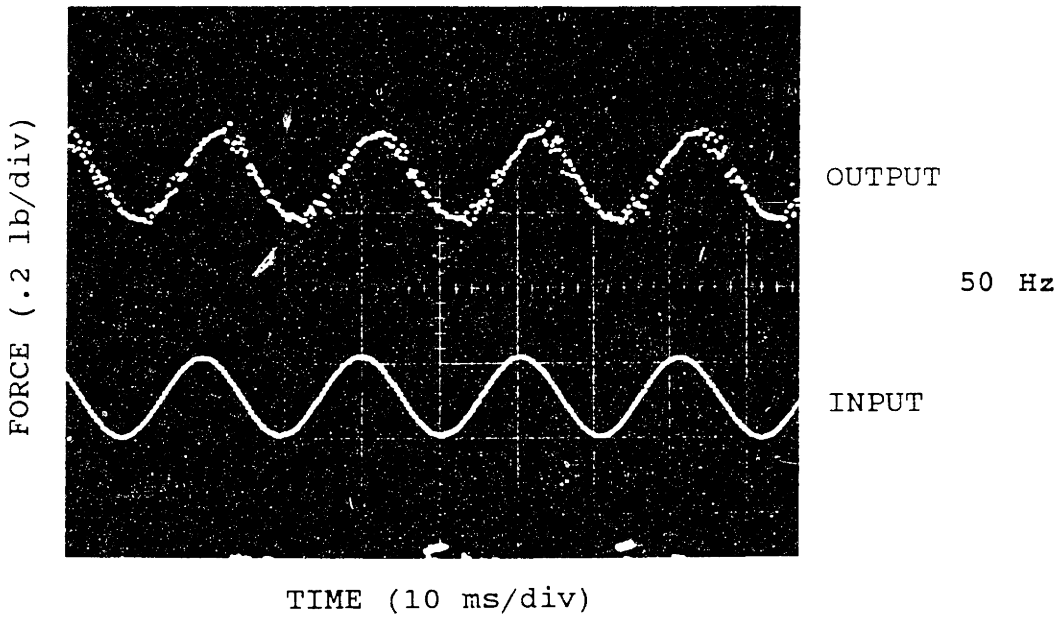

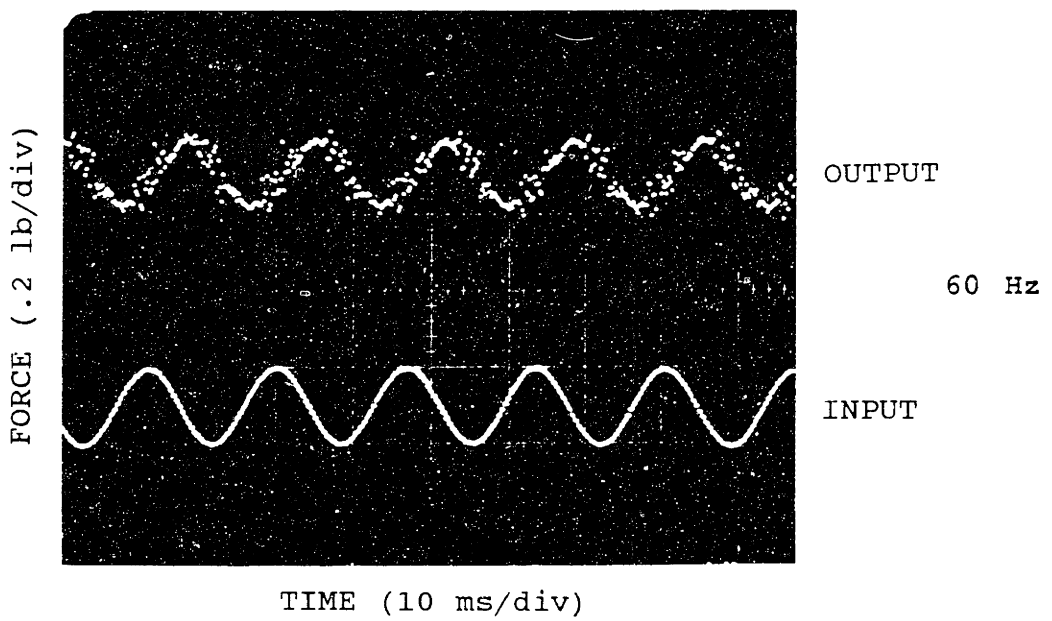

Figure 6.16: (Cont'd)

high performance endpoint control. The ability of the system to regulate endpoint position and interface forces was shown to be greatly superior to that of a conventional robot.

An endpoint position control bandwidth of 28 Hz, 15 times higher than the frequency of the first structural mode of the macromanipulator, was achieved.

A force control bandwidth of 60 Hz, 32 times higher than the frequency of the first structural mode of the macro-manipulator, was achieved against an environment that is five times stiffer than the robot structure. This demonstrates that high bandwidth force control can indeed be achieved when the proper physical architecture is used.

Finally, it should be noted that while endpoint velocity feedback was analytically shown to be very beneficial in force control, it is very difficult to obtain in practice. The reason for this is that when the robot is in contact with the environment, the resulting motion is generally below the resolution of the velocity transducer. Intrinsic damping, as close to the endpoint as possible, would help.

Chapter 7

GENERALIZATION OF CONCEPTS

While most of the research presented in this document pertains to a macro/micro manipulator system, some of the concepts developed are generic enough to be applicable to a wide range of problems. The scope of this chapter is to show the generality of these concepts.

7.1 Macro/Micro Separation Concept

The macro/micro manipulator was shown to be an inherently stable and well suited physical architecture for high performance control. The system was able to alleviate the problems caused by transmission line dynamics in conventional robots. A robot structure, however, is just one form of a transmission line. The macro/micro separation concept can be used to reduce the effect of undesirable dynamics associated with most transmission lines.

A generalized transmission line can be thought of as the path between two points. Any entity transferred from one point to another must be sent along a transmission line. The entity may be matter or non-matter. Examples include forces, fluids, heat, light, discrete manufacturing jobs, unemployment, inflation, etc.. Transmission lines may or may not give rise to undesirable dynamics. Vacuum, for example, is an excellent transmission line for light. A robot structure, on the other hand, is a terrible transmission line for sending forces from one point on the structure to another. This is

generally true of most transmission lines when using non-collocated control.

Consider the system shown in Figure 7.1 as an example of a fluidic transmission line. The diagram represents a vertical reservoir connected to two hoses. The fluid capacitance in the reservoir is denoted by C. The first hose is supplied fluid by a variable pressure source (P). There is a constriction (R_2) between the reservoir and the hoses. The fluid flowing in the supply hose experiences a line resistance (R_1) and exhibits an inertia (I_1). The fluid flowing through the second hose exhibits an inertia (I_2). It is desired to control the fluid output through the second hose by controlling the pressure source (P) in a closed loop fashion.

The bond graph characterizing this system is given in Figure 7.2a. The bond graph characterizing the robot structure of Figure 3.1a is reshown in Figure 7.2b for comparison. It is noted that the structure of the two bond graphs is the same. In fact, if generalized effort, flow, capacitance, inductance and resistance variables are used in both cases, the bond graphs become identical. Hence, the structure of the fluid system described is equivalent to that of the simple robot of Figure 3.1a. It can therefore be concluded that this fluidic system is inherently unstable and ill suited for high bandwidth control as well. Since the macro/micro separation concept was able to alleviate the problems caused by the undesirable transmission line dynamics of the robot structure, it should be able to help in this system as well.

Consider now the addition of another pressure source (p) supplying the second hose through a constriction (R_3), as shown in Figure 7.3. It is still desired to control the fluid output in a closed loop fashion. This time, however, both P

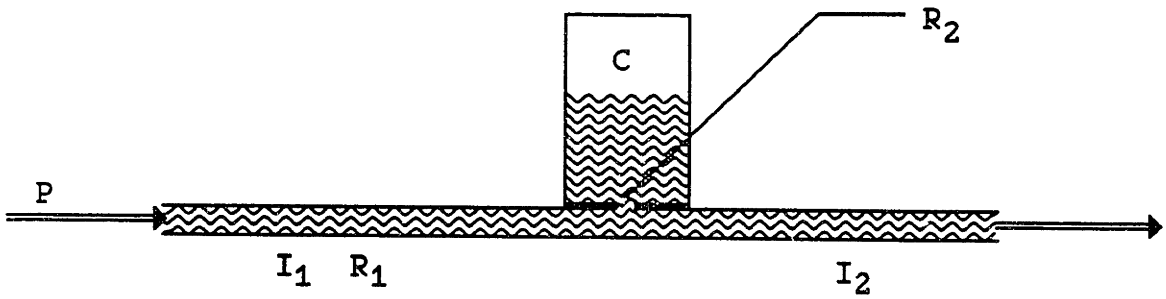

Figure 7.1: Fluidic Transmission Line.

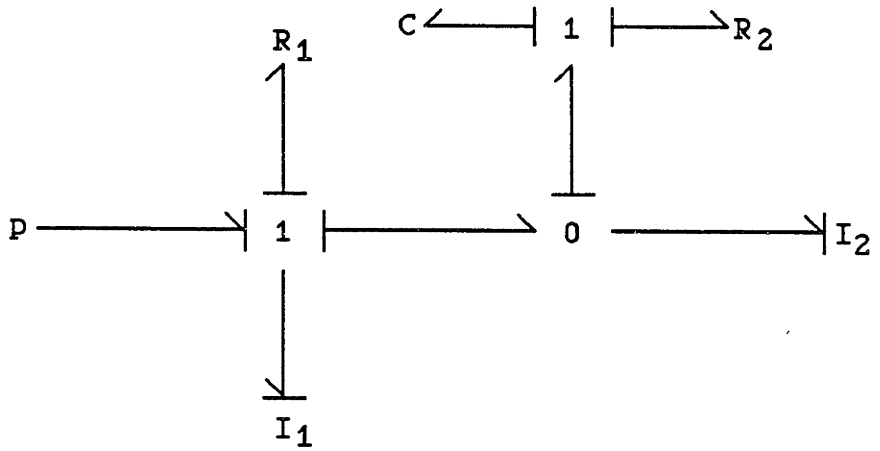

a.

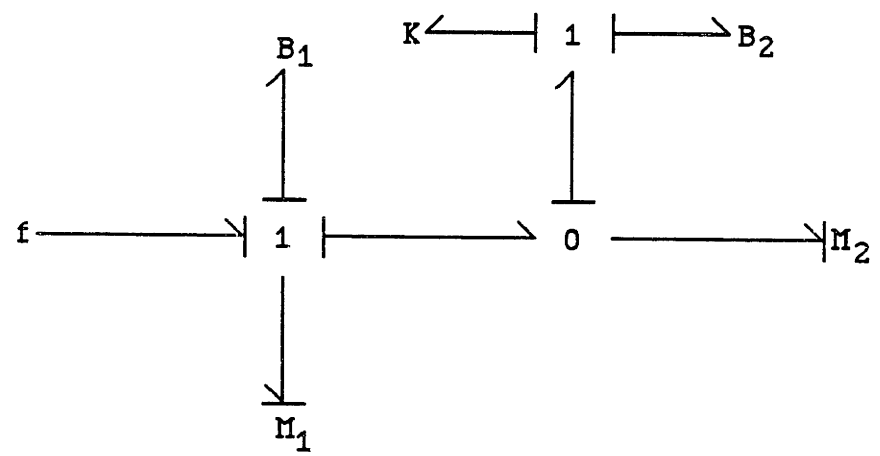

b.

Figure 7.2: a. Bond Graph of Fluidic Transmission Line.
b. Bond Graph of Robot Structure.

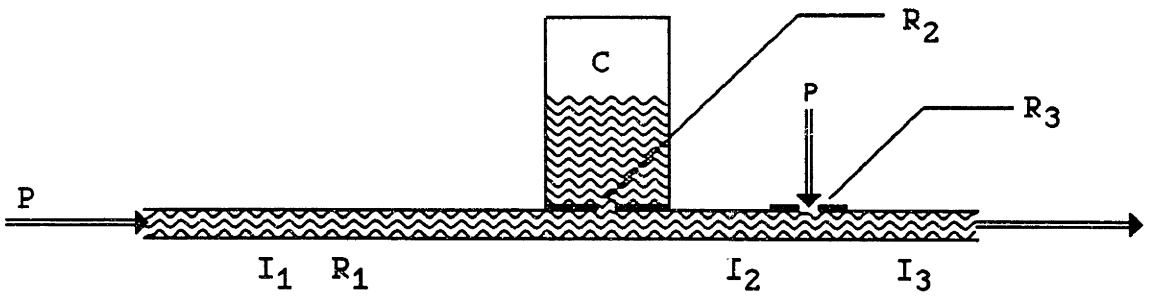

Figure 7.3: Modified Fluidic Transmission Line.

and p are utilized in the control.

The bond graph characterizing this system is given in Figure 7.4a. The bond graph characterizing the macro/micro manipulator of Figure 3.2 is given in Figure 7.4b. It is seen that both bond graphs have the same structure. If generalized variables are used in both cases, the bond graphs once again become identical. Thus, the system of Figure 7.3 is the fluidic equivalent of the mechanical macro/micro manipulator. The analysis developed for the macro/micro manipulator is therefore applicable to this system as well. It is hence concluded that this fluidic system is inherently more stable and better suited for high bandwidth control than the fluidic system of Figure 7.1.

The fluidic systems described in this section are not just academic examples. The system of Figure 7.1 represents a simple lumped parameter model of the transmission line associated with controlling a hydraulic piston through a long hose, using a servo-valve. The fluid capacitance represents the compressibility in the fluid. The servo-valve dynamics are neglected in this model. In many situations requiring high bandwidth, it is desired to minimize the moving inertia. Hence, in order to reduce that inertia, the servo-valve is placed at the stationary base of the system, rather than on the moving piston. The hydraulic fluid is then supplied to the piston through a long hose. As was explained previously, however, this limits the achievable bandwidth of the system due to the transmission line dynamics (fluid compressibility).

The system of Figure 7.3 represents a simple lumped parameter model of the transmission line dynamics associated with controlling a hydraulic piston using two servo-valves: one large (macrovalve), with high flow capability at the base.

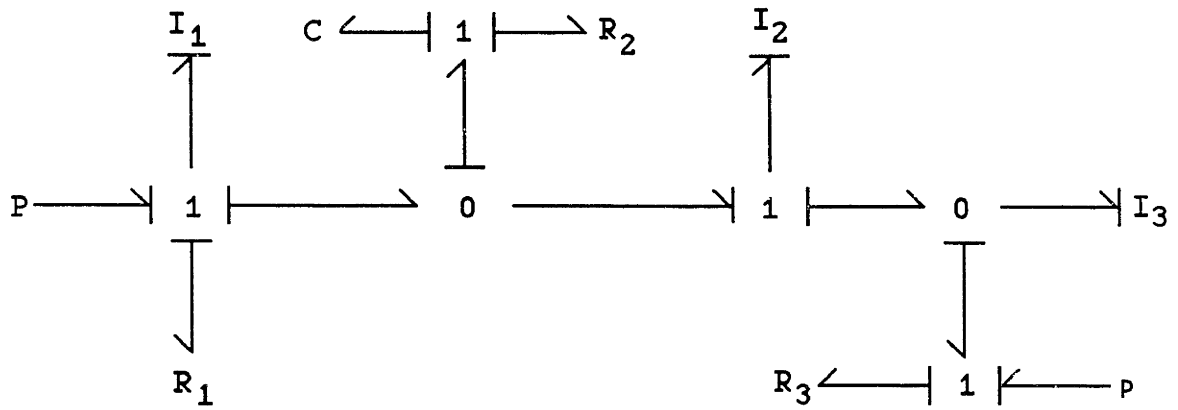

a.

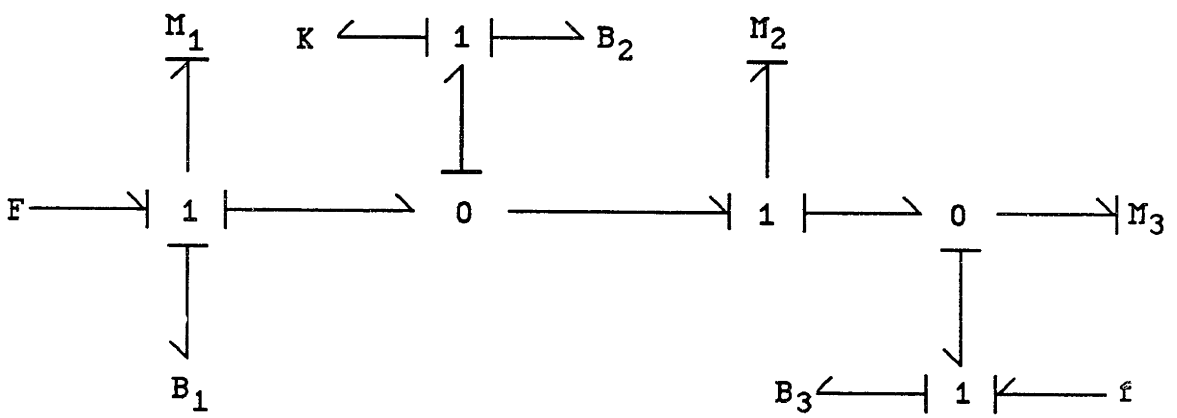

b.

Figure 7.4: a. Bond Graph of Modified Fluidic Transmission Line.
b. Bond Graph of Macro/Micro Manipulator.

and one small (microvalve) with low flow capability right on the moving piston. The macrovalve supplies the nominal flow rate required, while the microvalve quickly compensates for deviations. The mass of the microvalve is much lower than that of the macrovalve. Hence, it can be attached directly to the moving piston without significantly increasing the moving inertia. This architecture is inherently more stable and better suited for high bandwidth control. Thus, the macro/micro separation concept is likely to be applicable to other systems besides mechanical robots.

7.2 Implications of Physical Equivalence

The concept of physical equivalence is very powerful. It states that for every controlled physical system, there exists a purely physical (no control) system whose behavior is identical. Hogan[23] postulates that "It is impossible to devise a controller which will cause a physical system to present an apparent behavior to its environment which is distinguishable from that of a purely physical system." Hence, a controller simply alters the behavior of one physical system such that it emulates another physical system. This implies that if a controlled system truly emulates a physical system whose behavior is known, then the complete controlled system can be characterized regardless of the details of how the controller accomplishes that task. For example, if a controlled system emulates a mass-spring-damper system, then it can be concluded that the system is stable, regardless of the implementation.

There are many possible control implementations that can make a physical system behave like a mass-spring-damper

system. Hence, physical equivalence is a high level abstraction of control systems. It is a many-to-one mapping, analogous to abstraction by specification in computer languages. In designing a complex computer program, abstraction is heavily used as means of focusing on what each procedure accomplishes rather than how it is implemented. This enables the programmer to concentrate on the task of the program without being cluttered with an unmanageable level of detail. Similarly, the control systems designer can use physical equivalence as a means of abstraction when designing control systems. This would be especially useful in complex systems.

Of course the details of the particular implementation are very important. Just as some implementations of abstraction in a computer program may be more robust or efficient than others, so is the case for control systems as well. Since in reality a controlled system does not perfectly emulate another physical system, the particular implementation will influence the quality and range of the emulation. Some of the reasons for imperfect emulation are: finite force sources, actuator dynamics including internal non-collocation, transmission line delays, etc. Thus, the details of implementation are extremely important. However, abstraction facilitates separation of design issues from implementation issues.

While selecting a target physical system to be emulated is relatively straightforward when stability is the sole criteria, selecting one based on desired behavior for a particular task is an open research question. It is not at all clear what the best system behavior is for a particular task. This is especially true in constrained, interactive tasks.

7.3 Control Systems Design Begins With Mechanical Systems Design

Control systems design is generally perceived as the manner in which measurement signals and predictions are conditioned and used to specify voltage or current levels applied to the actuators. This process is independent of the mechanical design process, and usually follows it. It is commonly assumed that the mechanical system already exists when it is "handed" over to the controls engineer. The author argues that this is a short sighted approach to controller design.

The time at which a mechanical or electro-mechanical design is specified is also the time when many restrictions are automatically placed on the controller design. Unfortunately, some traits that are considered beneficial from a mechanical design point of view may actually be detrimental from a controls point of view.

Consider, for example, the space shuttle arm. Its low mass is ideal for the application, since the cost of each kilogram of payload is phenomenal. On the other hand, its resulting low stiffness makes it extremely difficult to control.

Mechanical designers often strive to achieve as much shared functionality as possible. This reduces the number of components required in an assembly, perhaps improving reliability while reducing cost. This concept justifies the decision made by designers to incorporate only six actuators (not counting the gripper) into commercial robots. After all, this is the minimum number required to arbitrarily specify a position and orientation in space. From a mechanical point of view, there is no point in adding redundant actuators to the

system. It increases cost, increases complexity, and hence reduces reliability. Yet, the use of redundant actuators, properly located, is what makes the macro/micro manipulator inherently more stable and better suited for control.

Another example is the design tradeoff between structural stiffness and weight. From a mechanical point of view, a certain structural stiffness may be adequate. When enclosed within a control loop, however, this same structure may give rise to severe instability. Thus, specifying a particular mechanical design may inadvertently place detrimental restrictions on achievable controller performance.

It is suggested that control systems design begins with mechanical systems design, and hence a unified design approach should be taken.

7.4 Design in the Physical Domain

Design in the Physical Domain is proposed as a unified approach to control systems design. It attempts to unify mechanical systems design with control systems design. It is by no means claimed that the subject has been thoroughly understood or formalized. This may prove to be a lifetime's research goal. The ideas presented in this section are in their infancy, but are definitely a step in the right direction.

Consider the most common procedure for designing control systems. First, the system to be controlled is modeled using any of the established techniques. The equations of motion describing the system are then derived from that model. The next step usually involves Laplace transformation in order to

work in the S-plane, using the well known methods of classical control. If modern control is used, then instead of taking the Laplace transform, the system gains are determined in the time domain. Both of these approaches are very useful in that they provide a mathematical methodology for designing controllers. On the other hand, a great deal of physical insight is lost when working in the Laplace domain (S-plane), or when using the optimization theory of modern control.

Recall the macro/micro manipulator model of Figure 5.1. Examining its Bode plot (Figure 5.2) and root locus plot (Figure 5.3), it is noted that they contain a great deal of information regarding natural frequencies, phase lag, stability, etc. Yet, they provide no physical insight as to why the system is behaving the way it is. Working only with the root locus and Bode plot of the system, the author challenges the reader to see if he or she can reach the same conclusion that varying the base damping (B_1) alleviates the anti-resonance problem exhibited in the Bode plot. The author was definitely not able to do that. It was somewhat intuitive that raising the structural damping would help, but there was certainly no clue that the base damping was the key. Even less evident from the Bode plot and root locus, was the fact that raising the base damping arbitrarily high will actually hurt performance. Instead, this conclusion was reached by working directly with the physical system, applying the vast existing knowledge of physical systems behavior.

Since the concept of physical equivalence establishes that a controlled physical system is physical as well, why not design the control system in the physical domain? This would not only provide more physical insight into the system, but would also enable the designer to select a proper physical

configuration in terms of actuator location, sensor location, etc. Hence, control systems design would include mechanical design.

7.4.1 Controller Design Approach

Controller design in the physical domain is based on the following postulate:

Given ideal (no dynamics) actuators and sensors,

any physical system can be made to emulate the dynamic behavior of any other physical system, provided that actuators and sensors can be placed at any point in that system.

Ideal actuators and sensors, of course, do not exist. Hence, a controlled physical system cannot perfectly emulate the desired system. Nevertheless, it can closely approximate its dynamic behavior for a certain frequency range. Furthermore, actuators and sensors cannot be arbitrarily placed anywhere in a real system.

Thus, the "art" of designing controllers in the physical domain consists of:

1. **Selecting a target physical system that can be approximated with achievable actuation and sensing.**
2. **Wisely locating available actuators and sensors.**

The author claims that the second of these points is by far the most important and influential factor in achieving a desired control system. Yet, it is often considered part of

the mechanical or electro-mechanical design phase. It is therefore imperative that the mechanical design phase be an integral part of the control system design phase. Designing a controller after a mechanical design has been independently specified, is like challenging someone to a fencing duel with your hands tied behind your back. The mechanical architecture is the heart of the control system and should therefore be treated as such.

The first point is also very important and remains an open research question. It is often unclear what the best system behavior is for a given task. Furthermore, it is not only important to select the proper desired system behavior, but also one that can be achieved with available actuation and sensing.

The approach for designing controllers should consist of two steps:

1. **Designing the controller <u>structure</u> in the physical domain.**
2. **Fine tuning the controller parameters using common control techniques (S-plane, optimization theory, simulation, etc.).**

Designing the controller structure includes decisions such as: the proper target physical system for the task, the proper states to measure (sensor location), the proper states to actuate (actuator location), etc. This should be done in the physical domain where the most insight is available. Note that a great deal is automatically specified about the mechanical design in the process of designing the controller structure. It must be ensured, however, that these restrictions are not detrimental from a "mechanical" point of view, and in fact are feasible. A compromise may often have to be reached.

Once the structure of the control system is designed, the system parameters (gains, etc.) can be fine tuned using any of the common control techniques, if necessary. Thus, controller design in the physical domain is not presented as an alternative to classical or modern control. Rather, it is presented as a means of unifying existing control methodologies with mechanical design.

Consider, as an example, a conventional robot attempting to regulate interface forces against a rigid environment (Figure 4.1). One way of designing a controller is to derive the equations of motion, obtain the root locus (Figure 4.2), and attempt to design a compensator. Examining the root locus, however, reveals that instability occurs due to the interaction between the sensor dynamics and structural dynamics of the robot. Designing a compensator to alleviate this problem is extremely difficult (many have tried), however. Pole-zero cancellation would work in theory, but it is not robust and does not generally work in real systems. In fact, most methods that attempt to cancel dynamics require very accurate knowledge of the structure, and hence are not very robust. Furthermore, there is a fundamental physical limitation to performance, caused by the time it takes a wave to travel from the base of the structure to the other end.[6,30]

The error with the controller design approach taken above is that the mechanical architecture of a robot is assumed to be "cast in concrete." Why attempt to design a complex controller for a physical architecture that is inherently unstable and ill-suited for control?

Using the philosophy of designing controllers in the physical domain, the control structure is first established. This consists of selecting a desired target physical system

behavior. Lets take it to be a simple mass-spring-damper. It is known that this behavior will be stable. It is also known, from physical systems theory,[30] that the endpoint inertia of a structure cannot be changed by actuating at the base. Again, this is due to the finite propagation delay of the structure. Thus, it is established that in order to approximate the desired behavior (impedance) an actuator must be placed as close to the endpoint as possible. Hence, the mechanical architecture of the robot must be altered.

If an actuator is placed between the endpoint and ground, the desired behavior can be achieved since the actuator by-passes the undesirable dynamics of the structure. This can actually be accomplished by placing several local actuators near each task location, to which the robot would attach its endpoint. This is along the same lines as the local support concept,[4,5] where passive supports are replaced by active ones.

Placing an actuator between the robot endpoint and ground is feasible, but may at times be impractical. Yet, we know that in order to approximate the target physical system, an actuator is needed as close to the endpoint or task as possible. A feasible alternative is to attach a small actuator to the endpoint of the robot, making it the new endpoint (macro/micro manipulator). However, the base of this new actuator is attached to a dynamic system, rather than ground. It is thus desired to either bypass the structural dynamics or to reduce its undesirable aspects.

A passive local support can now mechanically bypass the structural dynamics, making the robot appear to be a ground. In other words, the macromanipulator would attach its endpoint (the base of the micromanipulator) to a passive local support

in the vicinity of the task, mechanically bypassing its structural dynamics. The micromanipulator would then apply and regulate the desired forces, achieving the target physical system behavior, as if it was attached directly to ground. The resulting system would have a large work space, as well as desirable endpoint dynamics in the vicinity of the task.

It was pointed out in Chapter 5, however, that local supports may reduce the versatility of the robot, especially as the workspace becomes more cluttered with other tools and fixtures. An alternative approach was presented, based on impedance matching, for alleviating the undesirable structural dynamics of the macromanipulator seen by the micromanipulator base. Either way, design in the physical domain leads to the macro/micro manipulator architecture, altering the mechanical configuration of conventional robots. It also leads to the already established local support concept, and confirms that it is a good means of altering endpoint dynamics.

It is admitted that a great deal of intuition was used in the design above, and not enough concrete ("cook book") procedural methodology. Also, hindsight was probably unconsciously used. Nevertheless, it can be seen, at least qualitatively, how several issues are tied together when using this approach.

Design in the Physical Domain is in an infant stage. It is a foundation on which a unified approach to control systems design can be built.

7.5 Chapter Summary

It was demonstrated in this chapter that some of the concepts developed for the macro/micro manipulator have gener-

al merit and applicability. The macro/micro separation concept was shown to be advantageous not only in robotics, but in other systems with transmission line dynamics as well. The transmission line need not necessarily be a mechanical structure, as was illustrated with a fluidic example. Both system stability and performance can be greatly improved using the macro/micro separation concept.

The concept of physical equivalence was presented as a means of abstraction, separating the control design issues from the implementation issues. This concept facilitates control systems design in the physical domain.

Control systems design was shown to begin with mechanical systems design. Hence, it is imperative that the two disciplines be combined.

Design in the Physical Domain was proposed as a unified approach to control systems design. A robot attempting to regulate interface forces was used as a case study. It was shown how controller design in the physical domain led to the macro/micro manipulator concept and the local support concept. It is admitted, however, that some hindsight may have been used in the design process.

Chapter 8

CONCLUSIONS

8.1 Research Contributions

The research presented in this document clearly demonstrates, both analytically and experimentally, that a macro/micro manipulator is an inherently more suitable configuration for endpoint control than a conventional robot. More specifically, the following key contributions are claimed:

I. Demonstrated mechanical feasibility of a macro/micro manipulator. Developed a small, light-weight, five-degree-of-freedom micromanipulator that can accelerate a 50 pound mass at 45G's.

II. Analytically and experimentally demonstrated that a macro/micro manipulator is an inherently stable physical architecture for endpoint control.

III. Demonstrated both analytically and experimentally that a macro/micro manipulator is an inherently well suited physical configuration for high performance control.

   Achieved an endpoint position bandwidth of 28 Hz (15 times higher than the frequency of the first structural mode of the macromanipulator).

   Achieved a force control bandwidth of 60 Hz (32 times higher than the frequency of the first structural mode of the macromanipulator).

IV. Proposed a design philosophy in the physical domain as a a unified approach to control systems design. This can help close the gap between control systems design and mechanical design.

V. Proposed the macro/micro separation concept as a general solution to the problem of transmission line dynamics.

At the outset of this research, the mechanical feasibili-

ty of a high-performance micromanipulator, that does not limit the payload capabilities of the macromanipulator, was not at all clear. This question was definitely answered by this research. Not only does the prototype micromanipulator not limit the capabilities of a macromanipulator, its performance is highly superior. Demonstrating physical feasibility of such a high performance micromanipulator is very important, since the applicability of the entire macro/micro manipulator concept relies on it.

Similarly, intuition would indicate that the addition of the micromanipulator, doubling the number of actuators and sensors, would complicate the control problem. The research demonstrated that this is not the case, and in fact the opposite is true. The addition of the extra actuators and sensors actually made the system inherently more stable and easier to control. It should be stressed that not only was the macro/micro manipulator shown to be capable of high performance position and force control, more importantly, it was demonstrated to be a stable and well suited physical architecture for high performance endpoint control. This is a crucial point. Just because high performance can be achieved by a certain system, it does not mean that it is the right approach to take. This ties in closely with the proposed concept of designing controllers in the physical domain. This procedure begins to close the gap between control systems design and mechanical design, leading to a better suited physical architecture for a given problem.

An inverted pendulum, for example, can certainly be stabilized with the proper control action. High performance (fixed orientation) can even be achieved if enough effort is put in. This does not mean, however, that an inverted

pendulum is the right approach for supporting a high rise building. Thus, achieving high performance endpoint position and force control using a macro/micro manipulator is certainly reassuring. Demonstrating that a macro/micro manipulator is in fact the right approach (perhaps the only one) is by far a greater contribution.

Finally, the macro/micro separation concept was proposed as a general solution to the problem of transmission line dynamics. This can be quite useful since almost all real systems consist of some sort a transmission line. The associated dynamics may not necessarily be harmful in all systems, however. This is dependent on the system and the desired behavior.

Besides the specific contributions listed above, the models developed throughout the analysis are believed to be a contribution as well. Their virtue is their simplicity, insight, and adequacy in characterizing the system. Also, although no new information is revealed, the assessment of problems in force control (Chapter 4) provides a great deal of insight to understanding the force control problem.

8.2 Future Work

The research presented in this document demonstrates the inherent characteristics and potential of a macro/micro manipulator system. The achieved performance is clearly superior to that of conventional robots. However, there is a great deal that can be done to further improve performance and applicability to manufacturing automation.

8.2.1 Sensing Technology

Sensing technology, or lack of it, is one of the most crucial factors in flexible automation. Regardless of how intelligent a system may be, it needs some data to work with. The quality of this data will play a major role in the achievable performance. Hence, the sensors used to gather this data must be accurate and reliable.

More specifically, in the case of the macro/micro manipulator, fast, accurate, and reliable non-contact endpoint position and velocity measurement is needed. Work must be done in the area of robust non-contact velocity measurement. Ultimately, it would be nice to have an absolute six-degree-of-freedom measurement of the robot's endpoint relative to ground. As an intermediary solution, accurate measurement of the tool relative to the work-piece would suffice.

Technology development is often driven by need. Before the introduction of the macro/micro manipulator concept, the need for non-contact endpoint velocity measurement in robotics did not widely exist. After all, conventional robots are actuated and controlled at the base, and endpoint control is inherently unstable. The advent of macro/micro manipulators creates a real need for non-contact endpoint velocity and position measurement. When there is a need, there is a way.

8.2.2 Actuation Technology

Even if perfectly accurate and robust sensor data is available, high performance actuators are necessary in order to translate this data into desired mechanical motion. This

is especially true in force control, as was explained in chapter 4. Hence, in order for the macro/micro manipulator to be more effective, high torque, low inertia "micro" actuators must be developed. These actuators should emulate torque sources and contain as little internal non-collocation as possible. This would enable the characterization of a macro/micro manipulator's ability to regulate forces against arbitrarily stiff environments. Achieving these goals in a microactuator is much more feasible than in a macroactuator, that must provide a large range of motion.

8.2.3 Desired Impedance

The macro/micro manipulator was shown to be very effective in regulating interface forces. This can be used to vary the apparent endpoint impedance of the robot and hence emulate a desired target physical system. While having the capability to achieve a wide range of impedances is advantageous, there must be a way of determining what a proper impedance specification for a given task should be. It is not clear, for example, what impedance to ask for when using a certain power tool.

Determining the proper impedance for a given task is an open research topic. A formal procedure for determining the proper impedance for a given task must be developed. What good is a high performance controller if it is not known what to do with it? A great deal of work must be done in this area if robots are to succeed in interacting with their environment.

Thus, treating a controller as a regulator is adequate,

and perhaps wise, in unconstrained motion. That is not the case in constrained motion. Specifying overshoot, settling time, bandwidth, etc., in a grinding operation is clearly not a good approach. Instead, the proper endpoint impedance must be specified. But again, what is the proper impedance?

8.2.4 Design in the Physical Domain

The concept of designing in the physical domain has been proposed as a unified approach to control systems design. It was shown how control systems design begins with mechanical systems design, and that this approach can close the gap between the two disciplines. Yet, it was also admitted that this concept is still in its infancy. It is a foundation to build on. A great deal of work can and should be done in this area.

A formal methodology must be developed. It should not only provide guidance through the design process, but also in assessing the best system performance compromise from both a mechanical and control point of view. This is very important since often there is a contradiction between the two.

8.2.5 Full Implementation

The time has come to attach a fully operational five or six degree-of-freedom micromanipulator to an industrial robot. Or, perhaps a better alternative, to design and build a complete, multi-axis, integrated macro/micro manipulator system. Either way, the purpose would be to study the behavior, and to

characterize the advantages of the system in a well monitored, prototype application. Premature implementation into real manufacturing could be detrimental to the concept.

Appendix A

EQUATIONS OF MOTION OF TWO-AXIS MACRO/MICRO MANIPULATOR

Free body diagrams are used to derive the equations of motion of the two-axes macro/micro manipulator model in Figure 3.14.

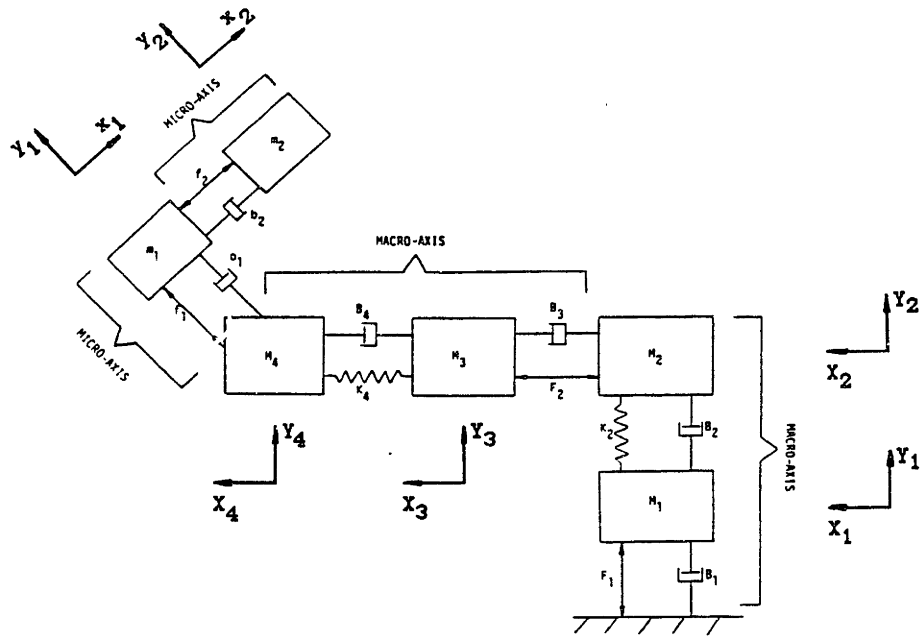

Note that all forces with "R" or "r" in the subscript refer to reaction forces introduced by the motion constraint along one axis.

M_1 :

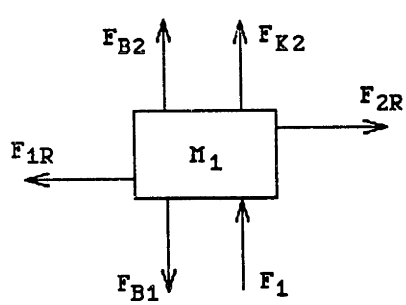

$$B_2(\dot{Y}_2 - \dot{Y}_1) + K_2(Y_2 - Y_1) - B_1\dot{Y}_1 + F_1 = M_1\ddot{Y}_1 \qquad \text{(a1.1)}$$

$$-F_{2R} + F_{1R} = 0 \qquad \text{(a1.2)}$$

M_2 :

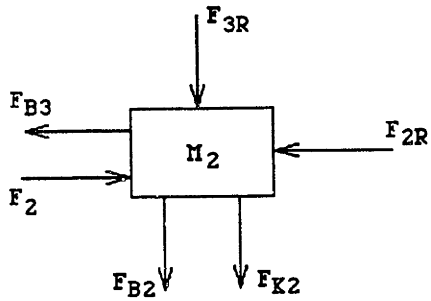

$$-F_{3R} - B_2(\dot{Y}_2 - \dot{Y}_1) - K_2(Y_2 - Y_1) = M_2\ddot{Y}_2 \qquad \text{(a1.3)}$$

$$B_3\dot{X}_3 - F_2 + F_{2R} = 0 \qquad \text{(a1.4)}$$

M_3 :

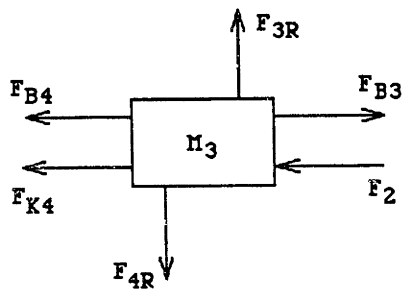

$$F_{3R} - F_{4R} = M_3\ddot{Y}_3 \qquad \text{(a1.5)}$$

$$B_4(\dot{X}_4 - \dot{X}_3) + K_4(X_4 - X_3) - B_3\dot{X}_3 + F_2 = M_3\ddot{X}_3 \qquad \text{(a1.6)}$$

M_4 :

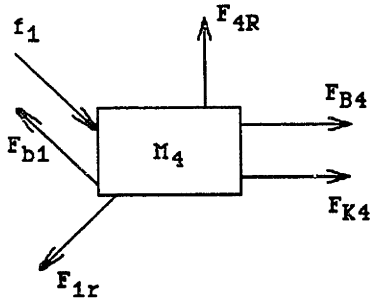

$$-0.707f_1 - B_4(\dot{X}_4 - \dot{X}_3) - K_4(X_4 - X_3) + 0.707F_{1r} + 0.707b_1(\dot{Y}_1 - 0.707\dot{Y}_4 - 0.707\dot{X}_4) = M_4\ddot{X}_4 \qquad \text{(a1.7)}$$

$$-0.707f_1 - 0.707F_{1r} + F_{4R} + 0.707b_1(\dot{Y}_1 - 0.707\dot{Y}_4 - 0.707\dot{X}_4) = M_4\ddot{Y}_4 \qquad \text{(a1.8)}$$

m_1 :

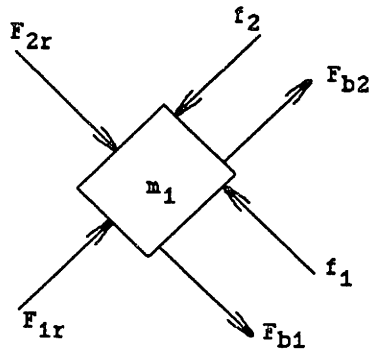

$$-f_2 + b_2(\dot{x}_2 - \dot{x}_1) + F_{1r} = m_1\ddot{x}_1 \quad \text{(a1.9)}$$

$$f_1 - b_1(\dot{y}_1 - 0.707\dot{Y}_4 - 0.707\dot{X}_4) - F_{2r} = m_1\ddot{y}_1 \quad \text{(a1.10)}$$

m_2 :

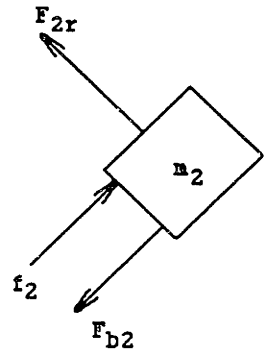

$$f_2 - b_2(\dot{x}_2 - \dot{x}_1) = m_2\ddot{x}_2 \quad \text{(a1.11)}$$

$$F_{2r} = m_2\ddot{y}_2 \quad \text{(a1.12)}$$

There are 12 equations with 18 unknowns. Hence 6 more kinematic equations are needed.

$$Y_1 = Y_2 \quad \text{(a1.13)}$$

$$Y_2 = Y_3 \quad \text{(a1.14)}$$

$$Y_3 = Y_4 \quad \text{(a1.15)}$$

$$X_1 = X_2 \quad \text{(a1.16)}$$

$$x_1 = -0.707X_4 + 0.707Y_4 \quad \text{(a1.16)}$$

$$y_1 = 0.707X_4 + 0.707Y_4 \quad \text{(a1.17)}$$

Eliminating reaction forces and using above kinematic constraints, the equations are placed in matrix form:

$$\dot{\underline{X}} = A*\underline{X} + B*\underline{U}$$

where the matrices and vectors are given below.

State Vector X

$$\begin{bmatrix} y_2 \\ \dot{y}_2 \\ x_2 \\ \dot{x}_2 \\ y_1 \\ \dot{y}_1 \\ x_3 \\ \dot{x}_3 \\ x_4 \\ \dot{x}_4 \\ y_4 \\ \dot{y}_4 \end{bmatrix}$$

Control Vector U

$$\begin{bmatrix} f_1 \\ f_2 \\ F_1 \\ F_2 \end{bmatrix}$$

A matrix:

This is a 12x12 matrix with the following elements:

$$A(1,2) = 1 \qquad \text{(a1.18)}$$

$$A(2,2) = -\frac{b_1}{m_1 + m_2} \qquad \text{(a1.19)}$$

$$A(2,10) = \frac{0.707b_1}{m_1 + m_2} \qquad \text{(a1.20)}$$

$$A(2,12) = \frac{0.707b_1}{m_1 + m_2} \qquad \text{(a1.21)}$$

$$A(3,4) = 1 \qquad \text{(a1.22)}$$

$$A(4,4) = -\frac{b_2}{m_2} \qquad \text{(a1.23)}$$

$$A(4,10) = -\frac{0.707b_2}{m_2} \qquad \text{(a1.24)}$$

$$A(4,12) = \frac{0.707b_2}{m_2} \qquad (a1.25)$$

$$A(5,6) = 1 \qquad (a1.26)$$

$$A(6,5) = -\frac{K_2}{M_1} \qquad (a1.27)$$

$$A(6,6) = -\frac{(B_1 + B_2)}{M_1} \qquad (a1.28)$$

$$A(6,11) = \frac{K_2}{M_1} \qquad (a1.29)$$

$$A(6,12) = \frac{B_2}{M_1} \qquad (a1.30)$$

$$A(7,8) = 1 \qquad (a1.31)$$

$$A(8,7) = -\frac{K_4}{M_3} \qquad (a1.32)$$

$$A(8,8) = -\frac{(B_3 + B_4)}{M_3} \qquad (a1.33)$$

$$A(8,9) = \frac{K_4}{M_3} \qquad (a1.34)$$

$$A(8,10) = \frac{B_4}{M_3} \qquad (a1.35)$$

$$A(9,10) = 1 \qquad (a1.36)$$

$$A(10,2) = \frac{(.3535m_1 b_1)/M + .707b_1}{D} \qquad (a1.37)$$

$$A(10,4) = \frac{(.3535m_1 b_2)/M - 0.707b_2}{D} \qquad (a1.38)$$

$$A(10,5) = \frac{(0.5m_1 K_2)/M}{D} \qquad (a1.39)$$

$$A(10,6) = \frac{(0.5m_1 B_2)/M}{D} \quad \text{(a1.40)}$$

$$A(10,7) = \frac{K_4}{D} \quad \text{(a1.41)}$$

$$A(10,8) = \frac{B_4}{D} \quad \text{(a1.42)}$$

$$A(10,9) = -\frac{K_4}{D} \quad \text{(a1.43)}$$

$$A(10,10) = \frac{[0.25m_1 (b_2 - b_1)]/M - 0.5b_1 - 0.5b_2 - B_4}{D} \quad \text{(a1.44)}$$

$$A(10,11) = -\frac{0.5K_2 m_1/M}{D} \quad \text{(a1.45)}$$

$$A(10,12) = -\frac{[m_1 (0.25b_1 + 0.25b_2 + 0.5B_2)]/M + 0.5b_1 - 0.5b_2}{D} \quad \text{(a1.46)}$$

$$A(11,12) = 1 \quad \text{(a1.47)}$$

$$A(12,2) = \frac{0.3535m_1 b_1/M_e + 0.707b_1}{E} \quad \text{(a1.48)}$$

$$A(12,4) = \frac{0.707b_2 - 0.3535m_1 b_2/M_e}{E} \quad \text{(a1.49)}$$

$$A(12,5) = \frac{K_2}{E} \quad \text{(a1.50)}$$

$$A(12,6) = \frac{B_2}{E} \quad \text{(a1.51)}$$

$$A(12,7) = \frac{0.5m_1 K_4/M_e}{E} \quad \text{(a1.52)}$$

$$A(12,8) = \frac{0.5B_4 m_1/M_e}{E} \quad \text{(a1.53)}$$

$$A(12,9) = -\frac{0.5K_4 m_1/M_e}{E} \quad \text{(a1.54)}$$

$$A(12,10) = -\frac{[m_1(0.5B_4 + 0.25b_1 + 0.25b_2)]/M_e + 0.5b_1 - 0.5b_2}{E} \quad \text{(a1.55)}$$

$$A(12,11) = -\frac{K_2}{E} \quad \text{(a1.56)}$$

$$A(12,12) = -\frac{[0.25m_1(b_1 - b_2)]/M_e + 0.5b_1 + 0.5b_2 + B_2}{E} \quad \text{(a1.57)}$$

All other elements in the A matrix are identically zero.

B Matrix

$$B(2,1) = \frac{1}{m_1 + m_2} \quad \text{(a1.58)}$$

$$B(4,2) = \frac{1}{m_2} \quad \text{(a1.59)}$$

$$B(6,3) = \frac{1}{M_1} \quad \text{(a1.60)}$$

$$B(8,4) = \frac{1}{M_3} \quad \text{(a1.61)}$$

$$B(10,1) = -\frac{0.3535m_1/M + 0.707}{D} \quad \text{(a1.62)}$$

$$B(10,2) = \frac{0.707 - 0.3535m_1/M}{D} \quad \text{(a1.63)}$$

$$B(12,1) = -\frac{0.3535m_1/Me + 0.707}{E} \quad \text{(a1.64)}$$

$$B(12,2) = \frac{0.3535m1/M_e - 0.707}{E} \quad \text{(a1.65)}$$

All other elements of matrix B are identically zero.

M, and M_e, D, and E above are defined as follows:

$$M = M_2 + M_3 + M_4 + 0.5m_1 \tag{a1.66}$$

$$M_e = M_4 + 0.5m_1 \tag{a1.67}$$

$$D = M_e - \frac{0.25m_1^2}{M} \tag{a1.68}$$

$$E = M - \frac{0.25m_1^2}{M_e} \tag{a1.69}$$

Appendix B

EQUATIONS OF MOTION OF A MANIPULATOR COUPLED TO A RIGID ENVIRONMENT

Free-body diagrams are used to derive the equations of motion of the manipulator in Figure 4.2.

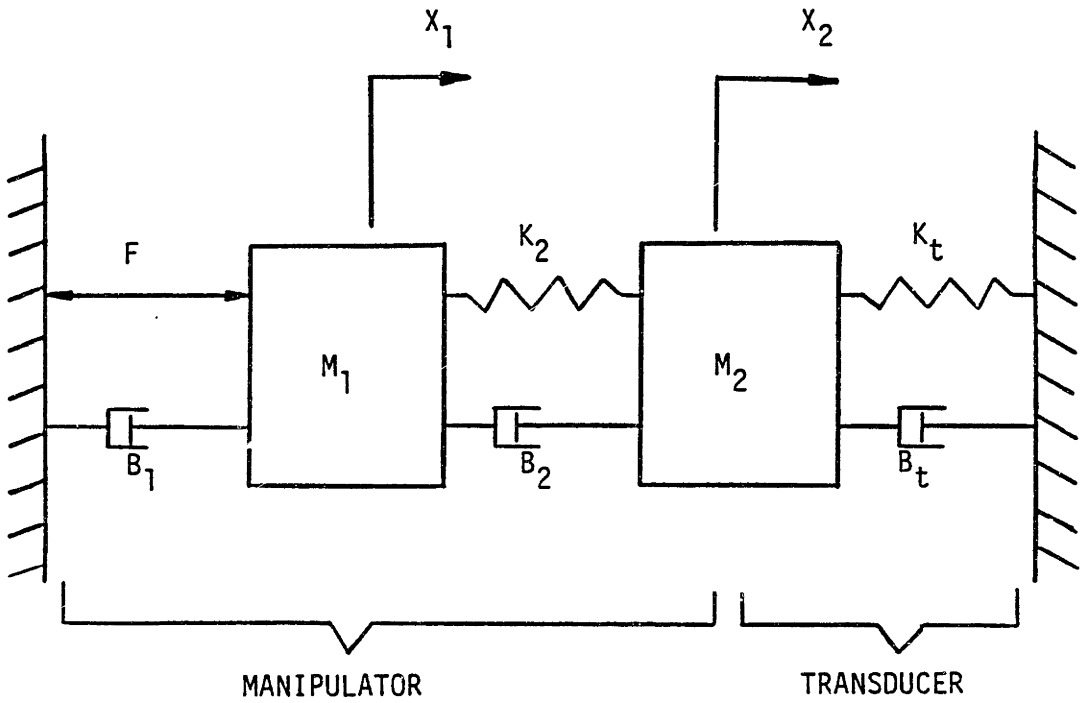

$$F + K_2 (X_2 - X_1) + B_2 (\dot{X}_2 - \dot{X}_1) - B_1 \dot{X}_1 = M_1 \ddot{X}_1 \qquad \text{(a2.1)}$$

$$-K_2 (X_2 - X_1) - B_2 (\dot{X}_2 - \dot{X}_1) - K_t X_2 - B_t \dot{X}_2 = M_2 \ddot{X}_2 \qquad \text{(a2.2)}$$

The force in the spring (F_t) is simply:

$$F_t = K_t X_2 \qquad \text{(a2.3)}$$

Placing equations in matrix form:

$$\dot{\underline{X}} = A*\underline{X} + B*\underline{U}$$

results in the following system equations:

$$\frac{d}{dt}\begin{bmatrix} X_1 \\ \dot{X}_1 \\ X_2 \\ \dot{X}_2 \\ F_t \end{bmatrix} = \begin{bmatrix} 0 & 1 & 0 & 0 & 0 \\ -\frac{K_2}{M_1} & -\frac{B_2+B_1}{M_1} & \frac{K_2}{M_1} & \frac{B_2}{M_1} & 0 \\ 0 & 0 & 0 & 1 & 0 \\ \frac{K_2}{M_2} & \frac{B_2}{M_2} & -\frac{K_2+K_t}{M_2} & -\frac{B_2+B_t}{M_2} & 0 \\ 0 & 0 & 0 & K_t & 0 \end{bmatrix} \begin{bmatrix} X_1 \\ \dot{X}_1 \\ X_2 \\ \dot{X}_2 \\ F_t \end{bmatrix} + \begin{bmatrix} 0 \\ \frac{1}{M_1} \\ 0 \\ 0 \\ 0 \end{bmatrix} \begin{bmatrix} F \end{bmatrix}$$

(a2.4)

Appendix C

EQUATIONS OF MOTION OF A MACRO/MICRO MANIPULATOR COUPLED TO A RIGID ENVIRONMENT

Free body diagrams are used to derive the equations of motion of the macro/micro manipulator model in Figure 5.1.

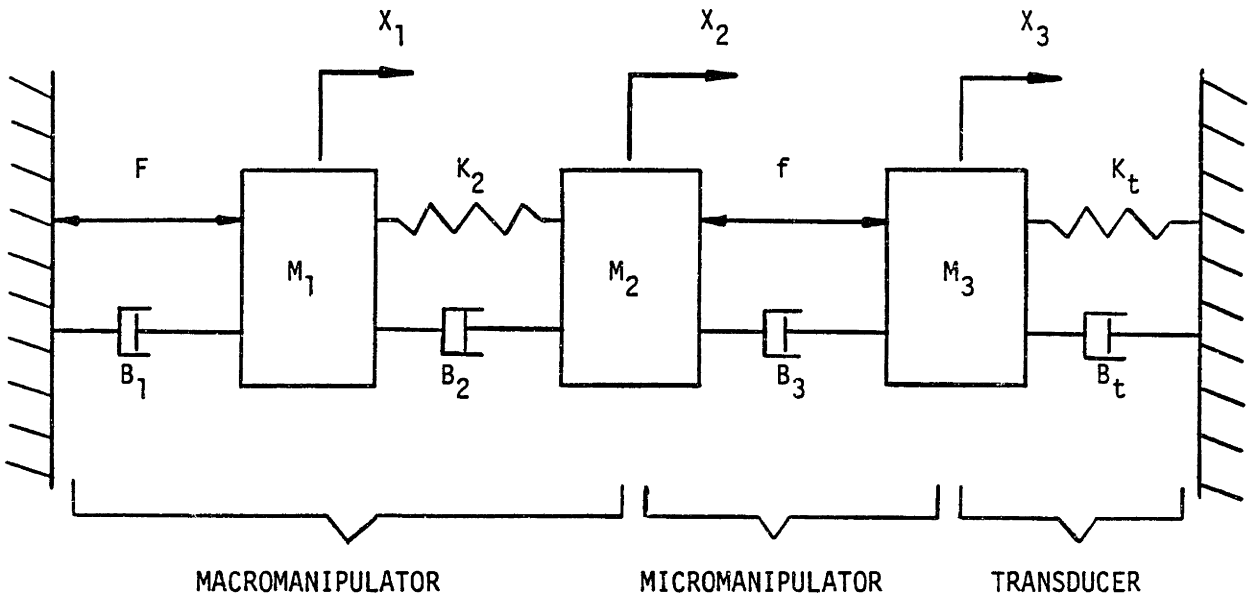

M_1 :

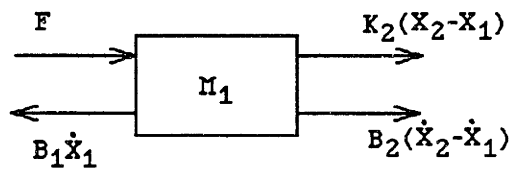

$$F - B_1\dot{X}_1 + K_2(X_2 - X_1) + B_2(\dot{X}_2 - \dot{X}_1) = M_1\ddot{X}_1 \qquad (a3.1)$$

M_2 :

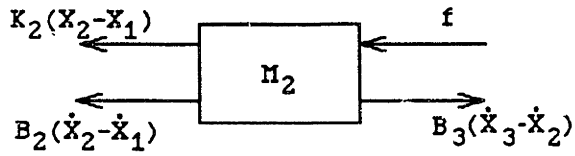

$$-f - K_2(X_2 - X_1) - B_2(\dot{X}_2 - \dot{X}_1) + B_3(\dot{X}_3 - \dot{X}_2) = M_2\ddot{X}_2 \qquad \text{(a3.2)}$$

M_3 :

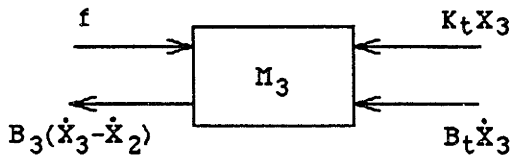

$$f - B_3(\dot{X}_3 - \dot{X}_2) - K_t X_3 - B_t \dot{X}_3 = M_3\ddot{X}_3 \qquad \text{(a3.3)}$$

The force in the spring (F_s) is simply:

$$F_t = K_t X_3 \qquad \text{(a3.4)}$$

Placing equations in matrix form:

$$\dot{\underline{X}} = A*\underline{X} + B*\underline{U}$$

results in the following:

$$\frac{d}{dt}\begin{bmatrix} X_1 \\ \dot{X}_1 \\ X_2 \\ \dot{X}_2 \\ X_3 \\ \dot{X}_3 \\ F_t \end{bmatrix} = \begin{bmatrix} 0 & 1 & 0 & 0 & 0 & 0 & 0 \\ -\frac{K_2}{M_1} & -\frac{(B_2+B_1)}{M_1} & \frac{K_2}{M_1} & \frac{B_2}{M_1} & 0 & 0 & 0 \\ 0 & 0 & 0 & 1 & 0 & 0 & 0 \\ \frac{K_2}{M_2} & \frac{B_2}{M_2} & -\frac{K_2}{M_2} & -\frac{(B_2+B_3)}{M_2} & 0 & \frac{B_3}{M_2} & 0 \\ 0 & 0 & 0 & 0 & 0 & 1 & 0 \\ 0 & 0 & 0 & \frac{B_3}{M_3} & -\frac{K_t}{M_3} & -\frac{(B_3+B_t)}{M_3} & 0 \\ 0 & 0 & 0 & 0 & 0 & K_t & 0 \end{bmatrix} \begin{bmatrix} X_1 \\ \dot{X}_1 \\ X_2 \\ \dot{X}_2 \\ X_3 \\ \dot{X}_3 \\ F_t \end{bmatrix} + \begin{bmatrix} 0 & 0 \\ \frac{1}{M_1} & 0 \\ 0 & 0 \\ 0 & \frac{1}{M_2} \\ 0 & 0 \\ 0 & \frac{1}{M_3} \\ 0 & 0 \end{bmatrix} \begin{bmatrix} F & f \end{bmatrix}$$

(a3.5)

REFERENCES

1. Book, W. J., "Characterization of Strength and Stiffness Constraints on Manipulator Control," Theory and Practice of Robots and Manipulators, 1976.

2. Burgam, P. M. ed., "The Push to Advanced Composites," Manufacturing Engineering, December, 1982.

3. Zalucky, A., and D. Hardt, "Active Control of Robot Structure Deflections," Robotics Research and Advanced Applications, November, 1982.

4. Asada, H., and H. West, "Design and Analysis of Braced Manipulators for Improved Stiffness," 3rd International Symposium on Robotics Research, October, 1985.

5. Book, W. J., S. Le, and V. Sangveraphunsiri, "The Bracing Strategy for Robot Operation," Theory and Practice of Robots and Manipulators, June, 1984.

6. Cannon, R. H., and E. Schmitz, "Initial Experiments on the End-Point Control of a One Link Flexible Experimental Manipulator," International Journal of Robotics Research, Fall, 1984.

7. Gevarter, W. B., "Basic Relations for Control of Flexible Vehicles," AIAA Journal, April, 1970.

8. Sharon, A., Enhancement of Robot Accuracy Using a Macro/Micro Manipulator System. S.M. Thesis, Mechanical Engineering Department, Massachusetts Institute of Technology, 1983.

9. Hollis, R. L., "Fine Positioner Increases Robot Precision," IBM Research Report, 1984.

10. Van Brussel, H., and J. Simmons, "The Adaptable Compliance Concept and its use for Automatic Assembly by Active Force Feedback Accommodations," 9th International Symposium on Industrial Robots, Washington, D.C., 1979.

11. Cutkosky, M. R., and P. K. Wright, "Position Sensing Wrists for Industrial Manipulators," 12th International Symposium on Industrial Robots, 1982.

12. Asakawa, K., F. Akiya, and F. Tabata, "A Variable Compliance Device and its Application for Automatic Assembly," Autofact 5 Conference, Detroit, November, 1983.

13. Kazerooni, H., and J. Guo, "Direct-Drive Active Compliant End-Effector (Active RCC)," IEEE International Conference on Robotics and Automation, March, 1987.

14. Whitney, D. E., "The Remote Center Compliance: What Can it Do?," Robotics Today, Summer, 1979.

15. Salisbury, J. K., "Design and Control of an Articulated Hand," 1st International Symposium on Design and Synthesis, Tokyo, July, 1984.

16. Jacobsen, S. C., et al, "The UTAH/MIT Dexterous Hand: Work in Progress," International Journal of Robotics Research, Vol. 3, No. 4, 1984.

17. Trimmer, W. S. N., and K. J. Gabriel, "The Micro Mechanical Domain," ASME Winter Annual Meeting, December, 1987.

18. Sharon, A., and D. Hardt, "Enhancement of a Robot's Accuracy Using Endpoint Feedback and a Macro/Micro Manipulator System," American Control Conference," June, 1984.

19. Chiang, W. W., End-point Position Control of a Flexible Manipulator with a Quick Wrist. Ph.D. Thesis, Department of Aeronautics and Astronautics, Stanford University, 1985.

20. Tilley, S. W. and R. H. Cannon Jr., "Experiments on End-Point Position and Force Control of a Flexible Arm With a Fast Wrist," AIAA Guidance and Control Conference, August, 1986.

21. Bailey, T., and J. E. Hubbard Jr. "Distributed Piezoelectric-Polymer Active Vibration Control of a Cantilever Beam," Journal of Guidance, Control, and Dynamics, September-October, 1985.

22. Raibert, M. H., and J. J. Craig, "Hybrid Position/Force Control of Manipulators," ASME Journal of Dynamic Systems, Measurement, and Control, Vol. 102, June, 1981.

23. Hogan, N., "Impedance Control: An Approach to Manipulation: Part 1 - Theory," ASME Journal of Dynamic Systems, Measurement, and Control, Vol. 107, March, 1985.

24. Wlassich, J. J., Nonlinear Force Feedback Impedance Control. S.M. Thesis, Mechanical Engineering Department, Massachusetts Institute of Technology. 1986.

25. Roberts R., Paul R., and B. Hillberry, "The Effect of Wrist Force Sensor Stiffness on the Control of Robot Manipulators," IEEE Conference on Robotics and Automation, 1985.
26. Whitney D., and J. Nevins, "Historical Perspective and State of the Art in Robot Force Control," IEEE Conference on Robotics and Automation, 1985.

27. Eppinger, S. D., and W. P. Seering, "On Dynamic Models of Robot Force Control," IEEE Conference on Robotics and Automation, 1986.

28. Townsend, W. T., The Effect of Transmission Design on Force Controlled Manipulator Performance. Ph.D. Thesis, Mechanical Engineering Department, Massachusetts Institute of Technology, 1988.

29. Bekefi, G., and A. H. Barret, Electromagnetic Vibrations, Waves, and Radiation. Cambridge, Massachusetts: The MIT Press, 1977.

30. Colgate, J. E., The Control of Dynamically Interacting Systems. Ph.D. Thesis, Mechanical Engineering Department, Massachusetts Institute of Technology, 1988.